# Ypts and TRAPPs in Golgi dynamics

BY

JANE J KIM
B.A. Kalamazoo College, 2008

THESIS

Submitted as partial fulfillment of the requirements
for the degree of Doctor of Philosophy in Biological Sciences
in the Graduate College of the
University of Illinois at Chicago, 2016

Chicago, Illinois

Defense Committee

Nava Segev, Advisor, Biochemistry and Molecular Genetics
Ron Dubreuil, Chair, Biological Sciences
Sojin Shikano, Biochemistry and Molecular Genetics
Simon Alford, Anatomy and Cell Biology
Dave Stone, Biological Sciences
Ben Glick, University of Chicago

## DEDICATION

I would like to dedicate my thesis to my parents, Joong Ki Kim and Heung Sook Kim for their years of inspiration, motivation, and support. From them, I've learned the art of persistence, which has served me well during my graduate school career. I would like to extend my deepest appreciation for friends and family, including a special thanks to Zhanna Lipatova, not only for the years of technical guidance and expertise, but also for the countless Starbucks trips and life advice. Last, but certainly not least, my deepest gratitude goes to Brian Grewe for the countless discussions, advice, and most helpful of all, the arguments.

## ACKNOWLEDGEMENTS

I offer the sincerest gratitude to my advisor, Nava Segev, for giving me the opportunity to join the lab and introducing me to a challenging but interesting research topic. I appreciate the continual guidance and encouragement that she has given me over these years. I wish to thank my current and former committee members, Sue Liebman, Ron Dubreuil, Simon Alford, Sojin Shikano, Ben Glick, and Dave Stone for their time and knowledge. Also, I would like to thank current and former lab members, including Zhanna Lipatova, David Taussig, XiuQi Zhang, Natalia Belogortseva, and Uddulak Majumdar as well as others for instructions and/or technical help.

## TABLE OF CONTENTS

## TABLE OF CONTENTS (continued)

## LIST OF TABLES

## LIST OF FIGURES

## LIST OF FIGURES (continued)

## LIST OF ABBREVIATIONS

| | |
|---|---|
| AD | activation domain |
| BiFC | bi-molecular fluorescence complementation |
| BD | binding domain |
| CC | coiled-coil |
| CFP | cyan fluorescent protein |
| ER | endoplasmic reticulum |
| FP | fluorescent protein |
| GAP | GTPase activating protein |
| GDP | guanine diphosphate |
| GEF | guanine nucleotide exchange factor |
| GFP | green fluorescent protein |
| GST | glutathione s-transferase |
| GTP | guanine triphosphate |
| IF | Immunofluorescence |
| KDa | kilodalton |
| mRFP | monomeric red fluorescent protein |
| PAS | pre-autophagosomal structure |
| PM | plasma membrane |
| TRAPP | transport protein particle |
| SEDT | spondyloepiphyseal dysplasia tarda |
| SEM | standard error of mean |
| STDEV | standard deviation |

## LIST OF ABBREVIATIONS (continued)

| | |
|---|---|
| Y2H | yeast-2-hybrid |
| yE | yeast enhanced |
| YFP | yellow fluorescent protein |

## SUMMARY

The conserved Ypt/Rab GTPases regulate the pathways of intracellular transport in eukaryotic cells. They accomplish this regulation in conjunction with their activators, guanine exchange factors (GEFs). Yeast Ypt1 (mammalian Rab1) and Ypt31/32 (mammalian Rab11) are essential for ER-to-Golgi and Golgi-to-PM trafficking, respectively. However, regulation of intra-Golgi processes, such as Golgi cisternal progression, by these Ypt/Rabs remains poorly understood. In this thesis, I report findings on Ypt1 and Ypt31 as well as their GEFs, the TRAPPI and TRAPPII complexes, within the Golgi. Using live-cell microscopy and immunofluorescence, I establish that Ypt1 and Ypt31 polarize to opposite ends of the Golgi, early and late, respectively. They co-localize on a compartment that contains both early and late Golgi proteins, which I termed transitional. Furthermore, using live-cell and time-lapse microscopy, I show that Ypt1 and Ypt31 regulate two distinct Golgi cisternal progression steps, early-to-transitional and transitional-to-late, respectively. Correspondingly, I provide evidence that the TRAPPII complex has a similar pattern of Golgi compartmental localization as Ypt31 and not of Ypt1. Together, these results show novel regulation for Golgi cisternal maturation by Ypt/Rab GTPases, clears up controversy for the placement of Ypt1 and Ypt31 to specific Golgi compartments, and places TRAPPII as the GEF for Ypt31 *in vivo*.

# CHAPTER 1. INTRODUCTION

## A. Intracellular trafficking overview

In every eukaryotic cell, proteins are shuttled through various pathways, e.g., the secretory pathway and autophagy. The shuttling process is known as intracellular trafficking. Membrane proteins, such as hormone receptors, and cytosolic proteins, such as hormones, are packaged as cargo in membrane-bound compartments called vesicles. These vesicles bud from an initial compartment and are then transported to their destination to fuse with the acceptor membrane (Caro and Palade 1964, Palade 1975, Farquhar and Palade 1981). Cellular destinations include various organelles or the plasma membrane, PM, where the cargo is deposited or secreted. These pathways can be constitutive or activated based on necessity. Regardless, they are highly regulated, as protein buildup or improper targeting could be detrimental to the cell. Due to the fundamentally essential nature of these pathways, small defects or changes in levels of functionality can cause widespread problems in cellular fitness and/or survival. Hence, because the proper regulation of these pathways is vital, it is Important to understand how these pathways are regulated and where defects lie in various diseases in hopes of developing better diagnostic and therapeutic strategies.

## B. Ypt/Rab GTPases

Ypt/Rab GTPases are monomeric G-proteins that function as key regulators of traffic. They are present in all eukaryotic cells, which speaks of their necessity. Originally, these GTPases were discovered in yeast, *Saccharomyces cerevisiae,* and named Ypts. The human homologs of Ypt, Rabs, were later discovered to be highly

conserved, not only in sequence but also in function (Lipatova et al. 2015). Ypt/Rab GTPases are small proteins, approximately 25 KDa in size, that act as molecular switches by altering their structural conformation upon the binding of GTP. There are over 70 Rabs in humans but only 11 Ypts in yeast. Accordingly, yeast is an excellent model organism to decipher the role of Ypt/Rab GTPases in protein trafficking.

i. GTPase cycle and accessory factors

All Ypt/Rab GTPases cycle between their active GTP-bound or inactive GDP-bound conformations. Structurally, upon binding to GTP, two regions undergo a conformational change, called the switch I and switch II domains (Sultana et al. 2011). Ypt/Rabs are prenylated on a cysteine in their C-terminal tail to enable attachment to the membrane of a compartment (Leung, Baron, and Seabra 2006, Lee, Mishra, and Lambright 2009). Once activated and attached to the membrane, they can interact with a variety of effectors, which organize subsequent transport steps. These effectors include motor proteins, scaffold proteins, tethering factors, and others. The GTPase-effector interaction mediates a wide array of transport steps including vesicle formation, movement, tethering, and fusion (Segev 2001b, a). In the GDP-bound state, the structural conformation of the GTPase changes, and it is extracted from the membrane into the cytosol for the next round of activation. Guanine Exchange Factors, GEFs, activate the GTPase by increasing the rate of GDP release, facilitating the cellularly abundant GTP to bind. Hence, GEFs are considered activators of GTPase activity (Goody and Hofmann-Goody 2002). GTPase Activating Proteins, GAPs, act as negative regulators. They provide catalytic activity for the hydrolysis of GTP to GDP, effectively

inactivating the GTPase (Tan, Vollmer, and Gallwitz 1991, Strom et al. 1993, Du, Collins, and Novick 1998, Albert, Will, and Gallwitz 1999) Figure 1.

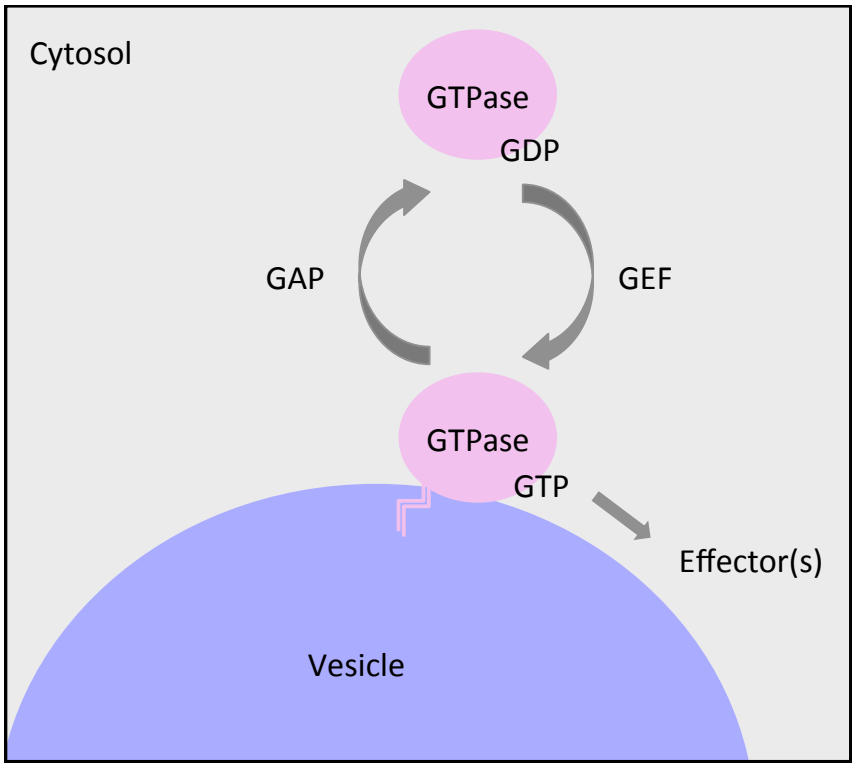


**Figure 1. Ypt/Rab GTPase cycle.** Ypt/Rab GTPases switch between GDP-bound inactivate state and GTP-bound active state. In their active state, they interact with downstream effectors. Guanine Exchange Factors (GEFs) facilitate the exchange between GDP to GTP bound state, and GTPase activating proteins (GAPs) catalyze the hydrolysis of GTP to GDP bound to the GTPase. Activated GTPases are modified with the addition of a prenyl group to their C-terminal tail, for insertion into the membrane of a vesicle or compartment.

ii. Regulation of individual transport steps

Five Ypt GTPases, Ypt1, Ypt31/32, Ypt6, and Sec4 regulate the secretory pathway in yeast. Initially, it was thought that each Ypt regulates one transport step in the pathway, however, further research has shown that Ypts coordinate multiple transport steps at particular cellular compartments.

One of the first GTPases to be discovered, Ypt1, is also the first GTPase in the secretory pathway (Segev and Botstein 1987, Segev, Mulholland, and Botstein 1988). In yeast, Ypt1 has been shown to be essential for ER-to-Golgi transport, as well as cis-to-medial Golgi transport (Jedd et al. 1995, Jones et al. 1995). A functionally conserved mammalian homolog has been identified as Rab1, which can replace Ypt1 functionally in yeast (Haubruck et al. 1989). Rab1 has also been shown to have ER-to-Golgi transport functions and localizes to a pre-Golgi intermediate complex in mammalian cells (Plutner et al. 1991, Tisdale et al. 1992, Marie et al. 2009). A later study concluded that Ypt1 plays a role at the late Golgi based on it's co-localization with Sec7, a late Golgi protein, and the cytosolic buildup of Snc1, a plasma membrane SNARE protein, in a Ypt1 mutant cell (Sclafani et al. 2010). Recently, Ypt1 and Rab1 have been implicated in regulation of general autophagy and ER-phagy (Lipatova et al. 2012, Lipatova et al. 2013, Lipatova and Segev 2015, Zoppino et al. 2010, Huang et al. 2011). The studies by Lipatova et al. show that the earlier result of Snc1 accumulation in Ypt1 mutant cells is a defect of ER-phagy and not a defect of secretion or recycling(Lipatova et al. 2013). However, the question still remains why does Ypt1 co-localize with the late Golgi protein, Sec7, without an apparent late Golgi function, which will be addressed in this thesis.

Ypt31/32 is a functionally redundant pair. These GTPases have been identified as regulators of cargo exit from the late Golgi (Jedd, Mulholland, and Segev 1997). More recently, Ypt31/32 has also been identified as a regulator of recycling from the endosome to the late Golgi (Chen et al. 2005, Chen, Shah, and Segev 2011). The closest mammalian homologs, Rab11a and Rab11, are also involved in regulation of post-Golgi transport steps (Ullrich et al. 1996, Takahashi et al. 2012, Welz, Wellbourne-Wood, and Kerkhoff 2014).

Ypt6 is the only non-essential GTPase in the secretory pathway in yeast. The mammalian homolog, Rab6, has a role in Golgi structural organization (Starr et al. 2010, Storrie et al. 2012). The role of Ypt6 has been controversial due to conflicting evidence. Specifically, experimental evidence identifies Ypt6 as a regulator of intra-Golgi traffic and other evidence shows Ypt6 as a regulator of retrograde traffic from late endosomes to the Golgi (Li and Warner 1996, Siniossoglou, Peak-Chew, and Pelham 2000, Luo and Gallwitz 2003).

Sec4 was one of the original GTPases discovered. It has been shown to regulate the Golgi-to-PM step of secretion (Salminen and Novick 1987, Goud et al. 1988, Salminen and Novick 1989). Due to the placement of Sec4 at the end of the transport pathway and lack of association with the Golgi, Sec4 will not be discussed in depth for this thesis. Figure 2.

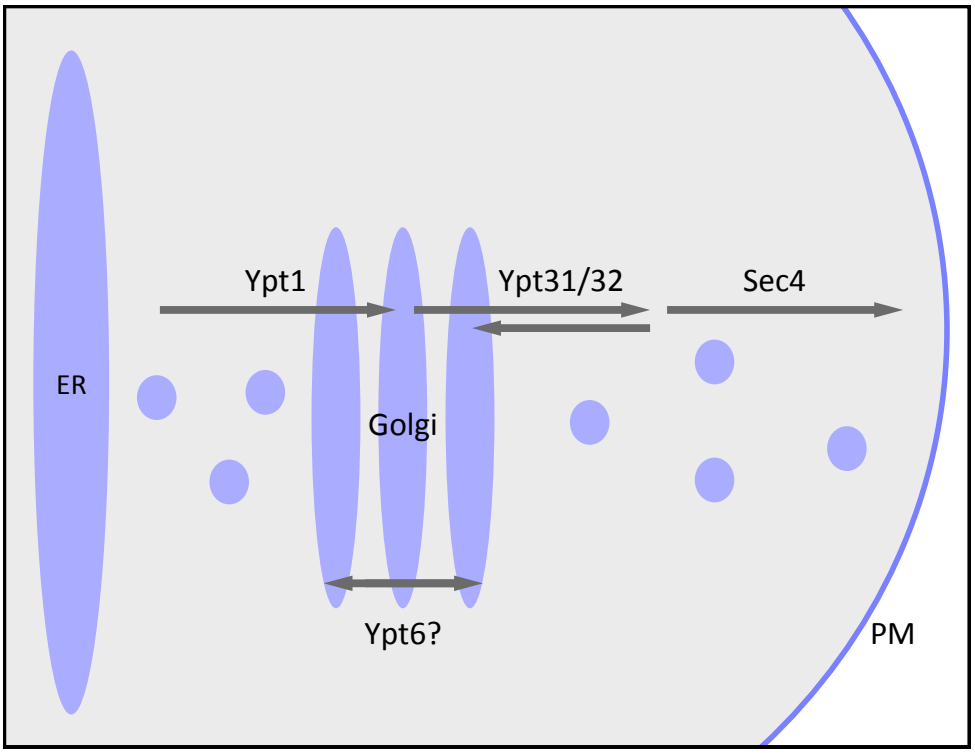


**Figure 2. Five Ypt GTPases regulate the secretory pathway in yeast.** Ypt1, Ypt31/32, Ypt6, Sec4 are placed with arrows that correspond with the transport steps they regulate. Ypt1 regulates ER to early Golgi transport. Ypt31/32 is required for cargo exit from the Golgi and recycling of components from endosomes back to the Golgi. Sec is responsible for the regulation of post-Golgi to PM transport. Ypt6 is placed with a question mark due to conflicting evidence in the field, but regardless has a role in Golgi based transport.

iii. GTPases and coordination

Individual transport steps have been studied in great detail and have led to emerging questions about how multiple transport steps are synchronized to coordinate traffic flow. One method of coordination is by a GTPase cascade, where one GTPase recruits the GEF of the Ypt/Rab that functions after it. A study by the Segev lab determined that there is a genetic interaction between Ypts and Arf GTPase GEFs and proposed that there may be a GTPase cascade to coordinate multiple steps of secretion (Jones et al. 1999). This proposal has led to several studies for various Ypt cascades. The first study found a Ypt32-to-Sec4 cascade, where activated Ypt32 interacts with Sec2, the GEF for Sec4 (Ortiz et al. 2002). This cascade was also observed in the mammalian homologs Rab11-to-Rab8 by Rabin8, the GEF for Rab8 (Knodler et al. 2010). Two other studies examined inactivation cascades where the earlier GTPase is inactivated by the recruitment of the GAP by the later GTPase. These studies found that Ypt32 recruits the GAPs for Ypt1 and Ypt6 (Rivera-Molina and Novick 2009, Suda et al. 2013). In mammalian cells, coordination of Rab5 and Rab7 on maturing endosomes has been visualized. Rab5 is shown to label the early endosome and Rab7 the late endosome. Following one endosome by time-lapse microscopy, the endosome seems to lose all Rab5 and gain Rab7 in a rapid manner (Rink et al. 2005).

Although Ypt32-GAP-Ypt1 cascade has been found, there are reservations about this study (Rivera-Molina and Novick 2009). First, the Ypt32 to Ypt1 cascade shown by time-lapse microscopy was not anchored to the Golgi, where these GTPase are functionally relevant. Secondly, the fluorescently labeled Ypts used in this study were not examined for functionality as a sole copy in the cell. Third, the GAP loss-of-function

mutant used in this study caused higher levels of Golgi proteins co-localization, which points to Golgi compartment disorganization (Rivera-Molina and Novick 2009). Therefore, work performed for this thesis aims to determine the Ypt1 and Ypt31 localization within the Golgi, determine any coordination between Ypt1 and Ypt31, and determine the relationship of these GTPases with Golgi sub-compartments.

## C. TRAPP complex

### i. TRAPP composition

TRAPP was originally identified as a protein complex that mediates ER-to-Golgi traffic (Sacher et al. 2000). The TRAPP complex is comprised of multiple protein subunits, which assemble to become three different TRAPP complexes. The core TRAPP components found in all three complexes consist of the essential Trs23, Trs31, Bet5, and two subunits of Bet3 (Cai et al. 2008). These four core subunits are necessary and sufficient for the GEF activity on Ypt1 (Jones et al. 2000, Wang, Sacher, and Ferro-Novick 2000). Pull-down studies suggest that TRAPPI contains the core TRAPP components with the addition of Trs20 and Trs33 (Kim et al. 2006). However, the roles of Trs20 and Trs33 in TRAPPI have yet to be shown. TRAPPIII contains the core TRAPP complex with the addition of Trs20 and Trs85, which targets the complex to autophagic pathways (Lynch-Day et al. 2010, Lipatova et al. 2012). Trs20 recently was shown to be required for the addition of Trs85 to the complex (Taussig, Lipatova, and Segev 2014). TRAPPII contains all the TRAPPI subunits with the addition of TRAPPII-specific subunits, Trs130, Trs120, and Trs65. Either Trs65 or Trs33 is required for the assembly of TRAPPII *in vivo* (Tokarev et al. 2009). Again, Trs20 was shown to

be required for interaction of TRAPPI with Trs20 to form TRAPPII which will be discussed in Chapter 2 of this thesis (Taussig et al. 2013). The structure of TRAPPII purified from yeast cell lysates was found to exist as a dimer where TRAPPII specific subunits are inserted between two complete TRAPPI complexes. With the deletion of the non-essential Trs65, the dimer was not detected in cell lysates (Yip, Berscheminski, and Walz 2010). The composition and approximate placement of the subunits in the three TRAPP complexes are modeled in Figure 3.

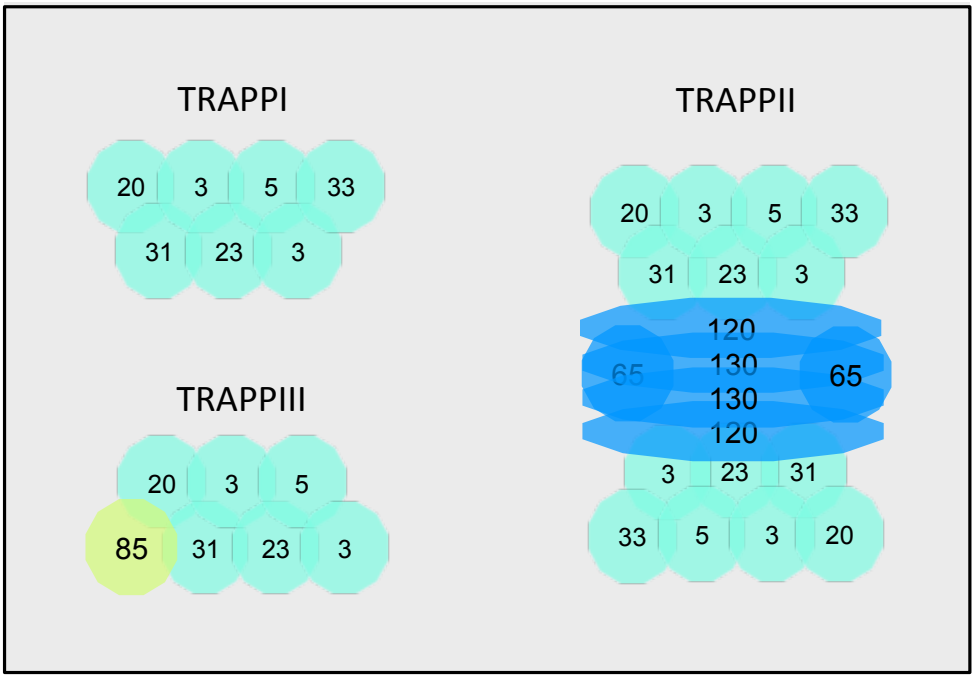


**Figure 3. Yeast TRAPP complexes.** TRAPPI, TRAPPII, and TRAPPIII are depicted here with their general composition. Numbers stand for TrsN, except for Bet3 and Bet5.

ii. TRAPP as a Ypt GEF

The idea that the TRAPP complex acts as a Ypt/Rab GEF is broadly accepted in the field, however, the GEF substrates of the individual TRAPP complexes are still disputed. In vitro studies show that TRAPPI has specific GEF activity for Ypt1 in ER to Golgi transport (Jones et al. 2000, Wang, Sacher, and Ferro-Novick 2000). However, there is a dispute on the specificity of the GEF activity of TRAPPII. Using biochemical and genetic approaches, the addition of TRAPPII specific subunits to TRAPPI was shown to switch GEF activity of TRAPP from Ypt1 to Ypt31/32 (Morozova et al. 2006). Studies from another group dispute this finding and conclude that TRAPPII is a GEF for Ypt1. That conclusion is based on mainly negative results described below. First, purified TRAPPII does not show any GEF activity on Ypt31/32 (Wang and Ferro-Novick 2002). Second, GST-Ypt31 or GST-Ypt32 was unable to pull-down any TRAPPII subunits. In this same study these authors make the argument that the addition of TRAPPII subunits does not change the structural face of GEF-Ypt binding or interaction. They draw the conclusion that TRAPPII must have GEF activity on Ypt1 as does TRAPPI (Yip, Berscheminski, and Walz 2010). The third argument for Ypt1 as the target of TRAPPII GEF activity is due to the placement of Ypt1 at the late Golgi (Sclafani et al. 2010). The views of the Segev lab about these arguments are as follows. The lack of evidence shown by the *in vitro* experiments can be due to the TRAPP complex structural changes during purification. Purification causes oligomerization and changes in complex size, which also affects the surface of the complex that binds the Ypt/Rab (Choi et al. 2011, Brunet et al. 2012, Brunet et al. 2013). Second, GST-Ypt31 and GST-Ypt32 were used for the pull-down studies that did not isolate TRAPPII subunits from

the yeast lysate. As will be discussed in the approach, using tags on Ypts could alter their functionality. Studies done by the Segev lab found that GEF assays could not be performed on GST tagged Ypts, the tag had to be removed by thrombin cleavage prior to the assay (Jones et al. 1995, Jones et al. 2000). Finally, the placement of Ypt1 at the late Golgi will be addressed Chapter 2.

Based on the TRAPP complex GEF activity on Ypt1 and Ypt31/32, this complex is the ideal candidate to coordinate these two GTPases. I propose that conversion of TRAPPI to TRAPPII on the Golgi occurs, potentially in tandem with Golgi cisternal progression, to coordinate their sequential activation (Figure 4). Analysis of TRAPPI complexes in vivo is needed to examine this model. To initiate the study of the TRAPP complex in the Golgi, the localization of TRAPPII will be addressed in Chapter 3.

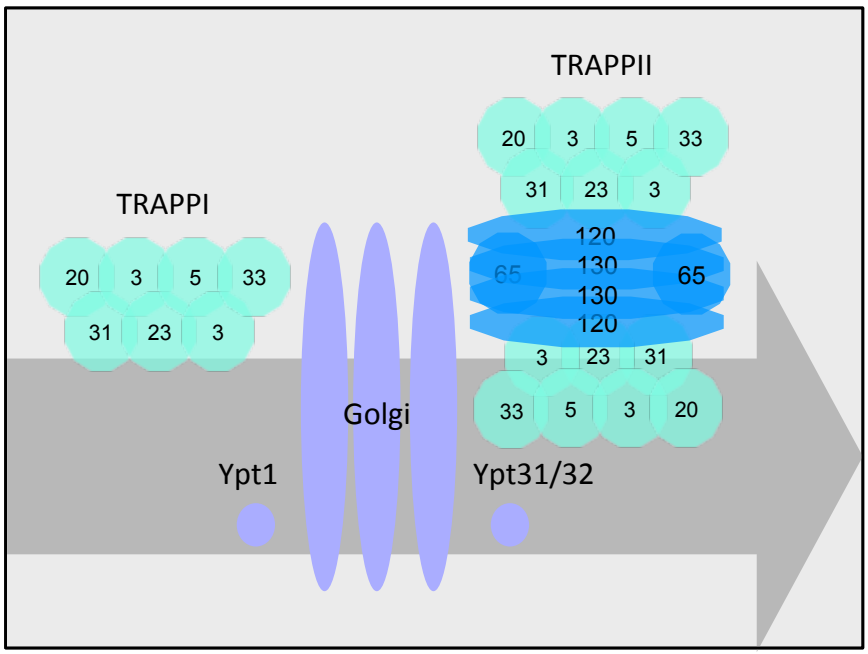


**Figure 4. Golgi TRAPP complexes involved with the secretory pathway.** TRAPPI is accepted as the GEF for Ypt1 for ER-to-Golgi transport. TRAPPII was shown to be the GEF for Ypt31/32, involved in vesicular exit from the late Golgi. However, the GEF activity of TRAPPII is disputed in the field.

## D. Golgi compartmental dynamics

The Golgi is the modification and sorting organelle of the cell (Farquhar and Palade 1981). Once proteins reach the Golgi, they may be modified with oligosaccharides or cleaved to form the mature functional version of the protein. These proteins are then packaged in vesicles and shuttled to their destination (Glick and Nakano 2009). Traditionally, the Golgi has been thought to be a static organelle, with three distinct functional cisternae. Based on the allocation of Golgi enzymes to three cisternae, they were named cis, medial, and trans (Farquhar and Palade 1981, Goldberg and Kornfeld 1983, Nilsson, Au, and Bergeron 2009). The anterograde vesicular transport model describes ER-derived cargo entering the Golgi membrane on the cis-Golgi face, which is then shuttled from one compartment of the Golgi to the next until it exits out of the trans-Golgi. In this model, the Golgi compartments remain static and unchanging (Orci et al. 1997, Orci et al. 2000).

Unfortunately, these three sub-compartments of the Golgi are difficult to visually distinguish in the cell. The mammalian Golgi is formed into parallel stacks with a surrounding tubular network (Rambourg and Clermont 1990). In yeast, the individual Golgi cisternae are spread throughout the cell, allowing for easier visualization of the separate cisternae (Preuss et al. 1992). Using this advantage, two research groups were able to visualize Golgi dynamics in yeast and came to the conclusion that the Golgi is not a static organelle. These groups determined that ER-derived vesicles form the early Golgi compartment, which then matures to the late Golgi, before becoming dispersed to Golgi-derived vesicles (Losev et al. 2006, Matsuura-Tokita et al. 2006). In this model, termed Golgi maturation or cisternal progression, the cargo is not moved

from one compartment to the next. Instead, the enzymes that define the identity of the Golgi cisternae are recycled backwards to allow maturation of the earlier compartment. Not only did these groups find that this process can be visualized by live-cell microscopy, they also showed that the rate of cargo flow through the Golgi agree with the rate of Golgi maturation (Losev et al. 2006, Matsuura-Tokita et al. 2006). Additionally, two groups provide genetic evidence supporting the Golgi cisternal progression model. They conclude that the Arf1 GTPase and Cop1, the coat protein involved with intra-Golgi and retrograde transport, are necessary for proper maturation (Bhave et al. 2014, Papanikou et al. 2015). In this thesis, I aim to show the regulation of Golgi compartmental dynamics by Ypt1 and Ypt31 GTPases.

## E. Approach

To address the Ypt and TRAPP questions underlined in the sections before, I used a combination of approaches. Immunofluorescence, live-cell, and time-lapse microscopy, optimization of fluorescent tags, and BiFC design and optimization will be described in this section.

### i. Immunofluorescence, live-cell, and time-lapse microscopy

Immunofluorescence, IF, and live-cell microscopy has been performed for decades, however, these tools can be modified to answer new questions. In this section, I will describe how these three techniques were used for this thesis.

The benefits of using IF include the ability to visualize endogenous proteins, with no modifications and expression at their native levels. This is very beneficial in systems where small changes in protein levels or functionality alter the cell. In yeast and other

model systems with a cell wall, a drawback of using IF is that it requires the removal of the cell wall and fixation with formaldehyde in order to allow the protein of interest's antibody to enter the cell to bind with its antigen. The process of fixation and cell wall removal may cause cellular damage, which may lead to incorrect experimental interpretation. Furthermore, since the cells are fixed, examination of protein movement and organelle dynamics cannot be done. Live-cell microscopy solves these issues by allowing visualization of fluorescently tagged protein in living cells. With light and confocal microscopy, visualization of yeast proteins can be accomplished efficiently. However, a drawback of using live-cell microscopy is the requirement of fluorescently labeled tags to be fused to the protein(s) of interest in order to visualize *in vivo* expression. Addition of these tags may alter cellular function, discussed below. In Chapter 2, I use both IF and live cell microscopy to determine the accurate localization of Ypt1 and Ypt31 in the Golgi. I also use a novel yeast technique of 3-color IF to visualize three proteins simultaneously in one cell. With this method, I visualized a yEGFP-tagged protein, an mRFP-tagged protein, and either Ypt1 or Ypt31 with its antibody and a secondary antibody with a far-red dye (see methods).

Once live-cell microscopy has been optimized for a set of proteins, fluorescent time-lapse microscopy can be performed. Fluorescence time-lapse microscopy is a powerful tool to study protein dynamics in yeast. Time-lapse microscopy refers obtaining a series of images over a passage of time. Rapid collection of images can be combined to produce a movie to follow proteins by fluorescent dots or puncta. There are experimental limitations that must be surpassed to obtain time-lapse movies (Rines et al. 2011). The major limitation is optimizing conditions while collecting the images.

There is a trade-off between lowering the excitation signal to prevent photo-bleaching, minimizing the signal-to-noise ratio, and lowering the image acquisition time to collect more frames per second.

First, the emission signal must be bright enough to follow the protein over several frames, if not sufficiently bright, higher levels of excitation signal must be used. However, with higher levels of excitation, more photo-bleaching occurs. Fluorophores become quenched, resulting in the signal not being detected after imaging several frames. To keep the signal-to-noise ratio low and prevent photo-bleaching, lower laser intensities can be used to excite the fluorophore. With this approach, more averaging of the image needs to be performed to remove background noise. However, with more averaging of the sample, the acquisition speed decreases and fewer frames are obtained per minute. To get effective time-lapse movies, the above conditions must be determined by trial and error for each protein. Previous studies performed by four research groups have been used as a starting point for the time-lapse analysis performed in Chapter 2 of this thesis (Matsuura-Tokita et al. 2006, Losev et al. 2006, Daboussi, Costaguta, and Payne 2012).

ii. Optimizing fluorescent tags

The first fluorescent protein, FP, observed was the green fluorescent protein, GFP, found in jellyfish (Shimomura, Johnson, and Saiga 1962). To this day, it is still the brightest fluorophore available to use as a tag. However, many alternative FPs are also widely used. The red FPs, mRFP, mCherry, and dsRed are commonly used to examine the possible co-localization of a protein tagged with a red FP to another protein tagged with a green FP. There are also less widely used FPs, such as the yellow, YFP, family

and the cyan, CFP, family of fluorescent proteins. All of these fluorescent proteins are roughly the same size at approximately 25kDa but have different structural characteristics. Novel mutations in FP are continuously being characterized for prevention of dimerization or oligomerization, and allowing for faster folding, brighter and more stable signal (i.e. less quenching).

Studying intracellular signaling and its regulation in yeast has many advantages. The structural morphology of the Golgi has been discussed above. Additionally, the ease of genetic modifications allows for the proteins to be labeled with FP tags quickly and effectively. If a protein loses functionality once tagged, it is much simpler to attempt an alternative tag. This has proven useful when attempting FP tagging on Ypts. Since the function of the GTPase is dependent on its architecture, large bulky tags often lead to a lower or non-functioning protein. Also, the tail of the GTPase is lipidated and inserted into the vesicular membranes, therefore, the C-terminal end cannot be modified. One study demonstrated that mCherry-Ypt1 maintain functionality when expressed in a Ypt1 temperature sensitive mutant strain (Rivera-Molina and Novick 2009). Although mCherry-Ypt1 was able to restore growth at restrictive temperatures when expressed with a temperature-sensitive Ypt1, our research determined that as a sole copy, mCherry-Ypt1 was non-functional, even at permissive temperature (see Chapter 2). To give the FP the best chance at functionality, yeast codon optimized FPs with the yE designation were used for the tagging of Ypt1 and Ypt31 (Sheff and Thorn 2004). Even with the yEFPs, the only tagged Ypt1 that was demonstrated to be functional as a sole copy is yEVenus-Ypt1. For the other proteins tagged with FPs in this study, often several different tags were tested to determine the best signal.

iii. BiFC design and optimization

BiFC, bimolecular fluorescence complementation, is a technique developed by the Kerppola Lab to visualize two proteins with one fluorescent signal (Hu, Grinberg, and Kerppola 2005). This protein complementation assay takes advantage of the property of fluorescent proteins such as YFP and CFP, to be split and expressed as N-terminal and C-terminal peptides. Each peptide by itself does not produce a fluorescent signal, but when in proximity to each other, proper folding occurs and produces a signal. The C-terminal tails of YFP and CFP have the same sequence, therefore the N-terminus determines the color of the fluorophore (Hu, Grinberg, and Kerppola 2005). Thus, the C terminal Y/CFP tagged protein will fluoresce when adjacent to either the N-terminal of YCP or YCP. This technique has been modified for multi-color BiFC experiments where 3 proteins can be viewed by 2 different fluorescent signals (Lipatova et al. 2012).

There are two limitations of the BiFC technique. The first is that the fluorescent protein halves cannot dis-assemble once folded. If the protein interaction or close localization is transitory, BiFC will force the attached proteins to remain together. It is possible to get a positive BiFC interaction without direct protein-protein interactions as proteins halves can reconstitute the fluorophore a distances above 7nm or 70 angstroms (Hu, Grinberg, and Kerppola 2005, Kerppola 2008). Therefore, any conclusions about interactions or complex formation can only be determined by BiFC with proper controls and should also be supported with other methods of detection (Lipatova, Kim, and Segev 2015).

With my help, the Segev lab optimized BiFC plasmids for use in yeast, described in a methods paper for which I am an author (Lipatova, Kim, and Segev 2015). First, the YFP/CFP split fragments were taken from yeast optimized FPs, yEVenus and yECFP. The length of the fragments was also adjusted to allow better assembly of the fluorophore. To allow flexibility to tag the BiFC fragment at either end of the protein of interest, plasmids were designed to allow both C-terminal and N terminal tagging. This allows proteins such as Ypts to be studied using BiFC, because they can only be tagged on their N-terminus (see above). To allow for multiple plasmids to be expressed in yeast, plasmids were also constructed with three different auxotrophic markers, *URA3*, *LEU2*, and *HIS3* (Lipatova, Kim, and Segev 2015). These optimized plasmids were used for the BiFC analysis performed in Chapter 3 as well as other studies performed by the Segev Lab (Lipatova et al. 2013, Taussig et al. 2013).

## F. Significance

As described earlier, Rab GTPases and the TRAPP complex regulate intracellular transport in human cells. These processes are vital for cellular health. Accordingly, it is not surprising that many human diseases have links with intracellular trafficking in general, and in particular with Rabs and the TRAPP complex. This section will highlight Rab1, Rab11, and the mammalian TRAPP, mTRAPP, related disorders. Due to the conservation between yeast and human Ypt/Rabs and TRAPP subunits and their importance for cell survival, it is expected that studies on the regulation of trafficking will be extremely useful for diagnostics and therapeutic targets for the future.

i. Rab1

Rab1 is the human homolog of Ypt1 also implicated in ER-to-Golgi transport. Due to its fundamental role of regulating ER-to-Golgi transport, Rab1 is implicated in many human disorders.

*Cancer*- The term cancer describes any disease where cells divide uncontrollably, by unregulated cell growth. In cancer cells, many genes and proteins are mis-regulated which leads to continuous growth and avoidance of cell death (Hanahan and Weinberg 2000). As GTPases have regulatory roles, it's not surprising to find that Rab expression levels are altered in cancerous cells. Rab1 specifically is overexpressed in various cancer cells (Calvo et al. 2002, Cheng et al. 2004, Shimada et al. 2005). Recently, a group found that Rab1a can act as an oncogene by activating the mTOR complex, which is a growth controller in eukaryotes (Xu et al. 2015, Thomas et al. 2014).

*Parkinson's*- Parkinson's disease is a neurodegenerative condition where mis-folded α-synuclein accumulates to form Lewy bodies (Beitz 2014). The normal function of α-synuclein is not known and neither is it known why an accumulation of this protein leads to such a devastating condition. A study by Cooper et. al, (2006) finds that when α-synuclein is expressed in yeast, ER-to-Golgi transport is blocked. This lethality can be rescued by over-expression of Ypt1. Additionally, elevated Rab1 expression was found to protect dopaminergic neuron loss in animal models of Parkinson's (Cooper et al. 2006). The potential rationale for this finding is that the build-up of α-synuclein causes ER-stress and strain on the ER-phagy pathway found to be regulated by Ypt1 (Lipatova et al. 2013, Lipatova and Segev 2015).

ii. Rab11

*Cancer-* As with Rab1, Rab11 is also shown to be associated with cancer. Unlike with Rab1, Rab11 expression levels are not altered in cancer cells. However, a suggested Rab11 GAP was found to be an oncogene and a Rab11 effector shows patterns of over-expression (Westlake et al. 2007, Zhang et al. 2009, Chung et al. 2014).

*Huntington's-* Huntington's disease is a neurodegenerative disorder caused by a region of the huntingtin gene. This region contains CAG repeats, which code for glutamines in the protein. The CAG repeats 36-120 times in patients with the disorder, compared to 10-35 times in non-affected individuals. More repeats correspond to higher levels of toxicity to neuronal cells (Landles and Bates 2004). Similar to the α-synuclein protein mentioned for Parkinson's disease, the function of the huntingtin protein is still unknown. Rab11 was found to be associated with the huntingtin protein through its GEF (Li et al. 2008). Also, recycling of the glutamate transporter in endosomes by Rab11 is shown to be impaired with a mutant huntingtin protein, and Rab11 over-expression is found to rescue neuronal cell death (Richards et al. 2011). Another study found that Rab11 regulates synaptic vesicle size that reduces defects caused by mutant huntingtin (Giorgini and Steinert 2013).

*Alzheimer's-* As another neurodegenerative disorder, Alzheimer's is described as an accumulation of amyloid precursor protein, APP, cleavage product into extracellular plaques (Hardy 2006). Rab11 was shown to regulate the endosomal recycling of the enzyme responsible for cleavage of APP to affect formation of the disease associated cleavage product (Udayar et al. 2013, Buggia-Prevot et al. 2014).

*Multiple sclerosis*- Also called MS, multiple sclerosis is an autoimmune disease where the immune system damages the myelin coat of nerve cells in the brain and spinal cord (Goldenberg 2012). The cause of MS is not known, but genetics and environmental conditions are thought to contribute to the disease. Mutations in the GAP of Rab11, EVI5, have found to be associated with MS (Dabbeekeh et al. 2007, Hoppenbrouwers et al. 2008).

*Cystic fibrosis*- Cystic fibrosis is an inherited disease caused by a mutation in the CFTR gene. The CFTR gene product is a PM anion channel (Rosenstein and Cutting 1998). Overexpression of Rab11 leads to an increased amount of CFTR at the PM while knockdown by RNAi causes reduced CFTR activity at the plasma membrane (Gentzsch et al. 2004, Silvis et al. 2009).

*Diabetes*- Diabetes is a group of diseases that results in high levels of blood glucose. Although there are several causes of diabetes, the glucose transporter, GLUT4 has been a target of treatment. The transporter functions at the PM and gets recycled to GLUT4 vesicles (Huang and Czech 2007). Rab11, already known to have a role in vesicular recycling, has been shown to be important for proper localization of GLUT4 in the following studies. Rab11 was found with GLUT4 in subcellular fractionation assays from rat cardiac muscle cells (Kessler et al. 2000). Overexpression or knockdown of Rab11 has shown changes in GLUT4 localization to either the GLUT4 vesicles or plasma membrane, respectively (Zeigerer et al. 2002, Schwenk, Luiken, and Eckel 2007).

iii. mTRAPP

Mutations in TRAPP subunits have been implicated in many human diseases (Brunet and Sacher 2014, Kim, Lipatova, and Segev 2016). The subunits of the yeast TRAPP complexes were described above and all have human homologs. However, there are mTRAPP subunits in humans with no yeast homolog. For this thesis, each mTRAPP subunit is not described in depth, but is mentioned for the disorder with which they are associated. mTRAPP subunits are named TrappCN with N ranging from 1 to 12 (Brunet and Sacher 2014).

*Spondyloepiphyseal dysplasia tarda, SEDT*- Four mutations in TrappC2, also called SEDL/Sedlin and homolog to yeast Trs20, cause an X-linked recessive disorder, SEDT. This disorder is characterized by skeletal tissue abnormalities, with early onset osteoarthritis. Very little is known about the cellular function of TrappC2, but analysis has revealed that the mutations disrupt proper protein folding, interactions, and TRAPP complex integrity. A more recent study determined that collagen secretion was inhibited in TrappC2 depleted cells (Venditti et al. 2012). One of the four mutations, D47Y, is a substitution of an amino acid that will be discussed in Chapter 3.

*Cancer*- As with Rab1 and Rab11, mTRAPP is also implicated in cancer. TrappC4 has been linked with tumorigenesis in colorectal cancer through interaction with the ERK2 MAP kinase in it's signaling pathway. Overexpression of TRAPPC4 increased cell growth and viability. Depletion of TrappC4 caused cell growth suppression and apoptosis (Zhao et al. 2011). TrappC9 has also been reported to meditate tumorigenesis of cancer cells through interaction with the transcriptional factor

Nuclear Factor kappa B. This transcriptional factor is found to have elevated activity in many types of human cancer (Zhang et al. 2015).

*Alzheimer's*- Discussed earlier, Rab11 is implicated with Alzheimer's disease. Reports found that TRAPPC6 is also associated in this disease (Hamilton et al. 2011, Chang et al. 2015). An isoform of TrappC6 contains an internal deletion of 14 amino acids. This specific isoform is found with Alzheimer's patients and becomes aggregated, leading to aggregation of Alzheimer's disease specific proteins or peptides (Chang et al. 2015).

Other newly added TRAPP related-disorders include a prospective link for miscarriage and the levels of TrappC2 (Wen et al. 2015). Also, there is a possible connection between TrappC9 mutations and neurological disorders such as autism and schizophrenia (Khattak and Mir 2014, McCarthy et al. 2014).

## CHAPTER 2. REGULATION OF GOLGI CISTERNAL PROGRESSION BY YPT/RAB GTPASES

The data presented in this chapter is taken verbatim from a publication where I am the first author (Kim et al. 2016). I produced all figures in this chapter with the following exceptions:

Figure 6

A-C: Zhanna Lipatova

Figure 11

A-B: Uddalak Majumdar

Figure 12

A-B: Uddalak Majumdar

## A. Abstract

Current models entail that transport through the Golgi — the main sorting compartment of the cell — occurs via cisternal progression/maturation, and that Ypt/Rab GTPases regulate this process. However, there is very limited evidence that cisternal progression is regulated, and no evidence for involvement of Ypt/Rab GTPases in such a regulation. Moreover, controversy about the placement of two of the founding members of the Ypt/Rab family, Ypt1 and Ypt31, to specific Golgi cisternae interferes with addressing this question in yeast, where cisternal progression has been extensively studied. Here, we establish the localization of Ypt1 and Ypt31 to opposite faces of the Golgi, early and late, respectively. Moreover, we show that they partially overlap on a transitional compartment. Finally, we determine that changes in Ypt1 and Ypt31 activity affect Golgi cisternal progression, early-to-transitional and transitional-to-late, respectively. These results show that Ypt/Rab GTPases regulate two separate steps of Golgi cisternal progression.

## B. Introduction

In the exocytic pathway, cargo is transported from the endoplasmic reticulum (ER), through the Golgi, to the plasma membrane (PM), whereas in the endocytic pathway, cargo is transported from the PM through endosomes to the lysosome, a major degradative compartment. The Golgi is the major sorting compartment of the cell. At its entry side, cis, cargo from the ER is sorted for forward and retrograde transport. At its exit side, trans, cargo is sorted for secretion to the PM or for delivery to endosomal compartments. Traditionally, the Golgi is considered to have three-stacked functional cisternae, cis, medial and trans, and two networks on each side (Shorter and Warren 2002). While a number of models exist regarding transport through the Golgi, the current view is that Golgi cisternae are transient, and forward transport probably occurs through cisternal progression/maturation (Glick and Luini 2011). The question is what regulates Golgi cisternal progression?

In budding yeast, the Golgi cisternae are not stacked but dispersed, which provides a convenient model system for studying cisternal maturation (Suda and Nakano 2012). Markers are established for the early (cis) and late (trans) compartments of the yeast Golgi, whereas the nature of the intermediate compartment is not clear (Papanikou and Glick 2014). Here, we propose that the intermediate Golgi cisterna is a transitional compartment on which early and late Golgi markers coincide.

Evidence for Golgi cisternal progression comes mostly from yeast and is based on observing dynamic switching of early and late Golgi markers on individual cisternae using time-lapse live-cell microscopy (Losev et al. 2006, Matsuura-Tokita et al. 2006). However, information about the mechanisms and regulation of Golgi cisternal

progression is very scarce. Recently, a role for Arf1 GTPase, a component of COPI vesicles, was proposed in early-to-late Golgi transition, based on slower Golgi maturation in *arf1*Δ mutant cells (Bhave et al. 2014). While Ypt/Rab GTPases were proposed to play a role in this process (Glick and Luini 2011, Suda and Nakano 2012), there is currently no experimental data supporting this idea. Here, we provide evidence that Ypt/Rabs regulate Golgi cisternal progression.

The conserved Ypt/Rab GTPases regulate all vesicle-mediated transport steps of the exocytic (secretory) and endocytic pathways. These GTPases are stimulated by nucleotide exchangers termed GEFs and, when in the GTP-bound form, interact with their multiple downstream effectors. These effectors then mediate the multiple steps of vesicular transport, from vesicle formation and motility to their tethering and fusion with the acceptor compartment (Segev 2001a). Recently, Ypt/Rab GTPases have also emerged as candidates for coordination of intra-cellular transport steps, with Ypt/Rab cascades or conversion as an example of coordination that drive compartment maturation (Segev 2011). An open question in the field is the nature of Ypt/Rab specificity: Are they specific to a particular transport pathway and/or a cellular organelle?

Our previous work has established that in budding yeast, two Ypts regulate Golgi entry and exit: Ypt1 regulates ER-to-cis Golgi transport and the functional pair Ypt31/Ypt32 regulates trans Golgi-to-PM transport (Jedd, Mulholland, and Segev 1997, Jedd et al. 1995, Segev 1991). The human functional homolog of Ypt1, Rab1, also regulates ER-to-Golgi transport (Haubruck et al. 1989, Pind et al. 1994).

While Ypt/Rab GTPases are considered to be specific to cellular compartments (Pfeffer 2005, Pfeffer 2013, Zerial and McBride 2001), currently there is controversy about the localization and function of Ypt1 and Ypt31/32 and their GEFs, the TRAPP complexes. Based on our cumulative data, we proposed that TRAPP I acts as the GEF for Ypt1 to regulate ER-to-Golgi traffic and TRAPP II stimulates Ypt31/32 to mediate traffic at the trans Golgi (Lipatova et al. 2015). However, based on ~60% co-localization of mCherry-tagged Ypt1 with Sec7, which is considered a late-Golgi marker (Sclafani et al. 2010, Suda et al. 2013), assignment of a role for Ypt1 in late Golgi (Sclafani et al. 2010), and different specificity of GEF activity assays (Cai et al. 2008), a different view exists in the field. This view entails that both TRAPP I and TRAPP II complexes act as Ypt1 GEFs and Ypt1 acts throughout the Golgi (Barrowman et al. 2010). We have recently shown that Ypt1 does not function at the late Golgi (Lipatova et al. 2013), and here we address its Golgi distribution compared to that of Ypt31/32. The uncertainty about the placement of Ypt1 and Ypt31 to specific Golgi cisternae hampered the ability to determine their possible role in cisternal progression in yeast, where cisternal progression was extensively studied (Suda and Nakano 2012).

Here, we define a set of markers for the early and late Golgi cisternae, determine their co-localization with the Ypts, and test the effect of altering the level and/or activity of the Ypts on the co-localization of the Golgi markers with each other. Our localization analysis provides evidence that Ypt1 and Ypt31 exhibit inverse polarization on the Golgi and overlap on a transitional compartment supporting the Ypt/Rab compartment specificity idea. The activity alteration analysis provides evidence for a role of Ypt/Rab GTPases in Golgi cisternal progression.

## C. Results

### i) Establishing marker pairs for early and late Golgi cisternae

To determine the distribution of Ypt1 and Ypt31 on the Golgi, we first established a set of four markers; we used two markers for each side of the Golgi: a vesicle coat subunit and an integral-membrane or membrane-associated protein. For the early Golgi, we used Cop1, a subunit of the COPI vesicle coat that mediates retrograde Golgi to ER transport, and Vrg4, an integral membrane GDP-mannose transporter with a role in glycosylation. Fluorescently tagged Cop1 and Vrg4 were used previously as markers for early Golgi (Huh et al. 2003, Losev et al. 2006). For the late Golgi we used Sec7, a membrane-associated Arf GEF, and Chc1, the heavy chain subunit of the clathrin vesicle coat. Fluorescently tagged Sec7 and Chc1 were previously used as markers for the late Golgi (Huh et al. 2003, Losev et al. 2006, Matsuura-Tokita et al. 2006).

When tagged with GFP, there are twice more puncta per cell for vesicle-coat subunits, Cop1 and Chc1 (~15), than for Golgi membrane proteins, Vrg4 and Sec7 (~7-8)(Figure 5A and B). This supports the idea that vesicle-coat proteins exist both on the Golgi and on vesicles, and agrees with the estimate of 6-10 early and late Golgi cisternae (Papanikou and Glick 2009).

The four Golgi markers were tagged at their C-termini with GFP or RFP and their co-localization with each other in different combinations was determined by live-cell confocal microscopy (Figure 5). As expected, the two early Golgi markers, Cop1 and Vrg4, exhibited 90% co-localization, and the two late Golgi markers, Sec7 and Chc1, showed >80% co-localization. The co-localization of early and late markers was ~10-

15% (Figure5G). We propose that the co-localization of early and late Golgi markers reflects their transient overlap on a transitional cisterna as discussed below.

**ii) Polarized localization of Ypt1 and Ypt31 to early and late Golgi, respectively**

To compare the distribution of Ypt1 and Ypt31 on the Golgi cisternae, we used live-cell and immuno-fluorescence (IF) microscopy. For live-cell microscopy, the two Ypts were tagged with a fluorescent moiety at their N, but not C-termini, because the latter has to be lipidated for membrane attachment and functionality (Segev 2001b). For this analysis, we wished to use tagged versions of Ypt1 and Ypt31 expressed from a *CEN* plasmid under their own promoter and terminator, which are capable of functioning as a sole copy. To determine functionality, the ability of a tagged Ypt expressed from a plasmid to support the growth of cells deleted for their endogenous Ypt, and carrying a *URA3* plasmid for expression of untagged Ypt1, was tested using the 5FOA assay. For Ypt1, we tested two versions: mCherry-Ypt1, whose localization was reported by Sclafani et al. (Sclafani et al. 2010) and Ypt1 tagged with yeast codon-optimized enhanced Venus (yEVenus), yEVenus-Ypt1. Both versions show clear fluorescent puncta when expressed in cells that also express endogenous Ypt1 (Figure 6A). However, the functionality assay showed that whereas yEVenus-Ypt1 could support cell growth as a sole Ypt1 copy, mCherry-Ypt1 could not do that (Figure 6B). Ypt31 tagged with yeast codon-optimized enhanced GFP (yEGFP), yEGFP-Ypt31, could function as a sole Ypt31/32 copy in cells deleted for both Ypt31 and Ypt32 (Figure 6C).

**A.**

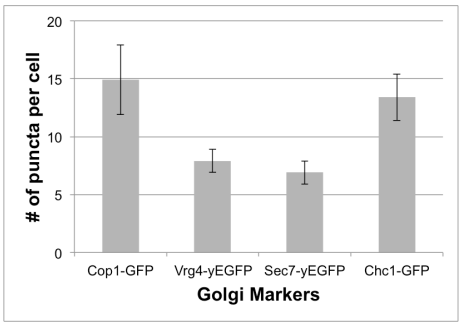


**B.**

| Puncta per cell | # of cells (n) | **average # of puncta** | std dev |
|---|---|---|---|
| Cop1-GFP | 10 | **14.9** | 3 |
| Vrg4-yEGFP | 10 | **7.9** | 1 |
| Sec7-yEGFP | 10 | **6.9** | 1 |
| Chc1-GFP | 10 | **13.4** | 2 |

**C.**

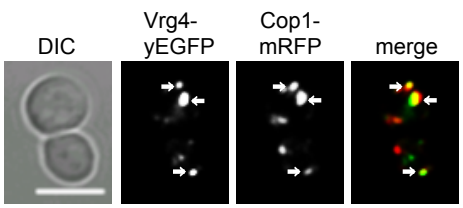


**D.**

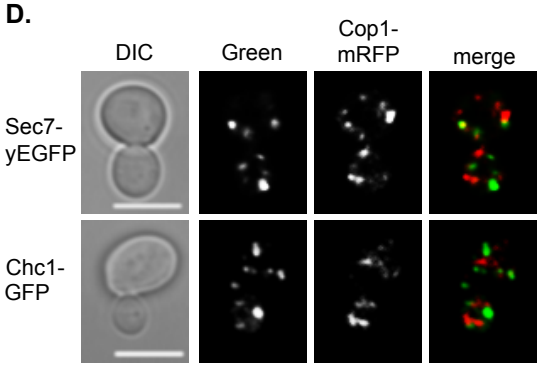


**E.**

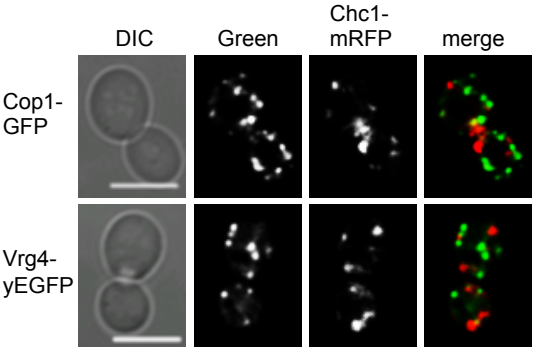


**F.**

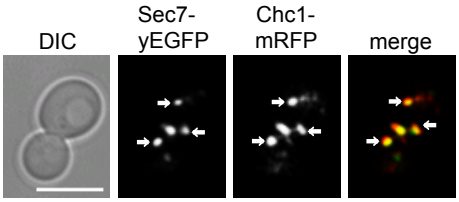


**G.**

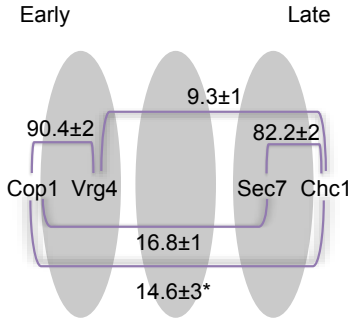


**H.**

| Red marker | Green Marker | # of cells (n) | **co-localization (%) of green** | std dev | # green puncta/slice | # co-localized puncta/slice |
|---|---|---|---|---|---|---|
| Cop1-mRFP | Vrg4-yEGFP | 30 | **90.4** | 2 | 4.3 | 3.8 |
| | Sec7-yEGFP | 40 | **16.8** | 1 | 4.4 | 0.8 |
| | Chc1-GFP | 24 | **16.8*** | 1 | 4.8 | 0.8 |
| Chc1-mRFP | Cop1-GFP | 20 | **12.3*** | 1 | 7 | 0.9 |
| | Vrg4-yEGFP | 30 | **9.3** | 1 | 4 | 0.4 |
| | Sec7-yEGFP | 40 | **82.2** | 2 | 4 | 3.3 |

**Figure 5. Co-localization pattern of early and late Golgi markers.** Four Golgi markers were tagged with GFP or RFP at their C-termini at their endogenous loci and visualized using live-cell confocal microscopy. **A**. Bar graph showing the number of GFP-tagged Golgi markers per cell. There are more puncta of vesicle subunit proteins (14-15) than Golgi membrane proteins (7-8) even though they are tagged with GFP and yEGFP, respectively. **B.** Table showing quantification from two independent experiments used for panel A. **C-H:** Co-localization of marker pairs was determined as follows: **C.** Early Golgi markers Cop1-mRFP with Vrg4-yEGFP; **D**. Early Golgi marker Cop1-mRFP with late Golgi markers Sec7-yEGFP or Chc1-GFP; **E**. Late Golgi marker Chc1-mRFP with early Golgi markers Vrg4-yEGFP and Cop1-GFP; and **F**. Late Golgi markers Sec7-yEGFP and Chc1-mRFP. C-F, Shown from left to right: DIC, GFP, RFP, merge (yellow). White arrows point to co-localized signal. Bar, 5 μm. **G.** Diagram showing the relative distribution of Golgi markers used here. Whereas the ~90% of the two early markers and ~80% of the late markers co-localize with each other, early and late markers exhibit only 10-15% co-localization. **H.** Table showing quantification from two independent experiments for panels C-F, bolded numbers were used for the diagram in panel G (asterisk in G is an average of values marked by asterisks in H. Error bars and +/- represent STDEV.

**A.**

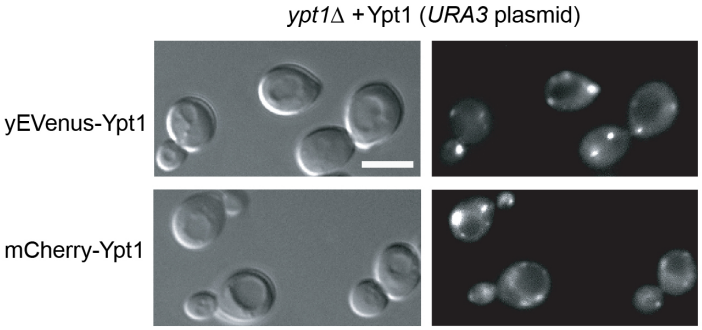


**B.**

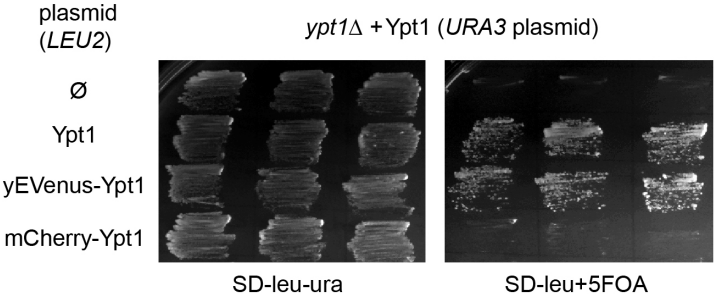


**C.**

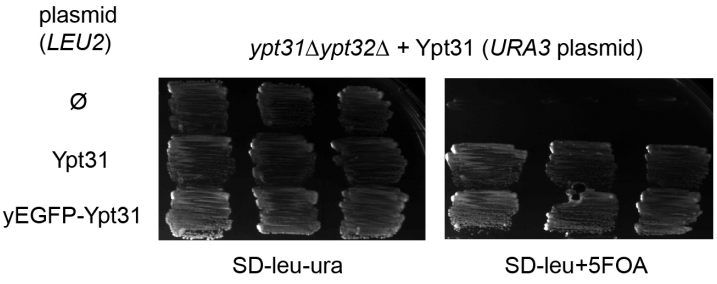


**D.**

| **Puncta per cell** | # of cells (n) | **# of puncta average** | std dev |
|---|---|---|---|
| yEVenus-Ypt1 | 10 | **10.3** | 2 |
| *yEGFP-YPT31 /ypt32Δ* | 10 | **11.5** | 2 |

**Figure 6. Functionality of fluorescently tagged Ypt1 and Ypt31. A.** Both yEVenus-Ypt1 and mCherry-Ypt1 show punctate fluorescence signal. Cells expressing the fluorescently tagged Ypt1 proteins from a *CEN* plasmid were visualized by live-cell microscopy. Shown are: DIC (left) and yEVenus-Ypt1 or mCherry-Ypt1 (right). Bar 5 mm. **B.** yEVenus-Ypt1, but not mCherry-Ypt1, is functional as a sole copy. Cells carrying *ypt1*Δ on the chromosome and expressing *YPT1* from a *CEN URA3* plasmid were transformed with a *CEN LEU2* plasmid expressing Ypt1 from it own promoter and terminator (from top to bottom): Ø (empty vector control), Ypt1, yEVenus-Ypt1 (Ypt1 tagged at its N-terminus with yeast-codon-optimized enhanced Venus), or mCherry-Ypt1. Growth of transformants is shown on SD-Ura-Leu (left), and the ability of cells to lose the *URA3* plasmid is shown on SD-Leu+5FOA (right). Whereas Ypt1 and yEVenus-Ypt1 are functional, mCherry-Ypt1 is not. **C.** yEGFP-Ypt31 is functional as a sole copy. Cells carrying *ypt31*Δ *ypt32*Δ on the chromosome and expressing *YPT31* from a *CEN URA3* plasmid were transformed with a *CEN LEU2* plasmid expressing Ypt31 from its own promoter and terminator (from top to bottom): Ø (empty vector control), Ypt31, yEGFP-Ypt31 (Ypt31 tagged at its N-terminus with yeast-codon-optimized enhanced GFP). Growth of transformants is shown on SD-Ura-Leu (left), and the ability to lose the *URA3* plasmid is shown on SD-Leu+5FOA (right). Both Ypt31 and yEGFP-Ypt31 can support cell growth. Results shown in this figure represent at least two independent experiments. **D.** Table shows quantifications from two independent experiments of total number of puncta of Ypt1 and Ypt31 per cell by live-cell microscopy.

The co-localization of yEVenus-Ypt1 with red Golgi cisternal markers, Cop1-mRFP, Sec7-mCherry, and Chc1-mRFP, was determined using live-cell microscopy (Vrg4 tagged with a red fluorescent moiety was too dim for this analysis). The highest co-localization of the yVenus-Ypt1 was with the early Golgi Cop1 (>85%), ~60% co-localized with Sec7, and <15% co-localized with the late Golgi marker Chc1 (Figure 7A and 7C). IF microscopy showed a similar distribution pattern, with the highest co-localization of Ypt1 with the early Golgi markers Cop1 and Vrg4 (~70 and 60%, respectively), ~40% with Sec7 and <15% with Chc1 (Figure 7B and 7C). While the polarized localization of the Ypt1 to the early Golgi is similar in both the live-cell and IF microscopy, the levels of co-localization are higher in the live-cell microscopy (also true for Ypt31, see below). We interpret this phenomenon to be the result of higher levels of Ypts expressed from a plasmid than their endogenous level (see below).

The co-localization of Ypt1 with Sec7 was previously taken as evidence for the presence of Ypt1 on late Golgi (Sclafani et al. 2010). To better understand this observation, the co-localization of Ypt1 with Sec7 was further analyzed using three-color IF microscopy using anti-Ypt1 antibody and Sec7-yEGFP, with the third color being mRFP-tagged Cop1 or Chc1 (Figure 8A-B). The pairwise co-localization patterns in the triple-color analyses were similar to those observed in the double-color analyses, albeit with lower levels: ~55% of the Ypt1 puncta co-localize with Cop1, ~25% with Sec7 and 12% with Chc1 (Figure 8C). Therefore, the triple-color IF corroborates the double-color IF observation that Ypt1 co-localizes best with the early Golgi marker Cop1, less with Sec7, and very little with Chc1. Similarly, the triple-color IF corroborates the double-color IF observation that Sec7 co-localizes mostly with Chc1, less with Ypt1, and

very little with Cop1 (Figure 8D). Analyses of triple-color IF indicate that the Ypt1-Sec7 puncta also contain Cop1 and/or Chc1 (Figure 8E). Even though only a small fraction of Sec7 co-localizes with Cop1 (~15%), Ypt1 completely overlaps with this compartment. Similarly, even though only a small fraction of Ypt1 co-localizes with Chc1 (~15%), Sec7 completely overlaps with this compartment (Figure 8F). Thus, we propose that the co-localization of Ypt1 with Sec7 represents localization of Ypt1 to a transitional compartment marked by Sec7, Cop1 and/or Chc1, and not to late Golgi marked only by Sec7 and Chc1.

The co-localization of Ypt31 with Golgi cisternal markers was also determined using live-cell and IF microscopy. In live-cell microscopy analysis, yEGFP-Ypt31, expressed from a *CEN* plasmid, showed >90 and >75% co-localization with the late Golgi markers Sec7 and Chc1, respectively, and <15% co-localization with the early Golgi marker Cop1 (Figure 9A and 9C). The IF microcopy showed a co-localization pattern similar to that of the live-cell microscopy, with lower numbers: ~60% with the late Golgi markers Sec7 and Chc1, 25% with Vrg4 and <5% with Cop1 (Figure 9B and 9C).

Together, this localization analysis establishes that Ypt1 and Ypt31 are polarized to opposite sides of the Golgi, early and late, respectively (Figure 10A).

**A.**

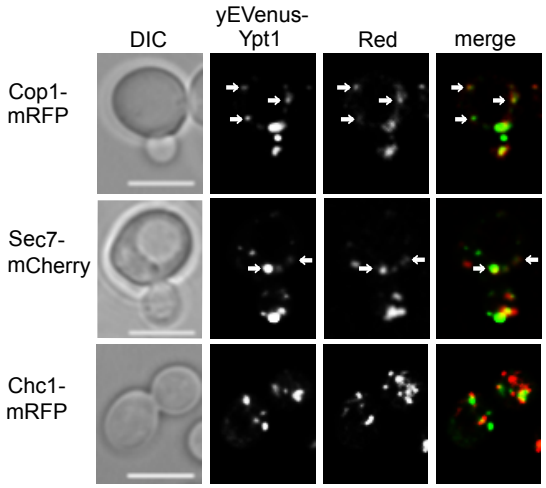


**B.**

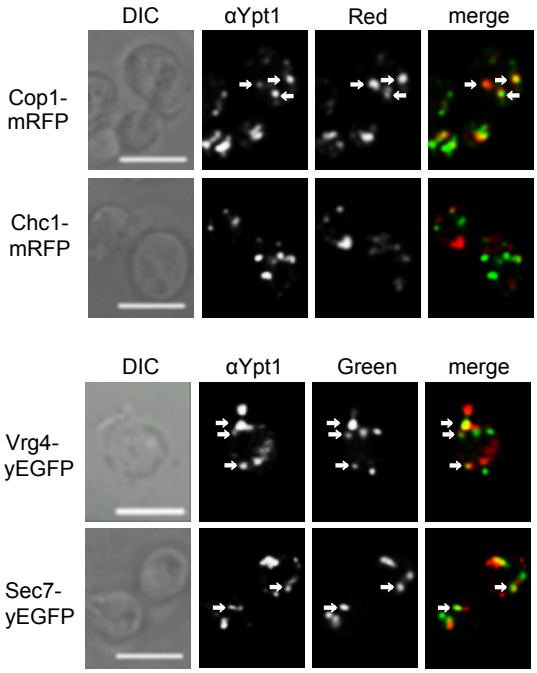


**C.**

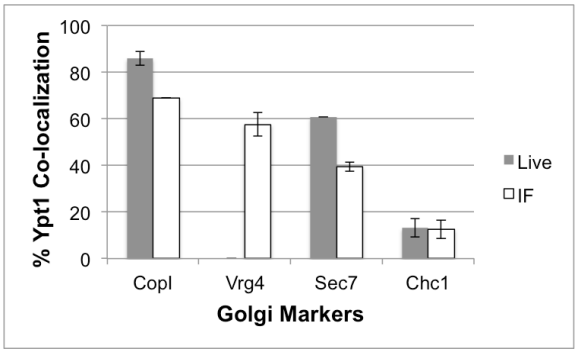


**D.**

| Ypt1 | Golgi Marker | # of cells (n) | **co-localization (%) of Ypt1** | std dev | # Ypt1 puncta/slice | # co-localized puncta/slice | co-localization (%) of green | std dev | # green puncta/slice |
|---|---|---|---|---|---|---|---|---|---|
| yEVenus-Ypt1 (plasmid) | Cop1-mRFP | 50 | **86** | 3 | 3.4 | 2.8 | n/a | n/a | n/a |
| | Sec7-mCherry | 20 | **60.8** | 0 | 3.3 | 2 | n/a | n/a | n/a |
| | Chc1-mRFP | 50 | **13.2** | 4 | 3.6 | 0.5 | n/a | n/a | n/a |
| α-Ypt1 (endogenous) | Cop1-mRFP | 40 | **69** | 0 | 5.3 | 3.6 | n/a | n/a | n/a |
| | Vrg4-yEGFP | 24 | **57.6** | 5 | 5.1 | 2.9 | 66.6 | 3 | 4.4 |
| | Sec7-yEGFP | 49 | **39.5** | 2 | 6.3 | 2.3 | 58.2 | 4 | 4 |
| | Chc1-mRFP | 40 | **12.6** | 4 | 5.6 | 0.7 | n/a | n/a | n/a |

**Figure 7. Polarized distribution of Ypt1 from early to late Golgi. A.** Co-localization of Ypt1 using live cell microscopy. Cells expressing a Golgi marker tagged with red fluorescence were transformed with a *CEN* plasmid for expression of yEVenus-Ypt1. Co-localization was determined using live-cell confocal microscopy. The Golgi markers shown from top to bottom: Cop1-mRFP, Sec7-mCherry and Chc1-mRFP. Shown from left to right: DIC, Ypt1 (green), Golgi marker (red) and merge (yellow). **B.** Co-localization of Ypt1 using IF microscopy. Cells expressing fluorescently tagged Golgi markers were processed for IF analysis using anti-Ypt1 antibodies. The secondary antibody was conjugated with green (FITC) or red (Texas Red) fluorescent dye depending on the tag of the Golgi marker. Co-localization was determined using confocal microscopy. Shown from left to right: DIC, Ypt1, Golgi marker and merge (yellow). Top panels: Red Golgi markers Cop1-mRFP and Chc1-mRFP. Bottom panels: Green Golgi markers Vrg4-yEGFP and Sec7-yEGFP. For panels A-B: White arrows point to co-localized signals; Bar, 5 μm. **C.** Bar graph summarizing the quantification of Ypt1 co-localization with the different Golgi markers using live-cell (panel A, grey bars) and IF (panel B, white bars) microscopy. Left to right: Ypt1 co-localize with decreasing frequencies with Cop1, Vrg4, Sec7 and Chc1. **D.** Table shows quantification from two independent experiments of panels A-B; bolded numbers were used for graph in panel C. Error bars represent STDEV.

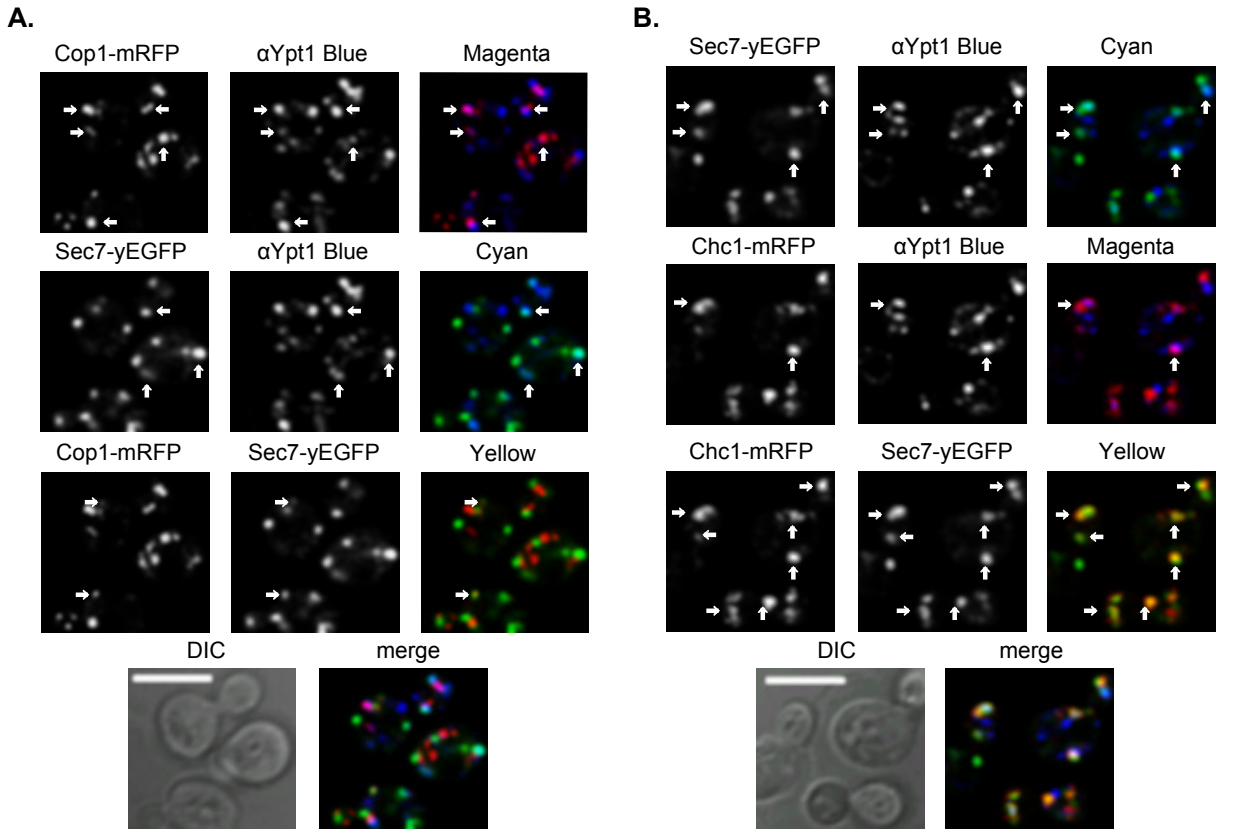
A.
Cop1-mRFP
αYpt1 Blue
Magenta
Sec7-yEGFP
αYpt1 Blue
Cyan
Cop1-mRFP
Sec7-yEGFP
Yellow
DIC
merge
B.
Sec7-yEGFP
αYpt1 Blue
Cyan
Chc1-mRFP
αYpt1 Blue
Magenta
Chc1-mRFP
Sec7-yEGFP
Yellow
DIC
merge

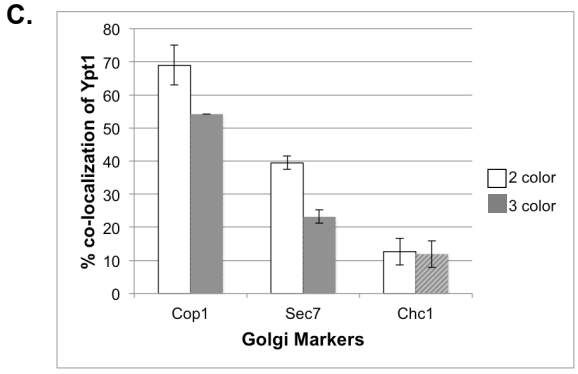
C.
% co-localization of Ypt1
80
70
60
50
40
30
20
10
0
Cop1
Sec7
Chc1
Golgi Markers
2 color
3 color

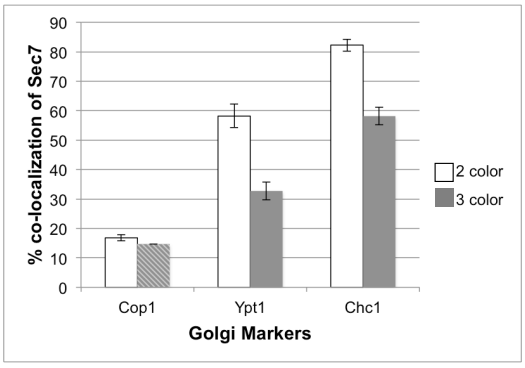
D.
% co-localization of Sec7
90
80
70
60
50
40
30
20
10
0
Cop1
Ypt1
Chc1
Golgi Markers
2 color
3 color

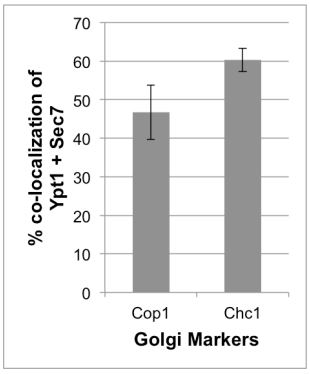
E.
% co-localization of Ypt1 + Sec7
70
60
50
40
30
20
10
0
Cop1
Chc1
Golgi Markers

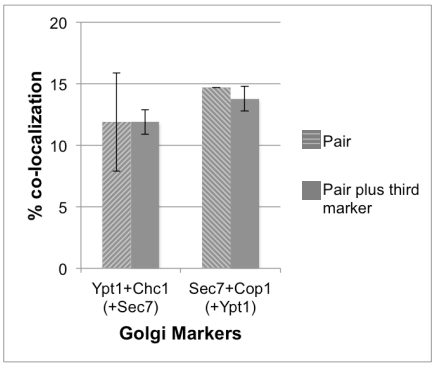
F.
% co-localization
20
15
10
5
0
Ypt1+Chc1
(+Sec7)
Sec7+Cop1
(+Ypt1)
Golgi Markers
Pair
Pair plus third marker

**Figure 8. Distribution of Ypt1 on the Golgi using three-color IF microscopy.** **A.** Three-color fluorescence microscopy of Sec7, Ypt1 and Cop1. IF microscopy was performed with cells expressing Sec7-yEGFP and Cop1-mRFP, using anti-Ypt1 antibodies (secondary antibodies conjugated with α-Alexa-fluor 647, false colored blue). **B.** Three-color fluorescence microscopy of Sec7, Ypt1 and Chc1. IF microscopy was preformed with cells expressing Sec7-yEGFP and Chc1-mRFP, using anti-Ypt1 antibodies (secondary antibodies conjugated with α-Alexa-fluor 647, false colored blue). A-B, shown from top to bottom: 3 pairwise co-localizations (single colors, and 2-color merge: magenta for red and blue; cyan for green and blue; yellow for red and green), DIC and 3-color merge (white). White arrows point to co-localized signal in the 2-color merge; bar, 5μm. **C.** Ypt1 co-localizes mostly with Cop1. Pairwise co-localization of Ypt1 (%) with the Golgi markers is compared between two-color (from Figure 2, white bars) and three-color (this figure, grey bars) IF analyses. The two analyses show similar co-localization patterns. **D.** Increasing co-localization levels of Sec7 with Cop1, Ypt1 and Chc1. Pairwise co-localization of Sec7 (%) with the Cop1, Ypt1 and Chc1 is compared between two-color (from Figure 5 and Figure 7, white bars) and three-color (from this figure, grey bars) microscopy analyses. The two analyses show similar co-localization patterns. **E.** Ypt1-Sec7 puncta co-localize with Cop1 or Chc1. Three-color analysis shows that 47 and 60% of the Ypt1-Sec7 puncta also contain Cop1 and Chc1, respectively. **F.** Ypt1-Sec7: The slight co-localization of Sec7 with Cop1 and Ypt1 with Chc1 (~15%, striped bars in panels C and D, respectively) fully overlaps the other protein, Ypt1 and Sec7, respectively. Three-color analyses of Sec7-Cop1 with Ypt1 and Ypt1-Chc1 with Sec7 were performed. White bars show pairwise co-localization and grey bars show triple co-localization with the third marker: Ypt1 (left) and Sec7 (right). Error bars represent STDEV. Quantifications from two independent experiments are detailed in Table 1.

**Table I. Distribution of Ypt1 on the Golgi using three-color IF microscopy (related to Figure 8).**

| | | | | | | | | |
|---|---|---|---|---|---|---|---|---|
| Cop1-mRFP Sec7-yEGFP α-Ypt1 | # of cells (n) | co-localization (%) of Sec7 with Ypt1 | std dev | # Sec7 puncta/slice | # co-localized puncta/slice | co-localization (%) of Ypt1 with Sec7 | std dev | # Ypt1 puncta/slice |
| | 24 | 33.1 | 3 | 5 | 1.5 | 23.4 | 2 | 6.6 |
| | | co-localization (%) of Sec7 with Cop1 | std dev | # co-localized puncta/slice | | co-localization (%) of Ypt1 with Cop1 | std dev | # co-localized puncta/slice |
| | | 14.7 | 0 | 0.7 | | 54.2 | 6 | 3.4 |
| co-localization of three markers | # of cells (n) | co-localization (%) of Ypt1+Sec7 with Cop1 | std dev | | # of cells (n) | co-localization (%) of Cop1+Sec7 with Ypt1 | std dev | |
| | 20 | 46.7 | 7 | | 14 | 93.8 | 9 | |
| Chc1-mRFP Sec7-yEGFP α-Ypt1 | # of cells (n) | co-localization (%) of Sec7 with Ypt1 | std dev | # Sec7 puncta/slice | # co-localized puncta/slice | co-localization (%) of Ypt1 with Sec7 | std dev | # Ypt1 puncta/slice |
| | 24 | 32.3 | 1 | 4.5 | 1.4 | 23 | 2 | 6.3 |
| | | co-localization (%) of Sec7 with Chc1 | std dev | # co-localized puncta/slice | | co-localization (%) of Ypt1 with Chc1 | std dev | # co-localized puncta/slice |
| | | 58.2 | 3 | 2.6 | | 11.9 | 4 | 0.66 |
| co-localization of three markers | # of cells (n) | co-localization (%) of Ypt1+Chc1 with Sec7 | std dev | | # of cells (n) | co-localization (%) of Ypt1+Sec7 with Chc1 | std dev | |
| | 12 | 100 | 0 | | 19 | 60.3 | 3 | |

**A.**

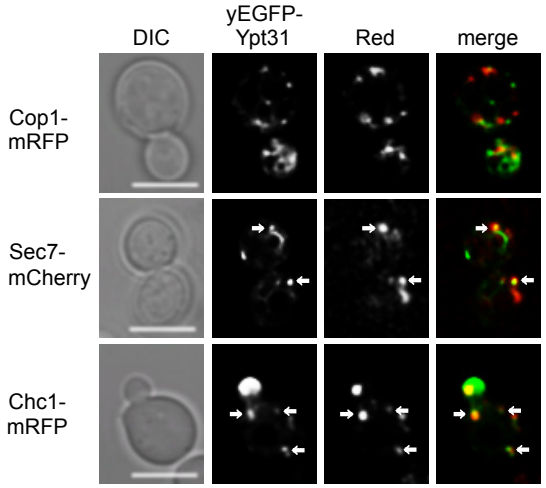


**B.**

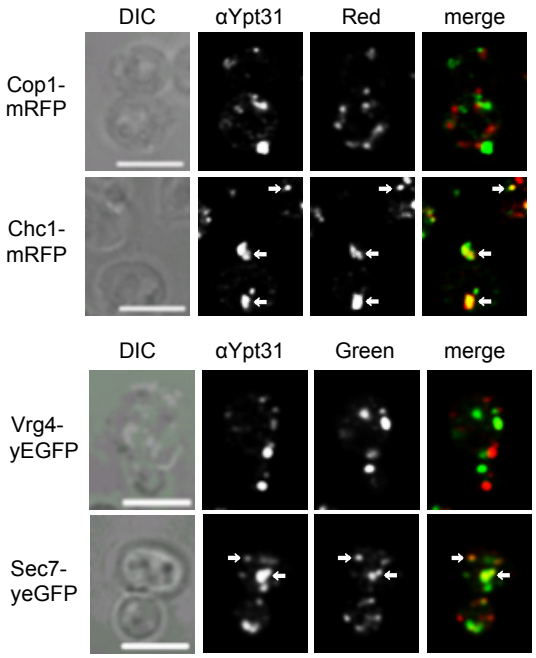


**C.**

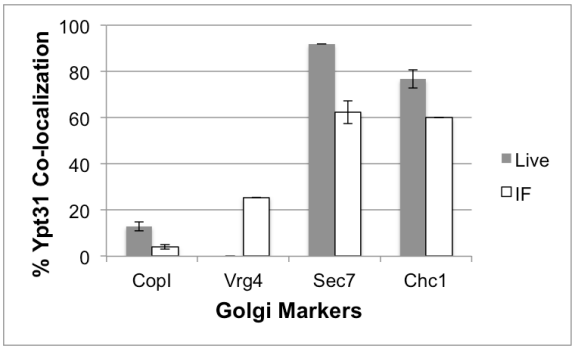


**D.**

| Ypt31 | Golgi Marker | # of cells (n) | **co-localization (%) of Ypt31** | std dev | # Ypt31 puncta/slice | # co-localized puncta/slice | co-localization (%) of green | std dev | # green puncta/slice |
|---|---|---|---|---|---|---|---|---|---|
| yEGFP-Ypt31 (plasmid) | Cop1-mRFP | 29 | **13** | 2 | 4.1 | 0.6 | n/a | n/a | n/a |
| | Sec7-mCherry | 20 | **91.9** | 0 | 3.4 | 3 | n/a | n/a | n/a |
| | Chc1-mRFP | 29 | **76.7** | 4 | 5.4 | 3.8 | n/a | n/a | n/a |
| α-Ypt31 (endogenous) | Cop1-mRFP | 30 | **4.1** | 1 | 5.2 | 0.2 | n/a | n/a | n/a |
| | Vrg4-yEGFP | 24 | **25.5** | 0 | 5.2 | 1.2 | 27.5 | 0 | 4.7 |
| | Sec7-yEGFP | 28 | **62.2** | 5 | 5.2 | 3 | 74 | 0 | 4.1 |
| | Chc1-mRFP | 30 | **60** | 0 | 4.7 | 2.7 | n/a | n/a | n/a |

**Figure 9. Polarized distribution of Ypt31 towards the late Golgi. A.** Co-localization of Ypt31 using live cell microscopy. Cells expressing a Golgi marker tagged with red fluorescence were transformed with a *CEN* plasmid for expression of yEGFP-Ypt31. Co-localization was determined using live-cell confocal microscopy. The Golgi markers shown from top to bottom: Cop1-mRFP, Sec7-mCherry and Chc1-mRFP. Shown from left to right: DIC, Ypt31 (green), Golgi marker (red) and merge (yellow). **B.** Co-localization of Ypt31 using IF microscopy. Cells expressing fluorescently tagged Golgi markers were processed for IF analysis using anti-Ypt31 antibodies. The secondary antibody was conjugated with green (FITC) or red (Texas Red) fluorescent dye depending on the tag of the Golgi marker. Co-localization was determined using confocal microscopy. Shown from left to right: DIC, Ypt31, Golgi marker and merge (yellow). Top panels: Red Golgi markers Cop1-mRFP and Chc1-mRFP. Bottom panels: Green Golgi markers Vrg4-yEGFP and Sec7-yEGFP. For panels A-B: white arrows point to co-localized signals; Bar, 5 μm. **C.** Bar graph summarizing the quantification of Ypt31 co-localization with the different Golgi markers using live-cell (panel A, grey bars) and IF (panel B, white bars) microscopy. Left to right: Ypt31 co-localize in increasing frequencies with Cop1, Vrg4, Sec7 and Chc1. **D.** Table shows quantification from two independent experiments for panels A-B; bolded numbers were used for graph in panel C. Error bars represent STDEV.

**iii) Ypt1 and Ypt31 co-localize on the Sec7-marked Golgi cisterna.**

The localization of Ypt1 and Ypt31 to the late and early Golgi compartments, respectively, is very low. However, both Ypt1 and Ypt31 showed significant co-localization with one Golgi marker, Sec7, 40% and 60%, respectively (by two-color IF, Figure 10A). Therefore, we wished to determine whether the two Ypts co-localize with each other, and if they do, on which Golgi compartment it happens.

Endogenous Ypt31 was tagged at its N-terminus with yEGFP in cells in which the *YPT32* gene was deleted. The localization of Ypt1 in these cells was determined using IF microscopy and anti-Ypt1 antibodies. Approximately 20-25% of the Ypt1 and Ypt31 puncta co-localized with each other (Figure 10B-C). To determine on which Golgi cisterna this co-localization occurs, three-color IF experiment was done in cells that also express Sec7-mRFP. Approximately 95% of the puncta on which Ypt1 and Ypt31 co-localized, also contained Sec7 (Figure 10D-E). This indicates that Ypt1 and Ypt31, which are polarized to the two sides of the Golgi, overlap on the Sec7 marked Golgi cisterna. Based on these results and on the fact that all the Ypt1-Sec7 puncta co-localize also with Cop1 or Chc1 (see above), we propose that the Golgi compartment on which Ypt1 and Ypt31 co-localize is a transitional Golgi compartment that contains all these proteins (Figure 10F).

**A.**

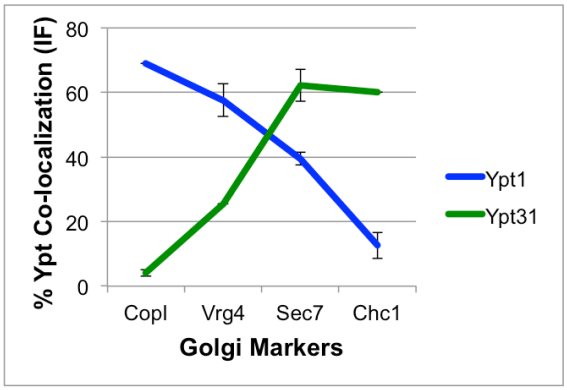


**B.**

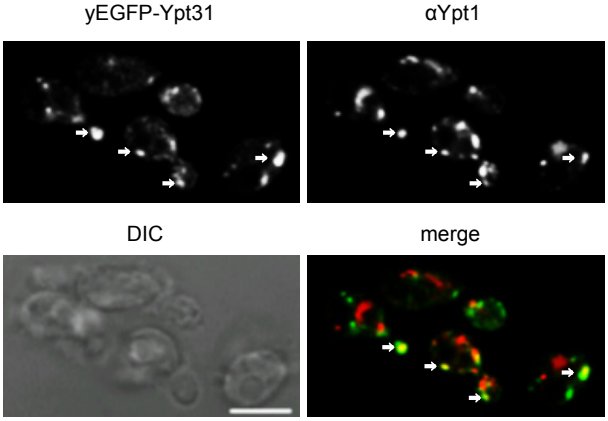


**C.**

| *yEGFP-YPT31/ypt32Δ α-Ypt1* | # of cells (n) | **co-localization (%) of Ypt1 with Ypt31** | std dev | # Ypt1 puncta/slice | # co-localized puncta/slice | **co-localization (%) of Ypt31 with Ypt1** | std dev | # Ypt31 puncta/slice |
|---|---|---|---|---|---|---|---|---|
| | 30 | **24** | 5 | 5.3 | 1.4 | **22.2** | 2 | 6.4 |

**D.**

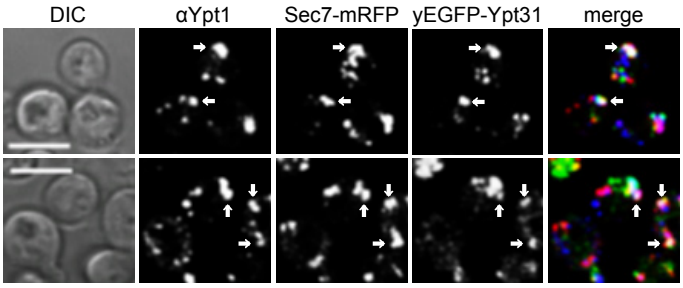


**F.**

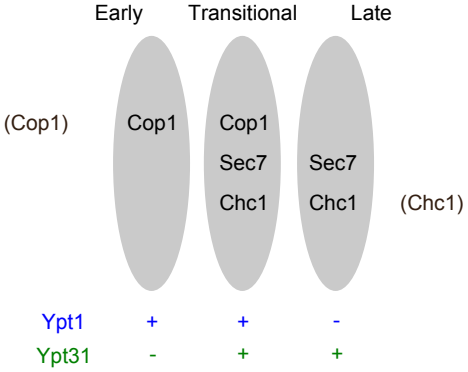


**E.**

| *yEGFP-YPT31/ypt32Δ* Sec7-mRFP α-Ypt1 | # of cells (n) | **co-localization (%) of Ypt1 with Ypt31** | std dev | # Ypt1 puncta/slice | # co-localized puncta/slice | **co-localization (%) of Ypt31 with Ypt1** | std dev | # Ypt31 puncta/slice |
|---|---|---|---|---|---|---|---|---|
| | 24 | **20.9** | 1 | 6.7 | 1.3 | **23.3** | 0 | 6 |
| | # of cells (n) | **co-localization (%) of Ypt1+Ypt31 with Sec7** | std dev | | | | | |
| | 24 | **93.8** | 3 | | | | | |

**Figure 10. Ypt1 and Ypt31 co-localize on a Sec7-marked Golgi compartment.** **A.** Both Ypt1 and Ypt31 show intermediate levels of co-localization with Sec7. Summary of IF analyses of Ypt1 (Figure 7B, red line) and Ypt31 (Figure 9B, green line) co-localization with the Golgi markers. **B.** About 20-25% of Ypt1 and Ypt31 co-localize with each other. Cells deleted for *YPT32* and expressing yEGFP-Ypt31 from its endogenous locus were processed for IF microscopy using anti-Ypt1 antibodies (secondary antibody conjugated with red (Texas Red) fluorescent dye). Shown: top panels: Ypt31 (green) and Ypt1 (red); bottom panels: DIC and merge (yellow). **C.** Table shows quantifications from two independent experiments for panel B; bolded numbers show the co-localization of the two Ypts. **D.** >90% of the Ypt1-Ypt31 puncta also contain Sec7 in a three-color IF microscopy. Cells deleted for *YPT32* and expressing yEGFP-Ypt31 and Sec7-mRFP from their endogenous loci were processed for IF microscopy using anti-Ypt1 antibodies (secondary antibody conjugated with α-Alexa-fluor 647, false colored blue). Shown from left to right: DIC, Sec7, Ypt31, Ypt1 and merge of 3 colors (white). Panels B and D: white arrows point to co-localized signal; bar, 5μm. **E.** Table shows quantifications from two independent experiments for panel D; bolded numbers show the 2 and 3-color co-localizations. **F.** Ypt1 and Ypt31 co-localize in a transitional Golgi compartment marked by Cop1, Sec7 and Chc1. A diagram showing three Golgi compartments: early, transitional and late and the distribution of Ypt1 (blue) and Ypt31 (green) in these compartments.

**iv) Effect of Ypt1 and Ypt31 level and/or activity on the Golgi**

While the idea that cisternal maturation underlies transport through the Golgi is largely accepted in the field, it is currently not clear what drives it. We hypothesized that Ypts have a role in this process. To test this hypothesis, the effect of altering the level and/or activity of Ypt1 and Ypt31 on the Golgi was determined using static fluorescence microscopy.

Determination of the levels of Ypt1 and Ypt31 expressed from a *CEN* plasmid, either tagged with yEVenus/yEGFP or not, showed that they are 10- and 5-fold higher than the endogenous levels, respectively (Figure 11A and 12A). This can explain the higher levels of co-localization of Ypt1 and Ypt31 with Golgi markers in live-cell microscopy than in IF (Figure 7 and 9). To determine the effect of higher Ypt levels on the Golgi, the wild type and activated (GTP-bound) untagged versions of Ypt1 (Q67L) and Ypt31 (Q72L) were expressed also from 2m plasmids, and 15- and 45-fold increases were observed, respectively (Figures 11B and 12B). Cells expressing a combination of green and red Golgi markers were transformed with one of the above plasmids and the effect of the higher levels of the Ypts on their co-localization was determined by live-cell microscopy (Figure 11-14). While overexpression of Ypt1 or Ypt31 did not affect the number of Sec7 puncta per cell (Figure 11E), it did affect the co-localization of Sec7 with Cop1 and Chc1 in different ways.

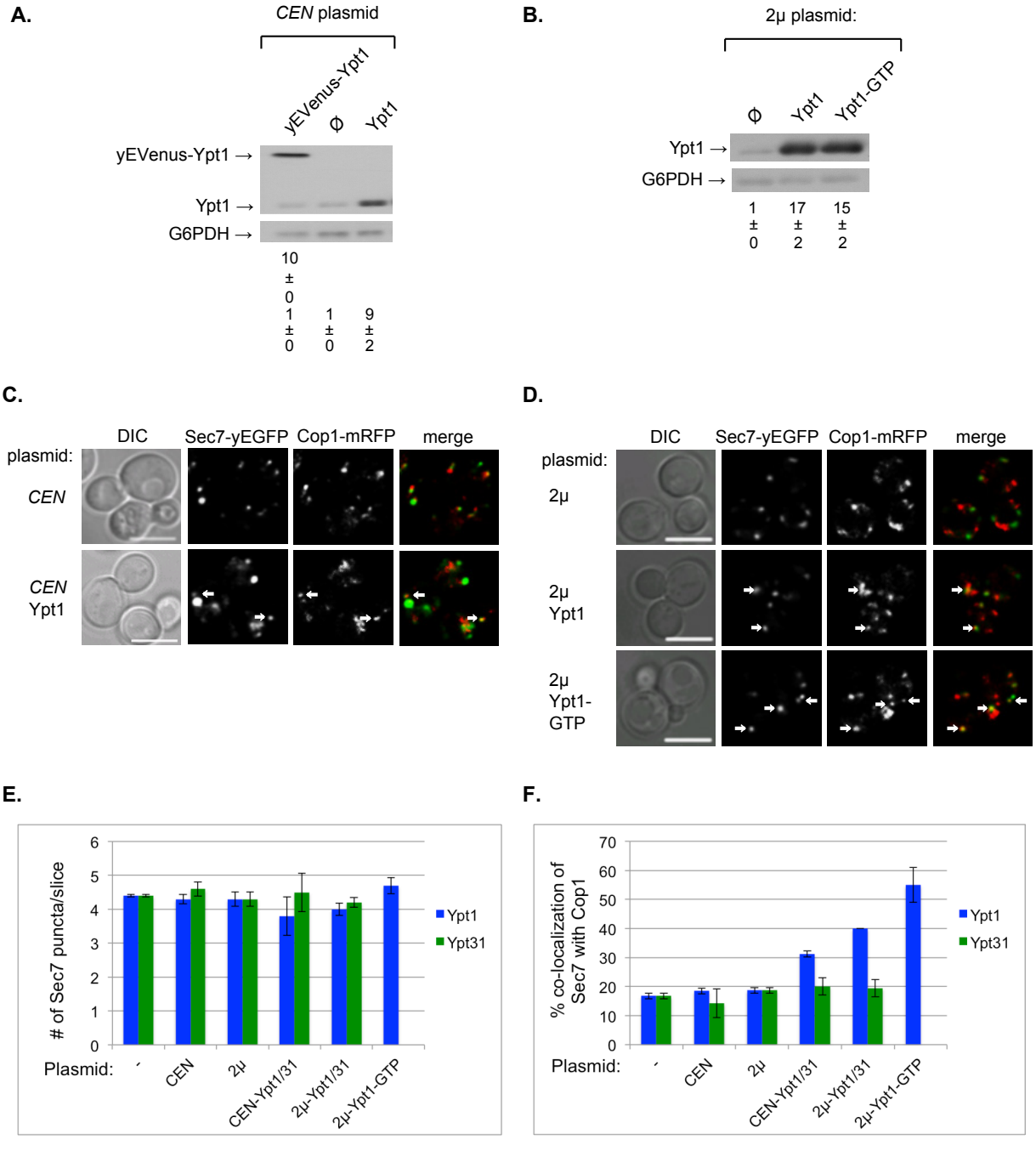
A.
CEN plasmid
yEVenus-Ypt1
Ø
Ypt1
yEVenus-Ypt1 →
Ypt1 →
G6PDH →
10 ± 0
1 ± 0
1 ± 0
9 ± 2
B.
2μ plasmid:
Ø
Ypt1
Ypt1-GTP
Ypt1 →
G6PDH →
1 ± 0
17 ± 2
15 ± 2
C.
DIC
Sec7-yEGFP
Cop1-mRFP
merge
plasmid:
CEN
CEN Ypt1
D.
DIC
Sec7-yEGFP
Cop1-mRFP
merge
plasmid:
2μ
2μ Ypt1
2μ Ypt1-GTP
E.
# of Sec7 puncta/slice
Plasmid:
-
CEN
2μ
CEN-Ypt1/31
2μ-Ypt1/31
2μ-Ypt1-GTP
Ypt1
Ypt31
F.
% co-localization of Sec7 with Cop1
Plasmid:
-
CEN
2μ
CEN-Ypt1/31
2μ-Ypt1/31
2μ-Ypt1-GTP
Ypt1
Ypt31

**Figure 11. Greater level of co-localization of Sec7 with Cop1 upon increased level and activity of Ypt1, but not Ypt31.** **A.** Expression of Ypt1 from a *CEN* plasmid results in a 10-fold increase of its level. The levels of Ypt1 protein in cells expressing it from its endogenous locus or a *CEN* plasmid were determined using immuno-blot analysis and anti-Ypt1 antibodies. Cells were transformed with a *CEN* plasmid expressing from left to right: yEVenus-Ypt1, empty plasmid (Ø), and Ypt1 (from its native promoter and terminator). Shown top to bottom: yEVenus-Ypt1, Ypt1, G6PDH (loading control), quantification of yEVenus-Ypt1 (left lane), and Ypt1 expressed as fold of endogenous level. **B.** Expression of Ypt1 from a 2m plasmid results in a ~15-fold increase of its level. The level of Ypt1 was determined as described for panel A. Cells were transformed with a 2m plasmid expressing from left to right: empty plasmid (Ø), Ypt1 and Ypt1-GTP (Ypt1-Q67L). Shown top to bottom: Ypt1, G6PDH (loading control), quantification of Ypt1 expressed as fold of endogenous level. **C.** The effect of expression of Ypt1 from a *CEN* plasmid on the co-localization of Cop1 and Sec7. Cells expressing Cop1-mRFP and Sec7-EGFP from their endogenous loci were transformed with a *CEN* plasmid (from panel A): empty (top) and for Ypt1 expression (bottom) and visualized by live-cell microscopy. Shown from left to right: DIC, Sec7, Cop1, and merge (yellow). **D.** The effect of expression of Ypt1 from a 2m plasmid on the co-localization of Cop1 and Sec7. Cells expressing Cop1-mRFP and Sec7-EGFP from their endogenous loci were transformed with a 2m plasmid (from panel B): empty (top), Ypt1 (middle) and Ypt1-GTP (bottom), and visualized by live-cell microscopy. Shown from left to right: DIC, Cop1, Sec7 and merge (yellow). Panels C-D: white arrows point to co-localized signal; bar, 5μm. **E.** The number of Sec7 puncta does not change upon overexpression of Ypt1 (blue bars) or Ypt31 (green bars). **F.** Co-localization (%) of Cop1 and Sec7 increases upon overexpression of Ypt1 (blue bars) but not Ypt31 (green bars). Shown from left to right in panels E-F: no plasmid (-), empty *CEN* and 2m plasmids, expression of wild-type Ypt from CEN, 2m, and Ypt-GTP from 2m plasmids. Error bars and +/- represent STDEV. Information about Ypt1 is from this figure, and Ypt31 is from Figure 14A. Quantifications from two independent experiments for Ypt1 and Ypt31 are detailed in Figures 13C and 14C, respectively.

For the Cop1 and Sec7 pair (Figures 11C-D and 14A), increased levels of Ypt1, but not Ypt31, resulted in a gradual increase of their co-localization: from <20% (no overexpression) to 30, 40 and 55% for wild-type Ypt1 overexpressed from *CEN* and 2m plasmids, and Ypt1-GTP overexpressed from 2m plasmid, respectively (Figure 11F). This reflects ~3-fold increase for the Cop1-Sec7 compartment upon overexpression of activated Ypt1.

The loss-of-function *ypt1ts* mutation resulted in an opposite effect on Cop1-Sec7 co-localization. Specifically, whereas activation of Ypt1 results in increase of co-localization of Cop1 with Sec7 (Figure 11F), there is a significant increase of Sec7-free Cop1 puncta (~30%) in *ypt1ts* mutant cells (Figure 15A-B). Neither activation nor inhibition of Ypt31 function affects this transport step. Together, the effects of increase and decrease in Ypt1 activity suggest that it regulates the recruitment of Cop1 to the Sec7-marked Golgi cisterna.

For the Sec7 and Chc1 pair (Figures 12C-D and 13), while their co-localization level did not change (Figure 12E), increased levels of Ypt31, but not Ypt1, resulted in a gradual increase in the number of Chc1 puncta that did not overlap with Sec7 (Figure 12F). This suggests that increase in Ypt31 activity does not affect the late Golgi, but the release of Chc1-vesicles from it.

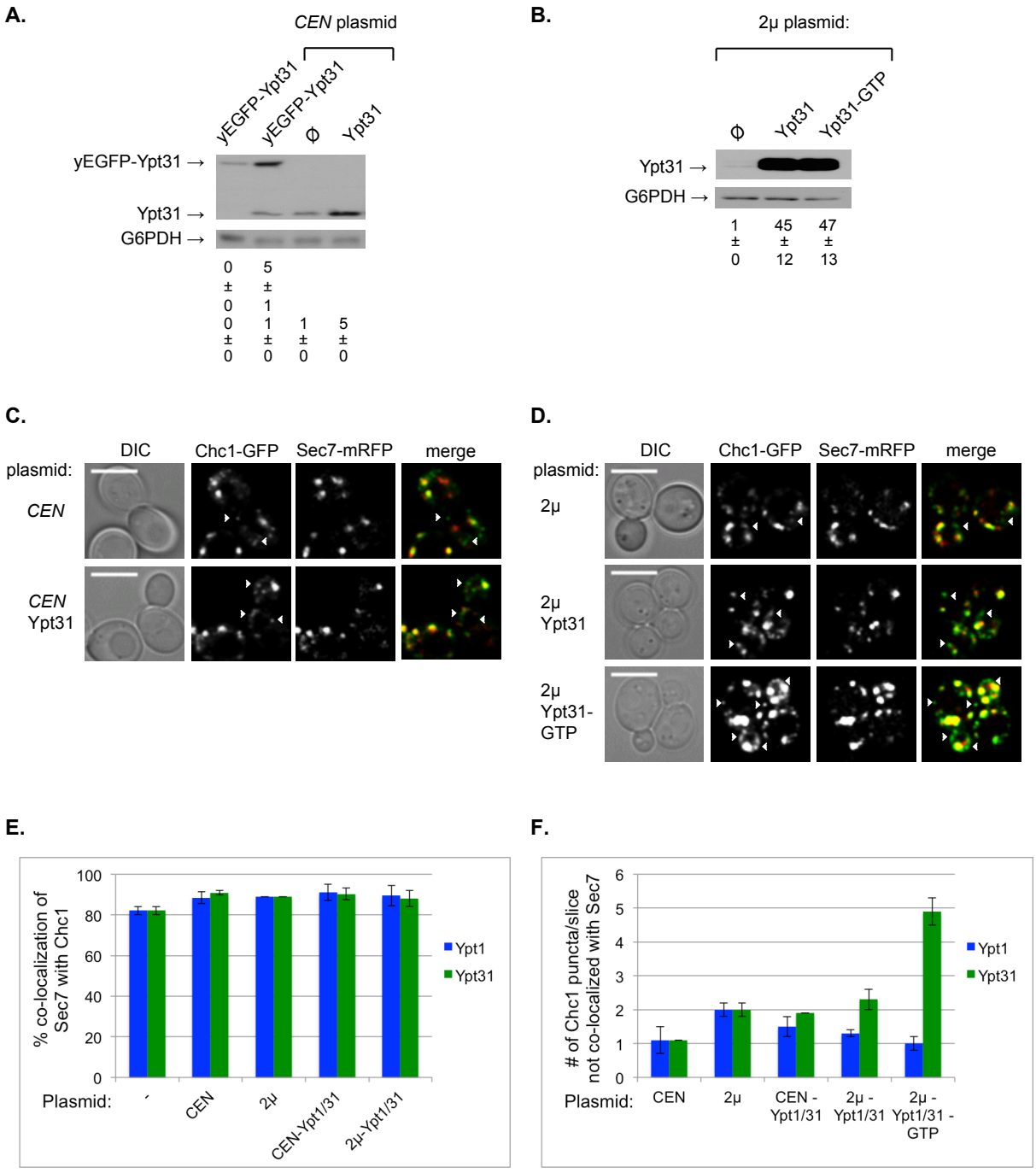
A.
CEN plasmid
yEGFP-Ypt31
yEGFP-Ypt31
Ø
Ypt31
yEGFP-Ypt31 →
Ypt31 →
G6PDH →
0 ± 0
5 ± 1
0 0 ± 0
1 1 ± 0
1 ± 0
5 ± 0
B.
2µ plasmid:
Ø
Ypt31
Ypt31-GTP
Ypt31 →
G6PDH →
1 ± 0
45 ± 12
47 ± 13
C.
DIC
Chc1-GFP
Sec7-mRFP
merge
plasmid:
CEN
CEN Ypt31
D.
DIC
Chc1-GFP
Sec7-mRFP
merge
plasmid:
2µ
2µ Ypt31
2µ Ypt31-GTP
E.
% co-localization of Sec7 with Chc1
100
80
60
40
20
0
Plasmid:
-
CEN
2µ
CEN-Ypt1/31
2µ-Ypt1/31
Ypt1
Ypt31
F.
# of Chc1 puncta/slice not co-localized with Sec7
6
5
4
3
2
1
0
Plasmid:
CEN
2µ
CEN - Ypt1/31
2µ - Ypt1/31
2µ - Ypt1/31 - GTP
Ypt1
Ypt31

**Figure 12. Higher number of Chc1 puncta that do not co-localize with Sec7 upon increased level and activity of Ypt31. A.** Expression of Ypt31 or yEGFP-Ypt31 from a *CEN* plasmid results in a 5-fold increase of its endogenous level. The levels of Ypt31 and yEGFP-Ypt31 proteins in cells expressing it from its endogenous locus or a *CEN* plasmid were determined using immuno-blot analysis and anti-Ypt31 antibodies. Left lane: *ypt32*Δ cells expressing yEGFP-Ypt31 from its endogenous promoter (used in Figure 10); *CEN* plasmid lanes: Cells (wild type) were transformed with a *CEN* plasmid expressing (from left to right): yEGFP-Ypt31, empty plasmid (Ø), and Ypt31 (from its native promoter and terminator). Shown top to bottom: yEGFP-Ypt31, Ypt31, G6PDH (loading control), quantification of yEGFP-Ypt31 (left lanes), and Ypt31 expressed as fold of endogenous level. **B.** Expression of Ypt31 from a 2m plasmid results in a ~45-fold increase of its level. The level of Ypt31 was determined as described for panel A. Cells were transformed with a 2m plasmid expressing from left to right: empty plasmid (Ø), Ypt31 and Ypt31-GTP (Ypt31-Q72L). Shown top to bottom: Ypt31, G6PDH (loading control), quantification of Ypt31 expressed as fold of endogenous level. **C.** The effect of expression of Ypt31 from a *CEN* plasmid on the co-localization of Sec7 and Chc1. Cells expressing Sec7-mRFP and Chc1-GFP from their endogenous loci were transformed with a *CEN* plasmid (from panel A): empty (top) and for Ypt31 expression (bottom) and visualized by live-cell microscopy. Shown from left to right: DIC, Chc1, Sec7 and merge (yellow). **D.** The effect of expression of Ypt31 from a 2m plasmid on the co-localization of Sec7 and Chc1. Cells expressing Sec7-mRFP and Chc1-GFP from their endogenous loci were transformed with a 2m plasmid (from panel B): empty (top), Ypt31 (middle) and Ypt31-GTP (bottom), and visualized by live-cell microscopy. Shown from left to right: DIC, Chc1, Sec7 and merge (yellow). Panels C-D: white arrowheads point to Chc1-GFP puncta that do not co-localize with Sec7-mRFP; bar, 5μm. **E.** The % co-localization of Sec7 with Chc1 does not change upon overexpression of Ypt1 (blue bars, from Figure 13A) or Ypt31 (green bars, Figure 14B). **F.** The number of Chc1 puncta that do not co-localize with Sec7 increases upon overexpression of Ypt31 (green bars, from this figure), but not Ypt1 (blue bars, Figure 13B). Shown from left to right in panels E-F: no plasmid (-), empty *CEN* and 2m plasmids, expression of wild-type Ypt from *CEN* and 2m, and Ypt-GTP from 2m plasmids. Error bars and +/- represent STDEV. Quantifications from two independent experiments are detailed in Figures 13C and 14C.

**A. Sec7 and Chc1 (yEGFP/mRFP)**

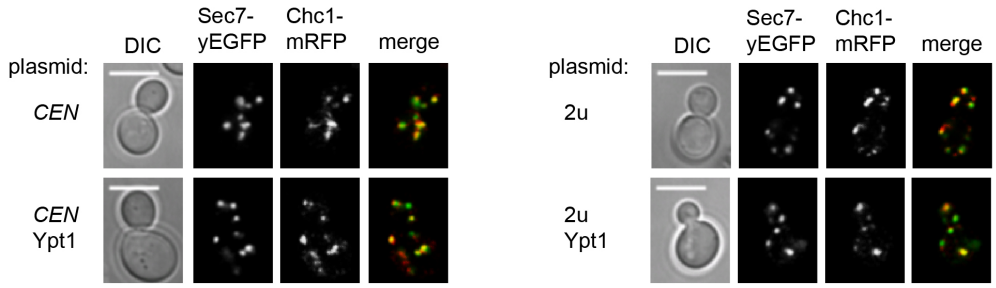


**B. Sec7 and Chc1 (mRFP/GFP)**

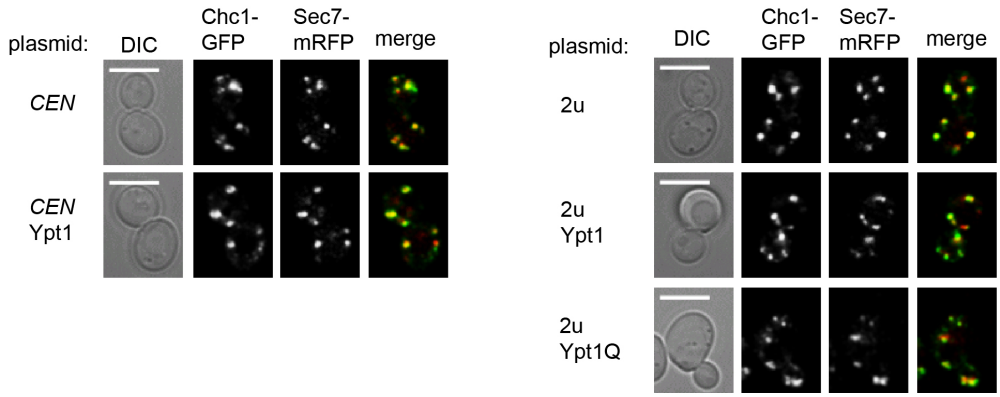


**C.**

| Strain | Plasmid | # of cells (n) | co-localization (%) of Green with Red | std dev | # Green puncta/slice | std dev | # co-localized puncta/slice | # not co-localized puncta/slice | std dev |
|---|---|---|---|---|---|---|---|---|---|
| Cop1-mRFP Sec7-yEGFP | Ø *CEN* | 20 | 18.5 | 1 | 4.3 | 0.1 | 0.9 | | |
| | Ypt1 *CEN* | 20 | 31.2 | 1 | 3.8 | 0.6 | 1.1 | | |
| | Ø 2µ | 20 | 18.7 | 1 | 4.3 | 0.2 | 0.9 | | |
| | Ypt1 2µ URA3 | 20 | 42.6 | 1 | 3.6 | 0.2 | 1.4 | | |
| | Ypt1 2µ LEU2 | 30 | 40 | 0 | 4 | 0.2 | 1.5 | | |
| | Ypt1-GTP 2µ | 30 | 55 | 6 | 4.7 | 0.2 | 2.5 | | |
| Sec7-mRFP Chc1-GFP | Ø *CEN* | 28 | 78.8 | 3 | 5.2 | | 4 | 1.2 | 0.4 |
| | Ypt1 *CEN* | 28 | 75.1 | 4 | 5.6 | | 4.1 | 1.5 | 0.3 |
| | Ø 2µ | 28 | 64.5 | 3 | 5.6 | | 3.6 | 2.1 | 0.2 |
| | Ypt1 2µ | 28 | 78.8 | 3 | 5.4 | | 4.1 | 1.3 | 0.1 |
| | Ypt1-GTP 2µ | 28 | 83.5 | 3 | 5.4 | | 4.4 | 1 | 0.2 |
| Sec7-yEGFP Chc1-mRFP | Ø *CEN* | 20 | 88.5 | 3 | 4.2 | | 3.6 | 0.6 | |
| | Ypt1 *CEN* | 20 | 91 | 4 | 3.7 | | 3.3 | 0.4 | |
| | Ø 2µ | 20 | 88.9 | 0 | 3.6 | | 3.1 | 0.5 | |
| | Ypt1 2µ | 20 | 89.5 | 5 | 3.9 | | 3.5 | 0.4 | |

**Figure 13. Ypt1 overexpression does not affect Sec7 and Chc1 co-localization.** **A.** Cells expressing Sec7-yEGFP and Chc1-mRFP from their endogenous loci were transformed with *CEN* (left) and 2µ (right) plasmids, empty (top) and for overexpression of Ypt1 (bottom). Information from this experiment was used in Figure 12E. **B.** Cells expressing Sec7-mRFP and Chc1-yEGFP from their endogenous loci were transformed with *CEN* (left) and 2µ (right) plasmids, empty (top) and for overexpression of Ypt1 (bottom). **C.** Table shows quantifications from two independent experiments for panels A and B of this figure and Figure 11 and 12. The co-localization level of the two markers was determined using live cell microscopy. Bar, 5µm.

**A. Cop1 and Sec7**

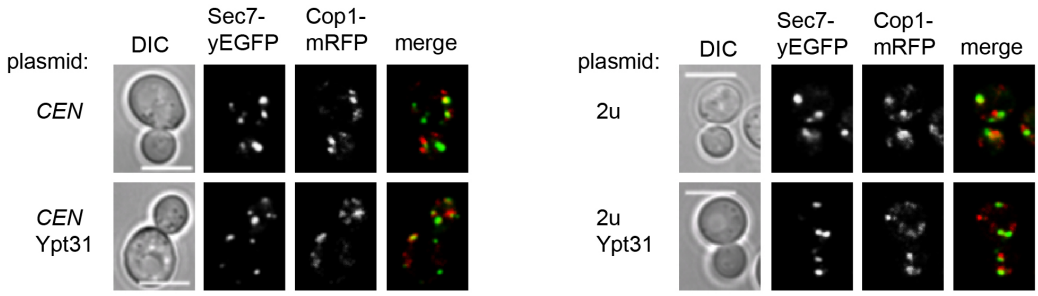


**B. Sec7 and Chc1**

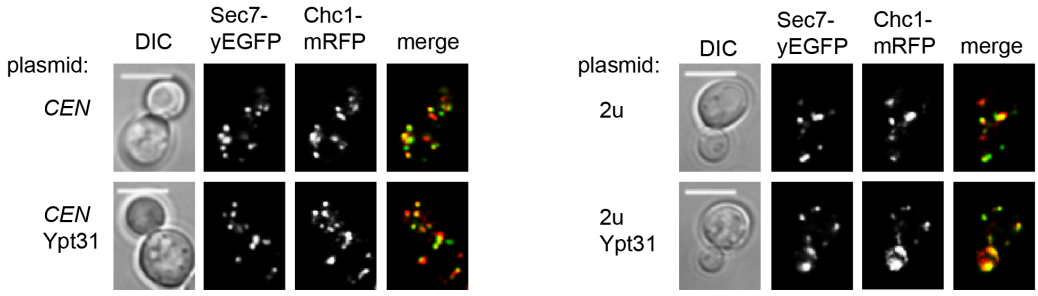


**C.**

| Strain | Plasmid | # of cells (n) | co-localization (%) of Green with Red | std dev | # Green puncta/slice | std dev | # co-localized puncta/slice | # not co-localized puncta/slice | std dev |
|---|---|---|---|---|---|---|---|---|---|
| Cop1-mRFP Sec7-yEGFP | Ø *CEN* | 20 | 14.3 | 5 | 4.6 | 0.2 | 0.7 | | |
| | Ypt31 *CEN* | 20 | 20.1 | 3 | 4.5 | 0.6 | 0.9 | | |
| | Ø 2µ | 20 | 18.7 | 1 | 4.3 | 0.2 | 0.9 | | |
| | Ypt31 2µ | 20 | 19.5 | 3 | 4.2 | 0.1 | 0.8 | | |
| Sec7-mRFP Chc1-GFP | Ø *CEN* | 20 | 81.1 | 1 | 5.2 | | 4.1 | 1.1 | 0 |
| | Ypt31 *CEN* | 20 | 70.5 | 3 | 6.3 | | 4.5 | 1.9 | 0 |
| | Ø 2µ | 28 | 64.5 | 3 | 5.6 | | 3.6 | 2.1 | 0.2 |
| | Ypt31 2µ | 28 | 64.4 | 4 | 6.3 | | 4 | 2.3 | 0.3 |
| | Ypt31-GTP 2µ | 28 | 45.1 | 3 | 8.4 | | 3.6 | 4.9 | 0.4 |
| Sec7-yEGFP Chc1-mRFP | Ø *CEN* | 20 | 90.9 | 1 | 4 | | 3.6 | 0.4 | |
| | Ypt31 *CEN* | 20 | 90.3 | 3 | 4.5 | | 4.1 | 0.4 | |
| | Ø 2µ | 20 | 88.9 | 0 | 3.6 | | 3.1 | 0.5 | |
| | Ypt31 2µ | 20 | 88 | 4 | 4.4 | | 3.9 | 0.5 | |

**Figure 14. Effects of Ypt31 overexpression on co-localization of Golgi markers.** **A.** Overexpression of Ypt31 does not affect the level of co-localization of Cop1 and Sec7. Cells expressing Sec7-yEGFP and Cop1-mRFP from their endogenous loci were transformed with *CEN* (left) and 2µ (right) plasmids, empty (top) and for overexpression of Ypt31 (bottom). Information from this experiment was used in Figure 11E-F. **B.** Overexpression of Ypt31 does not affect the level of co-localization of Sec7 with Chc1. Cells expressing Sec7-yEGFP and Chc1-mRFP from their endogenous loci were transformed with *CEN* (left) and 2µ (right) plasmids, empty (top) and for overexpression of Ypt31 (bottom). **C.** Table shows quantifications from two independent experiments for panels A and B of this figure and Figures 11 and 12. The co-localization level of the two markers was determined using live cell microscopy. Bar, 5µm.

The loss-of-function *ypt31Δ/ypt32ts* mutation resulted in an opposite effect on Sec7-Chc1 co-localization. Specifically, whereas activation of Ypt31 results in increase of the number of Chc1 puncta that do not co-localize with Sec7 (Figure 12F), there is a significant reduction (25%) in the number of Chc1 puncta that co-localize with Sec7 in *ypt31Δ/ypt32ts* mutant cells (Figure 15C-D). Neither activation nor inhibition of Ypt1 function affects this transport step. Together, the effects of increase and decrease in Ypt31 activity suggest that it regulates the recruitment of Chc1 to the Sec7-marked Golgi cisterna.

To support the idea that Ypt1 controls the formation of the transitional Golgi cisterna, the 3-color co-localization of Ypt1 and Ypt31 on the Sec7 compartment was determined when the GTP-restricted form of either Ypt1 or Ypt31 were expressed from a *CEN* plasmid. Triple-IF analysis of Ypt1, Ypt31 and Sec7 showed that the two Golgi Ypts co-localize on the Sec7 cisterna (Figure 10). As expected from the co-localization results of Golgi marker (Figures 11-12), when Ypt1, but not Ypt31, is activated there is a highly significant increase (67%) of its co-localization with Sec7. There is also a significant increase (~50%) in the co-localization of Ypt31 and Sec7 and co-localization of all three proteins when Ypt1 is activated (Figure 16). These results support the idea of a Ypt1-to-Ypt31 exchange in the Sec7-marked transitional Golgi cisterna.

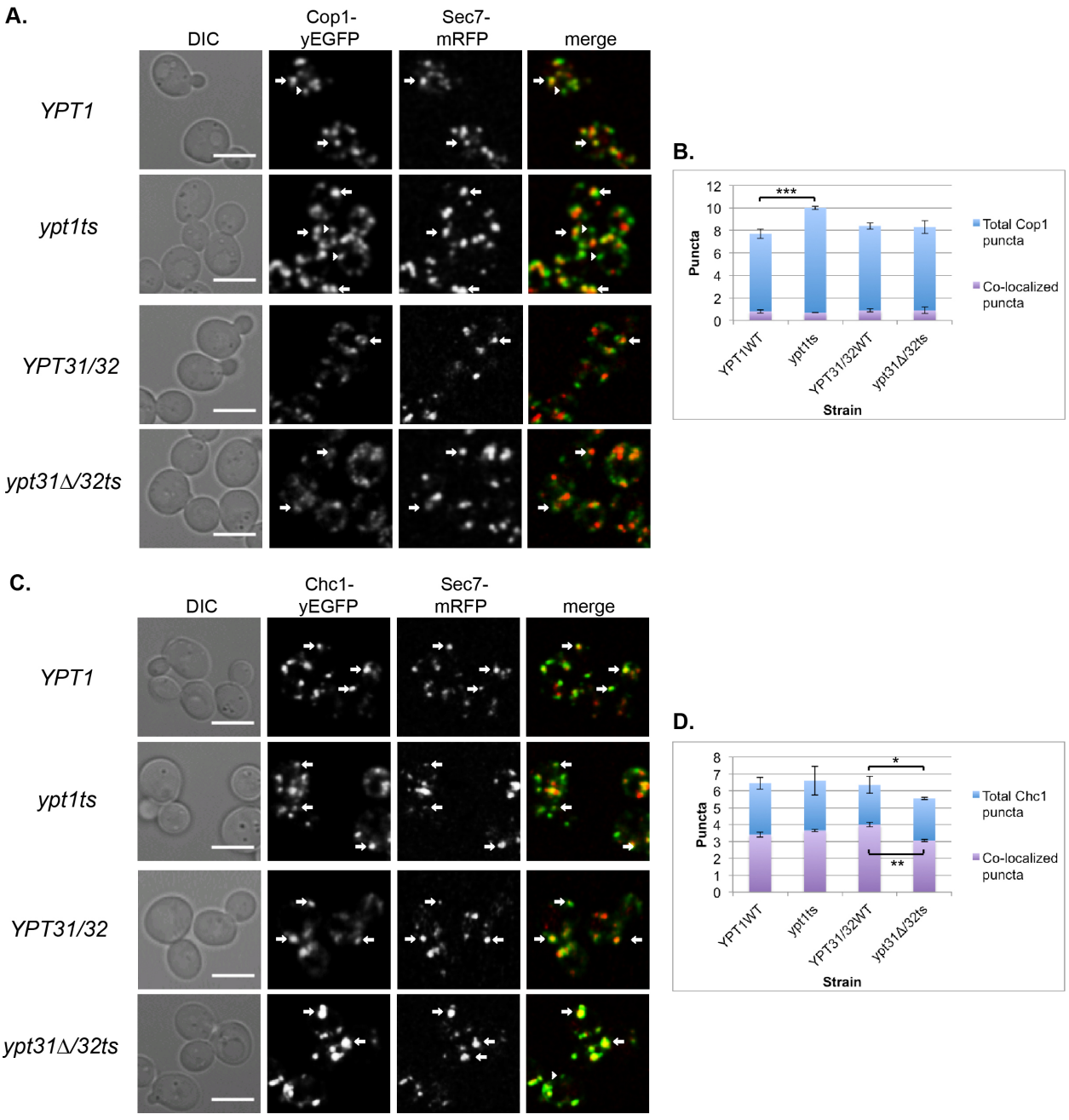
A.
DIC
Cop1-yEGFP
Sec7-mRFP
merge
YPT1
ypt1ts
YPT31/32
ypt31Δ/32ts
B.
Puncta
12
10
8
6
4
2
0
***
Total Cop1 puncta
Co-localized puncta
YPT1WT
ypt1ts
YPT31/32WT
ypt31Δ/32ts
Strain
C.
DIC
Chc1-yEGFP
Sec7-mRFP
merge
YPT1
ypt1ts
YPT31/32
ypt31Δ/32ts
D.
Puncta
8
7
6
5
4
3
2
1
0
*
**
Total Chc1 puncta
Co-localized puncta
YPT1WT
ypt1ts
YPT31/32WT
ypt31Δ/32ts
Strain

**Figure 15. The effect of *ypt1* and *ypt31/32* loss-of-function mutations on the co-localization of Golgi markers.** The effect of *ypt1ts* and *ypt31Δ/32ts* mutations on the co-localization of Golgi markers was determined at the permissive temperature using live-cell fluorescence microscopy: **A-B.** Cop1-Sec7. **C-D.** Sec7-Chc1. Wild type and mutant cells expressing tagged Golgi markers from their endogenous promoters were analyzed as described for Figures 6-7. Panels A and C: Shown from top to bottom: WT (*YPT1)*, *ypt1ts*, WT (*YPT31/YPT32)*, *ypt31Δ/32ts*. Arrows show co-localization; arrowheads show green-only puncta. Bar, 5μm. Bar graphs showing the number of Cop1 (B) or Chc1 (D) puncta: Total puncta (blue+purple bars), and puncta that co-localize with Sec7 (purple bars). Error bars and +/- represent STDEV; brackets with stars represent p-value from significant (*) to highly significant (***); p-values of all other pairs were not significant. Quantifications from two independent experiments are detailed in Table II.

**Table II. The effect of *ypt1* and *ypt31/32* loss-of-function mutations on the co-localization of Golgi markers (related to Figure 15).**

| | Strain | # of cells (n) | co-localization (%) of green with Sec7 | std dev | **# green puncta/slice** | **std dev** | **p-value** | **# co-localized puncta/slice** | **std dev** | **p-value** |
|---|---|---|---|---|---|---|---|---|---|---|
| Sec7-mRFP Chc1-GFP | *YPT1* | 20 | 11.1 | 2 | **7.7** | **0.4** | **n/a** | **0.8** | **0.1** | |
| | *ypt1ts* | 20 | 7.8 | 1 | **10.0** | **0.1** | **0.0007*** ** | **0.7** | **0** | |
| | *YPT31/32* | 20 | 11.9 | 1 | **8.4** | **0.3** | **n/a** | **0.9** | **0.1** | |
| | *ypt31Δ/32ts* | 20 | 11.0 | 4 | **8.3** | **0.6** | **0.8297** | **0.9** | **0.3** | |
| Sec7-mRFP Cop1-GFP | *YPT1* | 20 | 54.9 | 1 | **6.5** | **0.4** | **n/a** | **3.4** | **0.1** | |
| | *ypt1ts* | 20 | 56.8 | 1 | **6.6** | **0.8** | **0.7318** | **3.7** | **0.1** | **0.0374*** |
| | *YPT31/32* | 20 | 63.6 | 7 | **6.4** | **0.5** | **n/a** | **4.0** | **0.1** | |
| | *ypt31Δ/32ts* | 20 | 56.6 | 3 | **5.6** | **0.1** | **0.0395*** | **3.1** | **0.1** | **0.0042**** |

Bolded numbers were used for graphs in Figure 15B,D.

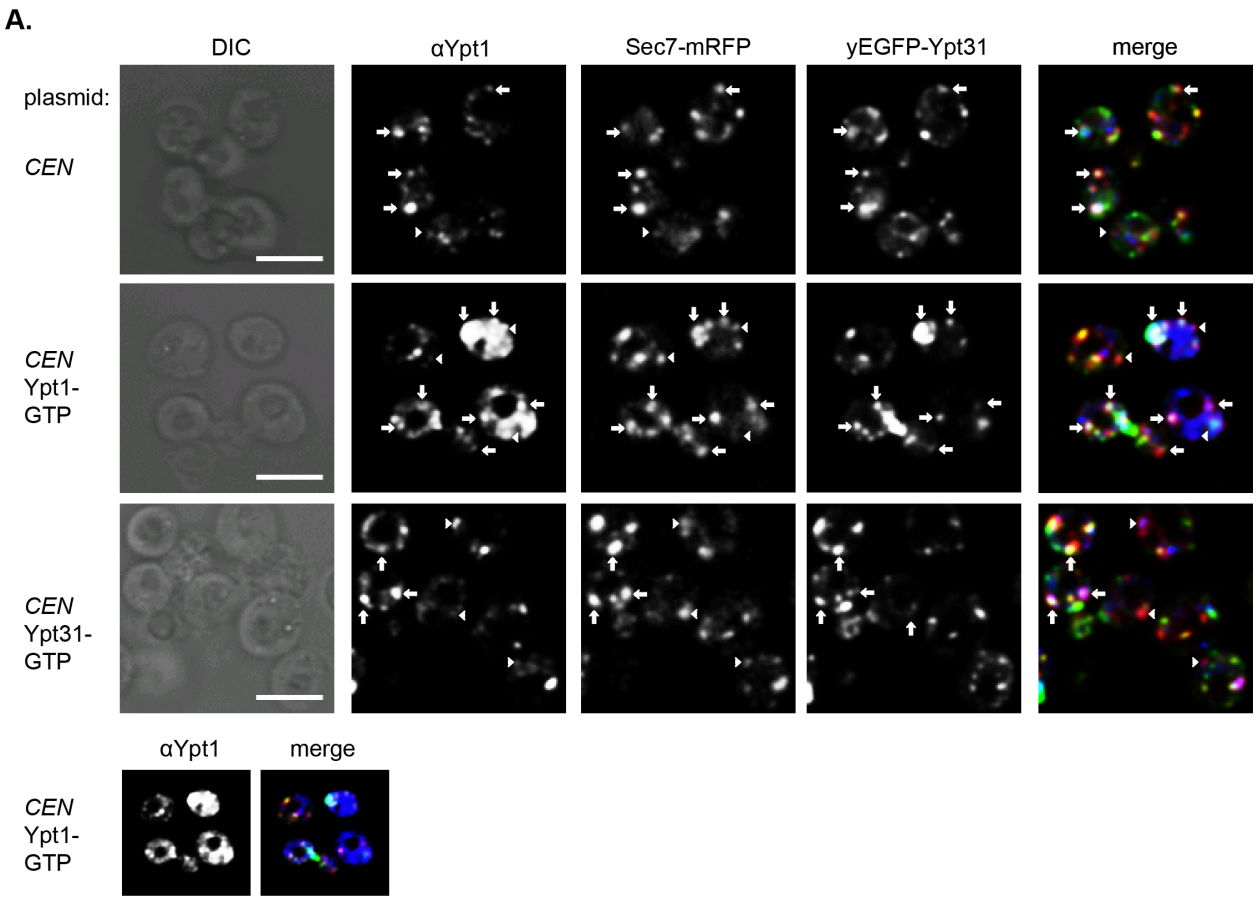
A.
DIC
αYpt1
Sec7-mRFP
yEGFP-Ypt31
merge
plasmid:
CEN
CEN Ypt1-GTP
CEN Ypt31-GTP
αYpt1
merge
CEN Ypt1-GTP

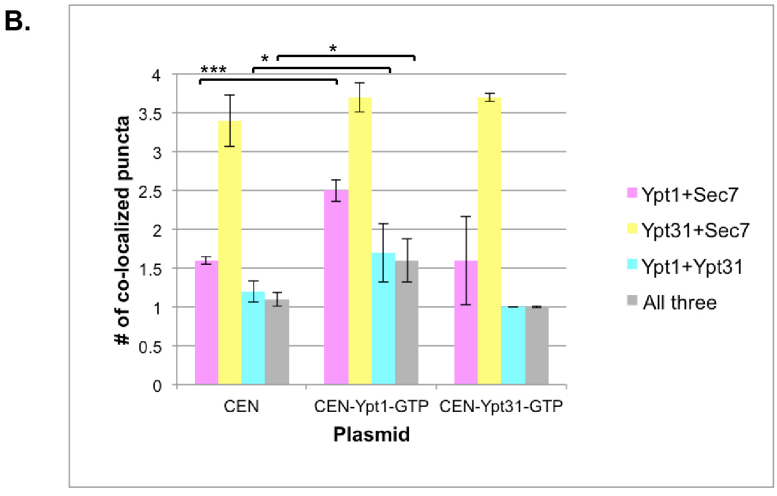
B.
***
*
*
# of co-localized puncta
0
0.5
1
1.5
2
2.5
3
3.5
4
CEN
CEN-Ypt1-GTP
CEN-Ypt31-GTP
Plasmid
Ypt1+Sec7
Ypt31+Sec7
Ypt1+Ypt31
All three

**Figure 16. The effect of Ypt1 or Ypt31 activation on their co-localization at the Sec7-marked Golgi compartment. A.** Cells were transformed with a CEN plasmid: empty (top), expressing Ypt1-GTP (middle), or Ypt31-GTP (bottom). Three-color IF microscopy was done as described in the legend for Figure 5C. The brightness of the Ypt1 staining in cells overexpressing Ypt1-GTP was reduced to enable the co-localization analysis (two bottom panels show the cells before the adjustment). Bar, 5μm. **B.** Bar graph showing the number of puncta in transformants of the three plasmids (from left-to-right): empty (CEN), Ypt1-GTP and Ypt31-GTP. The effect of each plasmid on co-localization of two or three proteins is color-coded (see key on the right): Ypt1+Sec7 (pink), Ypt31+Sec7 (yellow), Ypt1+Ypt31 (blue), and all three proteins (grey). Error bars and +/- represent STDEV; brackets with stars represent p-value; p-values for all other pairs were not significant. Quantifications from two independent experiments are detailed in Table III.

## Table III. The effect of Ypt1 or Ypt31 activation on their co-localization at the Sec7-marked Golgi compartment (related to Figure 16)

| ***yEGFP-YPT31/ypt32Δ* Sec7-mRFP α-Ypt1** | | **# of Ypt1+Ypt31 puncta** | % coloc Ypt1 with Ypt31 | % coloc Ypt31 with Ypt1 | **# of Ypt1+Sec7 puncta** | % coloc Ypt1 with Sec7 | % coloc Sec7 with Ypt1 | **# of Ypt31+Sec7 puncta** | % coloc Ypt31 with Sec7 | % coloc Sec7 with Ypt31 |
|---|---|---|---|---|---|---|---|---|---|---|
| **CEN** | **ave** | **1.17** | 0.20 | 0.20 | **1.57** | 0.28 | 0.35 | **3.43** | 0.57 | 0.77 |
| n=30 | **±** | **0.14** | 0.02 | 0.04 | **0.05** | 0.02 | 0.00 | **0.33** | 0.05 | 0.09 |
| **CEN-Ypt1-GTP** | **ave** | **1.73** | 0.29 | 0.27 | **2.50** | 0.43 | 0.54 | **3.73** | 0.60 | 0.81 |
| n=30 | **±** | **0.38** | 0.04 | 0.07 | **0.14** | 0.02 | 0.04 | **0.19** | 0.02 | 0.02 |
| | | **p=0.0240** | | | **p=0.0006** | | | **p=0.3474** | | |
| **CEN-Ypt31-GTP** | **ave** | **1.00** | 0.16 | 0.16 | **1.60** | 0.28 | 0.40 | **3.70** | 0.61 | 0.83 |
| n=30 | **±** | **0.00** | 0.01 | 0.01 | **0.57** | 0.11 | 0.17 | **0.05** | 0.06 | 0.02 |
| | | **p=0.4038** | | | **p=0.8926** | | | **p=0.3934** | | |

| ***yEGFP-YPT31/ypt32Δ* Sec7-mRFP α-Ypt1** | | # of red Sec7 | # of green Ypt31 | # of blue Ypt1 | **# of puncta co-loc of all three** | % of Ypt1+Ypt31 with Sec7 |
|---|---|---|---|---|---|---|
| **CEN** | **ave** | 4.43 | 6.03 | 5.67 | **1.07** | 0.92 |
| n=30 | **±** | 0.05 | 0.24 | 0.38 | **0.09** | 0.03 |
| **CEN-Ypt1-GTP** | **ave** | 4.63 | 6.33 | 5.97 | **1.60** | 0.93 |
| n=30 | **±** | 0.05 | 0.00 | 0.52 | **0.28** | 0.04 |
| | | | | | **p=0.0350** | |
| **CEN-Ypt31-GTP** | **ave** | 4.43 | 6.27 | 5.90 | **0.93** | 0.93 |
| n=30 | **±** | 0.05 | 0.47 | 0.33 | **0.00** | 0.00 |
| | | | | | **p=0.5132** | |

Bolded numbers were used for graphs in Figure 16B.

**v) Effect of overexpressed hyperactive Ypt1 and Ypt31 on Golgi cisternal progression**

The results of the static microscopy suggest that the overexpression of active Ypts affect the Golgi cisternal progression. To test this idea directly, we used time-lapse microscopy. The dynamics of two pairs of Golgi markers, Cop1-Sec7 and Sec7-Chc1, was determined in cells expressing tagged markers from their endogenous loci and transformed with a 2m plasmid for overexpression of Ypt1-GTP or Ypt31-GTP (empty vector used as a control) (Figures 17 and 18).

Conversion of early to late Golgi markers was previously observed using tagged Vrg4 or Sed5 and Sec7, respectively (Losev et al. 2006, Matsuura-Tokita et al. 2006). In wild type cells (without overexpression of a Ypt), green Cop1 puncta converts to red Sec7 with a clear separation between the peaks (Figure 17A). Overexpression of Ypt1-GTP, but not Ypt31-GTP, results in ~2.5-fold decrease in the gap between the curves (Figure 17B-C). This result reflects a faster conversion of a Cop1- to Cop1-Sec7-marked compartment, and is in agreement with the ~3-fold increase in the co-localization of Cop1 and Sec7 upon overexpression of Ypt1-GTP observed in the static microscopy analysis (Figure 11).

Conversion of Sec7 to Chc1 has not been not previously reported. When their individual dynamics was compared to that of Gga2, they both peaked at the same time as Gga2 (Daboussi, Costaguta, and Payne 2012). Here, we followed their dynamics directly and observed a short gap between their appearance. In wild type cells (without overexpression of a Ypt), red Sec7 puncta acquire green Chc1 with a short gap of ~10 seconds, which is ~20% of their co-localization time (average ~50 sec) (Figure 17E).

This result is in agreement with ~25% higher overlap of Ypt1 with Sec7 than with Chc1 (Figure 5A) and with the idea that Ypt1 co-localizes with these markers at the transitional compartment. Overexpression of Ypt31-GTP, but not Ypt1-GTP, results in ~2.5-fold decrease in the gap between the curves (Figure 17F-G). This result reflects a faster conversion of the Sec7- to Sec7-Chc1-marked compartment. While this faster conversion does not significantly affect the Sec7-Chc1 co-localization, which is already high (80%), we observed ~2.5-fold increase in the release of Chc1 vesicles form the Golgi in the static microscopy analysis (Figure 12). Moreover, the decrease in Chc1-Sec7 co-localization in *ypt31Δ32ts* mutant cells (Figure 15) further supports the idea that Ypt31 regulates Sec7-to-Chc1 conversion.

Together, the static and time-lapse microscopy experiments show that overexpression of activated Ypt1 and Ypt31 affect two separate steps of Golgi cisternal progression: early-to-transitional and transitional-to-late.

**A.** 2µ

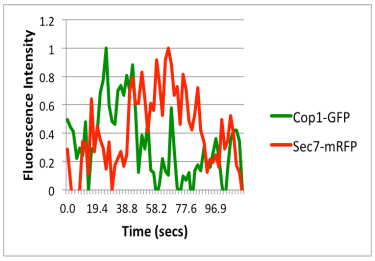


**B.** 2µ Ypt1-GTP

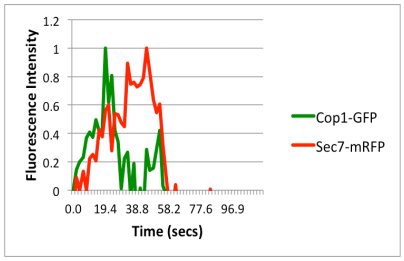


**C.** 2µ Ypt31-GTP

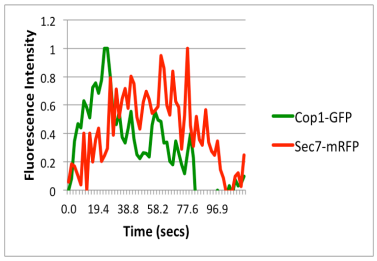


**D.**

| Cop1-yEGFP Sec7-mRFP | # puncta (n) | time Sec7 reaches 20% after Cop1 reaches 20% (s) | SEM | p-value | time Sec7 reaches 50% after Cop1 reaches 50% (s) | SEM | p-value |
|---|---|---|---|---|---|---|---|
| Ø 2µ | 10 | 13.7 | 2.4 | n/a | 19.4 | 2.8 | n/a |
| Ypt1-GTP 2µ | 10 | **5.8** | 1.2 | **0.0076**** | **7.6** | 1.9 | **0.0022**** |
| Ypt31-GTP 2µ | 10 | 17.1 | 5.3 | 0.5503 | 16.1 | 3.9 | 0.4889 |

**E.** 2µ

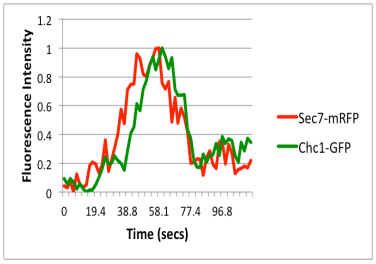


**F.** 2µ Ypt1-GTP

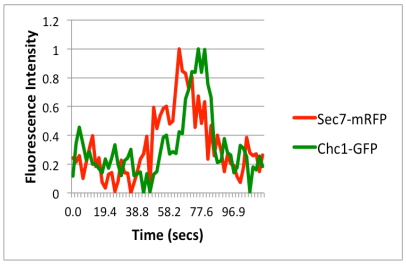


**G.** 2µ Ypt31-GTP

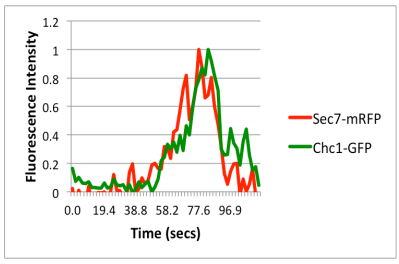


**H.**

| Sec7-mRFP Chc1-yEGFP | # puncta (n) | time Chc1 reaches 20% after Sec7 reaches 20% (s) | SEM | p-value | time Chc1 reaches 50% after Sec7 reaches 50% (s) | SEM | p-value |
|---|---|---|---|---|---|---|---|
| Ø 2µ | 10 | 12.0 | 2.4 | n/a | 9.9 | 2.1 | n/a |
| Ypt1-GTP 2µ | 10 | 7.6 | 1.8 | 0.1573 | 11.6 | 2.5 | 0.5978 |
| Ypt31-GTP 2µ | 10 | **3.7** | 1.1 | **0.0052**** | **3.9** | 0.9 | **0.0061**** |

**I.**

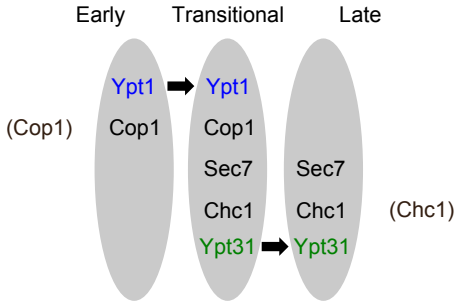

**Figure 17. The effect of overexpression of activated Ypt1 and Ypt31 on Golgi cisternal progression.** Time-lapse fluorescence microscopy was done with two pairs of Golgi markers: Cop1-Sec7 (A-C) and Sec7-Chc1 (E-G). **A-C:** Overexpression of Ypt1-GFP, but not Ypt31-GFP, results in ~2.5 fold increase in the rate of Cop1-to-Sec7 conversion. Cells expressing Cop1-GFP and Sec7-mRFP from their endogenous loci were transformed with a 2m plasmid (pRS425): empty (A), Ypt1-GTP (B), or Ypt31-GTP (C). D. Table shows quantifications from two independent experiments for panels A-C; bolded numbers show the significant change in Cop1-to-Sec7 conversion upon overexpression of Ypt1-GTP. **E-G:** Overexpression of Ypt31-GFP, but not Ypt1-GFP, results in ~2.5 fold increase in the rate of Sec7-to-Chc1 conversion. Cells expressing Sec7-mRFP and Chc1-GFP from their endogenous loci were transformed with a 2m plasmid (pRS425): empty (E), Ypt1-GTP (F), or Ypt31-GTP (G). **H.** Table shows quantifications from two independent experiments for panels E-G; bolded numbers show the significant change in Sec7-to-Chc1 conversion upon overexpression of Ypt31-GTP. Cells were analyzed by time-lapse live-cell microscopy. Graphs show normalized fluorescence intensity of representative switching puncta over time (secs); bottom: average of time between markers reaching 20 and 50% of their total average fluorescence level (n=10); +/- represent STDEV, (**, p value <0.01). Three-channel kymographs of puncta used for panels A-C and E-G are shown in Figure 18. **I.** Model summarizing the roles of Ypt1 and Ypt31 on Golgi cisternal progression. Based on results presented here we propose that Ypt1 regulates early-to-transitional cisternal progression whereas Ypt31 facilitates transitional-to-late cisternal maturation (see text for discussion).

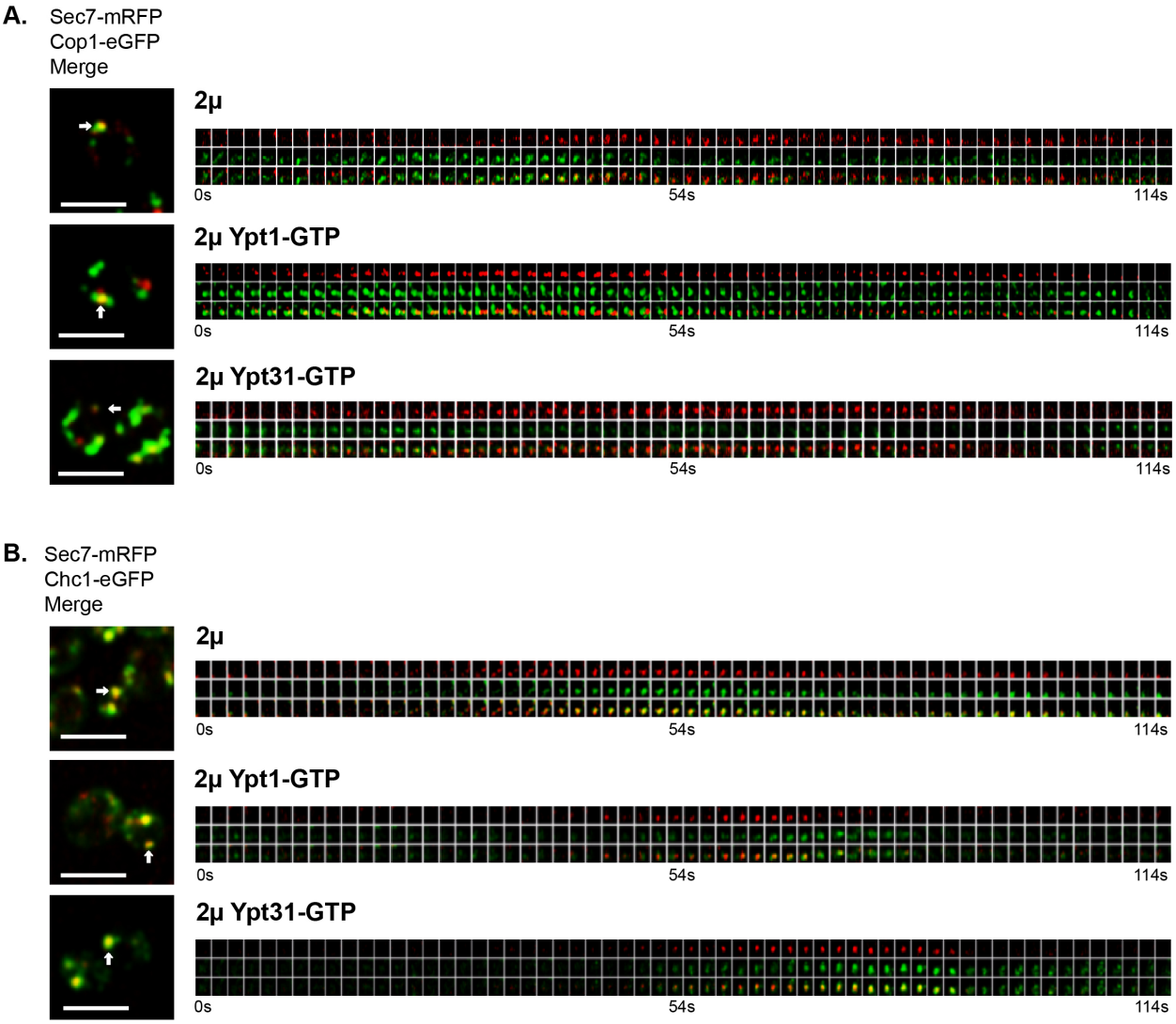


**Figure 18. Kymographs of the effect of overexpression of activated Ypt1 and Ypt31 on Golgi cisternal progression.** Three-channel kymographs of puncta used for graphs shown in Figure 17A-F. **A-C**: Cop1-GFP and Sec7-mRFP. **D-F**: Sec7-mRFP and Chc1-GFP. Cells expressing a Golgi marker pair were transformed with one of the indicated 2μ plasmids: empty, YPT1-GTP or Ypt31-GTP. For each transformant, left panel shows a merged live-cell image with a white arrow pointing to the punctum selected for the kymograph, which is shown to its right. For each kymograph, shown from top-to-bottom: mRFP, GFP, merge, time (secs). Bar, 5μm.

## D. Discussion

In this study we settle a long-standing controversy regarding the Golgi localization of two founding members of the Ypt/Rab GTPase family, Ypt1 and Ypt31. Our findings support a basic paradigm about compartment specificity of members of this family and allow us to determine a role for these GTPases in Golgi cisternal progression.

### i) Ypt/Rabs and compartment specificity

Using live-cell and IF microscopy, we clarify two important points about the distribution of Ypt1 and Ypt31/32 on the Golgi. First, Ypt1 and Ypt31 exhibit inverse polarized distribution to opposite sides of the Golgi, early and late, respectively. Second, the two Ypts display 20% co-localization with each other, and this co-localization overlaps with Sec7. We term the compartment on which these two Ypts and Sec7 overlap “transitional Golgi” and show that it also contains early and late Golgi markers, Cop1 and Chc1 (Figure 10F).

Two recent studies undermine the two other claims that form the basis for the idea that TRAPP I and TRAPP II complexes converge through a common Rab, Ypt1, which functions throughout the Golgi (Barrowman et al. 2010). First, we have shown that Ypt1 mutants used to implicate Ypt1 in late-Golgi transport (Sclafani et al. 2010) are instead defective in autophagy (Lipatova et al. 2013). Second, in vitro and in vivo studies support a role for TRAPP II at the late Golgi as a GEF for the *S. cerevisiae* Ypt31 (Morozova et al. 2006) and its *Aspergillus nidulans* ortholog RabE$^{RAB11}$ (Pinar et al. 2015). Thus, our and others cumulative data reinforce the idea that TRAPP I-stimulated Ypt1 regulates transport at the early Golgi, whereas TRAPP II-activated

Ypt31/32 regulate transport at the late Golgi. This placement agrees with the established roles of Ypt1 and Ypt31 on the two sides of the Golgi (Lipatova et al. 2015). It also supports the idea that although Ypt/Rab GTPases can regulate multiple transport steps (Lipatova and Segev 2014), they are specific to intracellular compartments (Zerial and McBride 2001).

What is the regulatory basis for Ypt1 versus Ypt31 localization? Mutations that deplete Ypt/Rab GEF activity affect the cellular localization of their Ypt/Rab substrate. For example, the TRAPP II-specific *trs130ts* mutation results in a diffuse distribution of Ypt31, but not Ypt1 (Morozova et al. 2006). Thus, we propose that TRAPP I and TRAPP II, which localize to early and late Golgi, respectively (Cai et al. 2005, Sacher et al. 2000), regulate the localization of Ypt1 and Ypt31 to the two faces of the Golgi.

How do we reconcile the controversy about the previously reported localization of Ypt1 to the late Golgi (Sclafani et al. 2010, Suda et al. 2013) and its documented function in the early Golgi (Jedd et al. 1995, Segev 1991)? First, the localization of Ypt1 to the late Golgi was based on 60% co-localization of tagged-Ypt1 with Sec7. We consider this an overestimate resulting from overexpression of the tagged Ypt1 (Figure 7), even though it was expressed from a low-copy *CEN* plasmid. Based on IF microscopy, we estimate that the Ypt1-Sec7 co-localization is 25-40%. Moreover, based on the finding that Ypt1 co-localizes less with Chc1, another late Golgi marker, we propose that the co-localization of Ypt1 and Sec7 reflects the presence of Ypt1 on a transitional compartment, and not at the late Golgi, where only Sec7 and Chc1 co-localize.

What is the transitional Golgi compartment? We propose that it is a transient compartment on which early and late Golgi markers and Ypts transiently overlap. The reason that we do not use the term “medial” is because it has been traditionally used to define a Golgi compartment in which specific cargo modifications reactions occur (Nilsson, Au, and Bergeron 2009).

Several lines of evidence presented here support the existence of the transitional Golgi compartment. First, early and late Golgi markers exhibit 10-15% co-localization, which we suggest occurs on the transitional compartment (Figure 5). Moreover, the frequency of the Cop1-Sec7 puncta and the rate of Cop1-to-Sec7 conversion increase by 2.5-3 fold upon overexpression of activated Ypt1 (Figures 11,12,17). These findings indicate that the Cop1-Sec7 co-localization reflects a distinct compartment after the early Golgi, marked by Cop1, Sec7 and Ypt1. Second, while Ypt1 shows 25-40% co-localization with Sec7, it shows only 15% co-localization with another late Golgi marker, Chc1 (Figure 7). This suggests that Ypt1 and Sec7 co-localize on a compartment distinct from the late Golgi marked by Sec7, Chc1 and Ypt31. Third, all the Ypt1-Sec7 puncta contain Cop1 and/or Chc1 (Figure 8E), Ypt1 is always present on the infrequent Cop1-Sec7 puncta, and Sec7 is always present on the infrequent Ypt1-Chc1 puncta (Figure 8F). This suggests that all these proteins are present, at least transiently, on one compartment. Fourth, 20-25% of Ypt1 and Ypt31 puncta overlap on a Sec7 marked compartment (Figure 10), which we consider the transitional compartment. Perhaps most importantly, progression into and out of the Sec7-marked transitional compartment is regulated independently by two different Ypts, Ypt1 and Ypt31, respectively (Figure 17).

Our combined evidence of the two-color and three-color IF and time-lapse microscopy suggest that Ypt1 localizes first to early Golgi marked with Cop1 and Vrg4, then to an transitional compartment marked by Sec7, Cop1 (Vrg4) and Chc1. Ypt31 also localizes to this transitional compartment, were it overlaps with Ypt1 and then to the late Golgi marked by Sec7 and Chc1 (Figure 10F). This data suggest the following dynamics: early Golgi that contains Ypt1 converts to an transitional compartment by acquiring Sec7, followed by recruitment of Ypt31 and late Golgi markers. Subsequent loss of Ypt1 and early Golgi markers indicates the transitional-to-late Golgi switch. These findings are in agreement with previous studies that showed that Sec7 appears on Ypt1-marked puncta, whereas Ypt31/32 appear on Sec7-marked puncta just before the disappearance of the Sec7 (McDonold and Fromme 2014, Suda et al. 2013). Moreover, the localization of Ypt1 and Ypt31 to opposite sides of the Golgi reported here, highlights the relevance of the Ypt1-to-Sec7 and Sec7-to-Ypt31 order previously reported by McDonald and Fromme to Golgi dynamics.

An interesting question is what regulates this early-to-transitional and transitional-to-late Golgi transitions.

**ii) Implications on Ypt/Rab GTPases and Golgi cisternal progression**

Concrete localization of Ypt1 and Ypt31 to opposite sides of the Golgi and characterization of a transitional Golgi compartment allowed us to study the effect of these Ypts on the dynamics of Golgi cisternal progression (Figure 17I). We show that increased levels and activity of the Ypts can stimulate the conversion rate of Golgi markers (Figure 17A-D). Increase in the activity of Ypt1, which functions at and localizes mostly to the early Golgi, resulted in an increase of conversion of Cop1-

marked early Golgi to Cop1/Sec7-marked transitional compartment and propagation of the latter (Figure 11). On the other hand, increase in the activity of Ypt31, which functions at and localizes mostly to the late Golgi, resulted in a faster conversion of transitional Golgi to the Sec7-Chc1-marked late Golgi (Figure 17E-H), and increased formation of Chc1-marked vesicles (Figure 12). In contrast to the effect of Ypt activation, the effects of loss-of-function *ypt1* and *ypt31/32* mutations is in agreement with a decrease in early-to-transitional and transitional-to-late Golgi switching, respectively (Figure 15). Although Ypt/Rab GTPases were proposed to regulate Golgi cisternal maturation (Suda and Nakano 2012) to our knowledge, this is the first evidence that substantiates a role for Ypt/Rab GTPases in this process.

Two Ypt GAP cascades have been reported. The first, a Ypt1-Gyp1-Ypt32 cascade was not anchored to specific Golgi cisterna (Rivera-Molina and Novick 2009) and the second, a Ypt6-Gyp6-Ypt32 cascade, was proposed to act during endosome-to-Golgi transport (Suda et al. 2013). Neither cascade provides evidence for the role of Ypts in Golgi cisternal maturation. In both cases, the second Ypt was proposed to recruit a GAP for the first Ypt to ensure that only one Ypt is active at a certain time and place. For both cascades, additional genetic evidence is needed to support this idea. For example, the *gyp1*$\Delta$ mutation used in the first report affects not only Ypt localization, but also results in permanent changes in Golgi morphology, e.g., increase in co-localization of Sec7 with Cog3, a subunit of a complex that mediates retrograde transport within the Golgi and endosome-to-Golgi transport (Rivera-Molina and Novick 2009). Regardless, the localization of Ypt1 and Ypt31/32 reported here provides context for the Ypt1-GAP-Ypt32 cascade to concrete Golgi cisterna.

Importantly, our findings add to the currently very limited genetic support for the existence of Golgi cisternal maturation. Recently, it has been reported that deletion of Arf1, a COPI component, resulted in slower and less frequent conversion of early, Vrg4-marked, puncta to Sec7-marked puncta (Bhave et al. 2014). We propose that this reflects a role of Arf1 in conversion of early (Vrg4) to transitional (Sec7) cisternal progression. Here, we show that Golgi cisternal progression can be accelerated when Ypt1 and Ypt31 are activated. Moreover, we show that two steps of cisternal maturation can be uncoupled: early (Cop1)-to-transitional (Sec7), and transitional (Sec7)-to-late (Chc1). Whereas Ypt1 increases the rate of first, but not the second, Ypt31 increases the rate of the second, but not the first. Interestingly, even though the Golgi Ypts exert their functions through effectors, an increase in their activity alone is enough to accelerate these conversions. This suggests that Ypt/Rabs GTPases regulate Golgi cisternal progression, whereas accessory proteins that mediate this process are readily available.

## CHAPTER 3. GOLGI TRAPP LOCALIZATION

The data presented in Figure 1 of this chapter comes from a publication (Taussig et al. 2013). Figure 2 and 3 contain previously unpublished material. The BiFC methods used in this chapter were described in a published methods paper where I am one of the two first co-authors (Lipatova, Kim, and Segev 2015). TRAPP complex information was also taken from a review article in which I am one of the two first co-authors (Kim, Lipatova, and Segev 2016). The following list reports the contribution of each author for the results.

Figure 19

A: Jane Kim

B: David Taussig

C: Jane Kim

D: Jane Kim

E: Zhanna Lipatova

F: Jane Kim and Zhanna Lipatova

Figure 20

Jane Kim- unpublished

Figure 21

Jane Kim- unpublished

## A. Introduction

The TRAPPII complex contains all the TRAPPI subunits, Bet3, Bet5, Trs23, Trs31, Trs20, and Trs33 as well as the TRAPPII specific subunits, Trs120, Trs130, and Trs65. The core TRAPP subunits, Bet3, Bet5, Trs23, and Trs31, are shown to be essential for GEF activity, however the roles of Trs20 and Trs33 in TRAPPI have not yet been determined. (Sacher et al. 1998, Sacher et al. 2000, Sacher et al. 2001, Morozova et al. 2006, Tokarev et al. 2009). Trs33 and Trs65 individually are non-essential, but at least one of them is required for assembly of TRAPPII (Tokarev et al. 2009). Trs20 is an essential subunit of TRAPP and is required for yeast cell viability, however not necessary for GEF activity (Kim et al. 2006). The human homolog of Trs20 is Sedlin, which in humans has been related to the disease Spondyloepiphyseal Dysplasia Tarda, or SEDT (Jang et al. 2002). To determine the localization and function of Trs20, Trs20 has been examined in Taussig et. al. in order to determine if an amino acid substitution mutation, Trs20D46Y or Trs20D, associated with SEDT has an effect the assembly of TRAPPII. Using a recombinant TRAPP complex from bacteria, it was shown that Trs20 is needed for TRS120 to interact with TRAPPI. A different Trs20 temperature sensitive, *trs20ts,* mutant is shown to affect the distribution of TRAPPII subunits within the Golgi. All TRAPP purified from yeast is shown to be restricted to TRAPPI in the *trs20ts* mutant and does not exhibit Ypt32 GEF activity. This study provides evidence that Trs20 has a role in the assembly of TRAPPII and includes Figure 19 used in this chapter (Taussig et al. 2013). Although the subunit composition of the TRAPPI and TRAPPII complexes are generally agreed upon in the field, the GEF substrate of TRAPPII is still debated.

In vitro studies found that TRAPPI has GEF activity for Ypt1 in ER-to-Golgi transport (Jones et al. 2000, Wang, Sacher, and Ferro-Novick 2000). Biochemical studies show that TRAPPII has GEF activity on Ypt31. Genetic analysis by the overexpression of Ypt31 rescues the growth defect of a temperature sensitive *trs130ts* mutant strain. In addition, mis-localizations of Ypt1 and Ypt31 in various TRAPP subunit mutant strains support the finding that TRAPPI is a Ypt1 GEF and TRAPPII is a Ypt31 GEF (Jones et al. 2000, Sacher et al. 2001, Morozova et al. 2006). Work from other groups dispute these findings and propose that TRAPPI and TRAPPII are both GEFs for Ypt1, albeit in different steps of trafficking. This model is based on mainly negative results. First, purified TRAPPII does not show GEF activity for Ypt31/32 (Wang and Ferro-Novick 2002). Secondly, GST tagged Ypt31 or Ypt32 is unable to pull-down any of the TRAPPII-specific subunits (Yip, Berscheminski, and Walz 2010). However, the process of purification can alter the TRAPP complex, leading to oligomerization or alteration in complex size (Choi et al. 2011, Brunet et al. 2012, Brunet et al. 2013). Also, the addition of GST tags on Ypt31/32 has been shown to alter their functionality for GEF assays, thus they were removed with a thrombin cleavage (Jones et al. 1995, Jones et al. 2000). Consequently, conclusions about the TRAPP complexes cannot be garnered solely from in vitro experiments. The model that both TRAPPI and TRAPPII are the Ypt31/32 GEF was further supported by the misconception that Ypt1 localizes mainly to the late Golgi due to its co-localization with Sec7 (Sclafani et al. 2010). However, I demonstrated, in the previous chapter, that Ypt1 is found mainly on the early Golgi and it only co-localizes with Sec7 at the transitional Golgi compartment.

*In-vivo* visualization of solely the TRAPPI complex has not yet been accomplished. A core TRAPP subunit tagged with a fluorescent marker will fluoresce in all the TRAPP complexes (TRAPPI, II, and III). Microscopy has been performed for two TRAPPII-specific subunits, Trs120 and Trs130, as these subunits are exclusive to TRAPPII. However, there remains a problem with visualizing one subunit (i.e. Trs130) and inferring the localization the entire complex (i.e. TRAPPII). Smaller sub-complexes may be formed while assembling the rest of the complex. For example, if Trs130 and Trs120 forms a sub-complex that attaches to TRAPPI to become TRAPPII, Trs130 signal would represent TRAPPII complex plus the Trs120-130 sub-complex. In this example, Trs130 would not be an accurate representation of the localization of the TRAPPII complex. Likewise, fluorescently tagged TRAPP subunits may be able to dimerize or oligomerize in vivo. These non-native aggregates would exhibit the brightest fluorescent signals and also confuse the true localization of the TRAPP complexes.

Live-cell microscopy of pairs of TRAPP subunits has equally proven to be difficult, due to low signal intensity when subunits are tagged with a red fluorescent protein. Therefore, a different technique was used. A protein complementation assay, PCA, named bimolecular fluorescence complementation, BiFC, is a technique used to visualize 2 proteins with one fluorescent signal (Hu, Grinberg, and Kerppola 2005). This technique takes advantage of the property of fluorescent proteins such as YFP and CFP, to be expressed as proteins halves. Each half of the fluorescent protein by itself does not produce an signal, but when in close proximity, fluorophore. . The drawback of the BiFC technique is that the fluorescent protein halves cannot separate again one they have folded, meaning that even if the protein interaction is transitory, BiFC signal

will continue once formed. Furthermore, the assembled BiFC fluorescent protein causes the proteins of interest to remain in close proximity whether or not they would in their native state. Therefore, protein-protein interactions or complexes can be visualized with BiFC with proper controls, (Lipatova, Kim, and Segev 2015). BiFC has been used to identify the GEF-Ypt-effector module, Trs85(TRAPPIII)-Ypt1-Atg11 module as the organizer for the pre-autophagosomal structure, PAS, in the autophagic pathway (Lipatova et al. 2012). This same technique was used to visualize multiple subunits of the TRAPP complex in this chapter.

In this chapter, I present evidence that TRAPPII is predominantly on the late Golgi with the same polarized localization pattern as Ypt31. I show the co-localization of Trs20-Trs120 BiFC and Trs130-Bet3 BiFC with the Golgi markers established in Chapter 2. To confirm the BiFC results, co-localization of Trs130 to the Golgi markers has been performed using the same Golgi markers. Further research will be necessary to determine if TRAPPI can be visualized as a distinct complex, what Golgi compartment TRAPPI localizes to in the Golgi, and if TRAPPI can be shown to convert to the TRAPPII complex. TRAPPI to TRAPPII conversion could allow for the coordinated activation of Ypt1 then Ypt31/32, allowing for the continuous movement of cargo from early to late Golgi.

## B. Results

### i) Trs20 and Trs120 interact and co-localize to the late Golgi

The following passage, including the figure and legend, has been quoted verbatim from Taussig et al., 2013. This publication establishes that Trs20 is necessary for the assembly of the TRAPPII complex. Figure 19 contributes to this finding by demonstrating that Trs20 interacts with Trs120 and the Trs20D mutant found in patients with SEDT is unable to form this interaction.

To verify the Trs20–Trs120 interaction and the effect of the D46Y mutation in vivo, we used the bimolecular fluorescence complementation, BiFC, assay (Kerppola 2008). Trs20 and Trs20-D46Y were tagged with the N-terminal fragment of YFP, and Trs120 was tagged with the C-terminal fragment of YFP. Yeast cells were transformed with plasmids expressing the two tagged proteins. Fluorescence in the YFP channel indicates that the two tagged proteins are physically interacting, thus bringing the two fragments of YFP into close proximity. BiFC can be observed in cells expressing Trs120 with wild-type Trs20, but not with the Trs20-D46Y mutant protein (Figure 19A). The expression of tagged Trs120, Trs20-WT and Trs20-D46Y was confirmed using immunoblot analysis (Figure 19B). The co-localization of the Trs20–Trs120 BiFC puncta with the cis- and trans-Golgi markers, CopI and Chc1, respectively, was determined in cells expressing red Golgi markers. If the two subunits interact to form TRAPP II, Trs20 and Trs120 should interact mostly on the trans-Golgi. Indeed, the Trs20-Trs120 BiFC puncta co-localize mostly with the trans-Golgi marker Chc1 (~87%), with very little co-localization with the cis-Golgi marker Cop (~10%; Figure 19C,D). In contrast to the Trs20-Trs120 BiFC interaction, both Trs20-WT and Trs20-D46Y interact with Bet3 in the

BiFC assay. In this case Bet3 was tagged with the N-terminus of CFP, and Trs20 and Trs20-D46Y were tagged with the C-terminus of CFP. The BiFC of Bet3 with Trs20 and Trs20-D46Y could be observed in the CFP channel (Figure 19E). This analysis further supports the idea that Trs20 interacts with Trs120 in vivo to form TRAPP II on the trans-Golgi, and that the D46Y mutation disrupts this interaction, but not the interaction of Trs20 with TRAPPI.

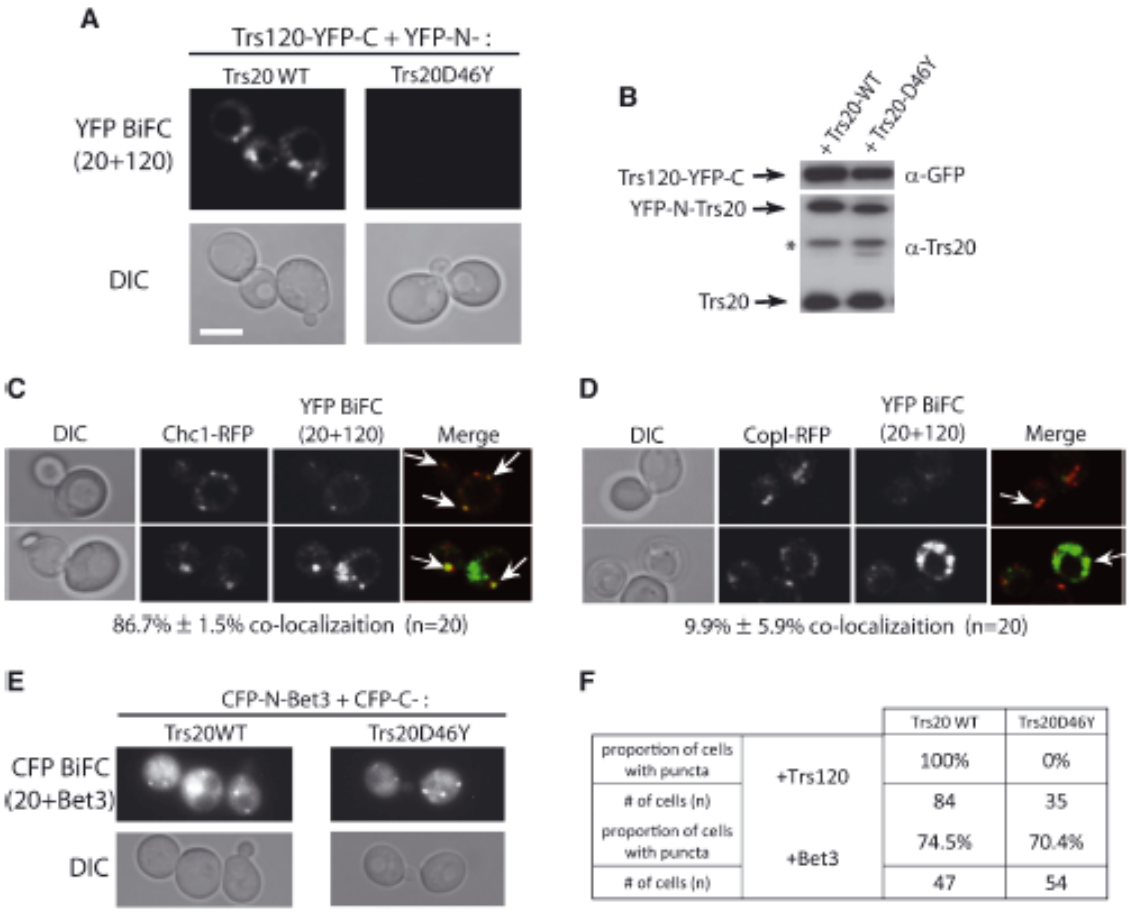


| | | Trs20 WT | Trs20D46Y |
|---|---|---|---|
| proportion of cells with puncta | +Trs120 | 100% | 0% |
| # of cells (n) | | 84 | 35 |
| proportion of cells with puncta | +Bet3 | 74.5% | 70.4% |
| # of cells (n) | | 47 | 54 |

**Figure 19. *In vivo* interactions with Trs20 on the trans-Golgi.**
A) Trs120 interacts with wild-type Trs20, but not with Trs20-D46Y, in the BiFC assay. Wild-type cells (NSY128) were transformed with two plasmids, one expressing Trs120-YFP-C and the other expressing YFP-N-Trs20 or YFP-N-Trs20-D46Y. Interaction was determined by YFP fluorescence, which was seen only in cells co-expressing Trs120 and wild type Trs20, but not Trs20-D46Y. Representative cells are shown: YFP (top), DIC (bottom) [see quantification in (F)]. B) Expression of Trs120-YFP-C was confirmed using immunoblot analysis and anti-GFP antibody (top), and expression of YFP-N-Trs20, wild type and D46Y, was confirmed using immunoblot analysis and anti-Trs20 antibody (bottom; endogenous Trs20, bottom band; *nonspecific band). C,D) Co-localization of the Trs120-Trs20 BiFC puncta with the trans-Golgi marker Chc1 (C), and the cis-Golgi marker CopI (D). Cells expressing RFP-tagged Golgi markers from their endogenous loci were transformed with Trs120-Trs20 (wt) BiFC plasmids (A). Whereas 87% of the BiFC puncta co-localize with Chc1, about 10% co-localize with CopI. E) Bet3 interacts with both Trs20 and Trs20-D46Y in the BiFC assay. Wild-type cells (NSY128) were transformed with two plasmids, one expressing CFP-N-Bet3 And the other expressing CFP-C-Trs20 Or CFP-C-Trs20-D46Y. Interaction was determined by CFP fluorescence seen in cells co-expressing Bet3 and Trs20 or Trs20-D46Y. F) Quantification of the BiFC interaction of Trs20, WT and D46Y, with Trs120 (A), or with Bet3 (E). Scale bar, 5 μm, arrows show co-localization, n is the number of cells. Results are representative of at least two independent experiments

### ii) Trs130 and Bet3 co-localize to the late Golgi (unpublished)

The co-localization of Trs130-GFP with has performed with the Cop1-mCherry and Chc1-mRFP Golgi markers in Trs20WT and *trs20ts* strains (Taussig et al. 2013). First this previous co-localization was confirmed in the BY4741 wild-type strain using Trs130 tagged with the yeast codon-optimized GFP, yEGFP. This newly tagged Trs130-yEGFP was co-localized with the mRFP-tagged Golgi markers used in Chapter 2 to localize the Ypts (Figure 20). Similar to the results from the earlier study, Trs130 mainly co-localized with the late Golgi markers Sec7 and Chc1 (~90%). <10% of the co-localization was with Cop1, therefore, Trs130 does not localize with the early Golgi. This result confirms that in the same wild-type background, using the same red-tagged markers, TRAPPI has the same polarized localization in the Golgi as Ypt31 (Figure 10).

To determine if this localization is true for just the Trs130 subunit or also the TRAPPII complex, BiFC was performed to visualize Trs130 with Bet3 (Figure 21). Due to the inclusion of Bet3 in both TRAPPI and TRAPPII, visualizing Bet3 only when in close proximity to Trs130 excludes all TRAPPI or TRAPPIII related Bet3 signals. Therefore all co-localized signal pertains only to the TRAPPII complex. Similar to the results of Trs130-yEGFP co-localization, the highest co-localization was seen with Chc1 at the late Golgi but it is less so (~68%). There is little co-localization with the early Golgi as well as the ER markers, Cop1 and Sec13, respectively (<10%). The Trs130-Bet3 signal was also co-localized with the endosomal marker Snf7, due to TRAPPII's role as a GEF for Ypt31/32 in recycling to the Golgi and also for later trafficking steps (20%) (Figure 21).

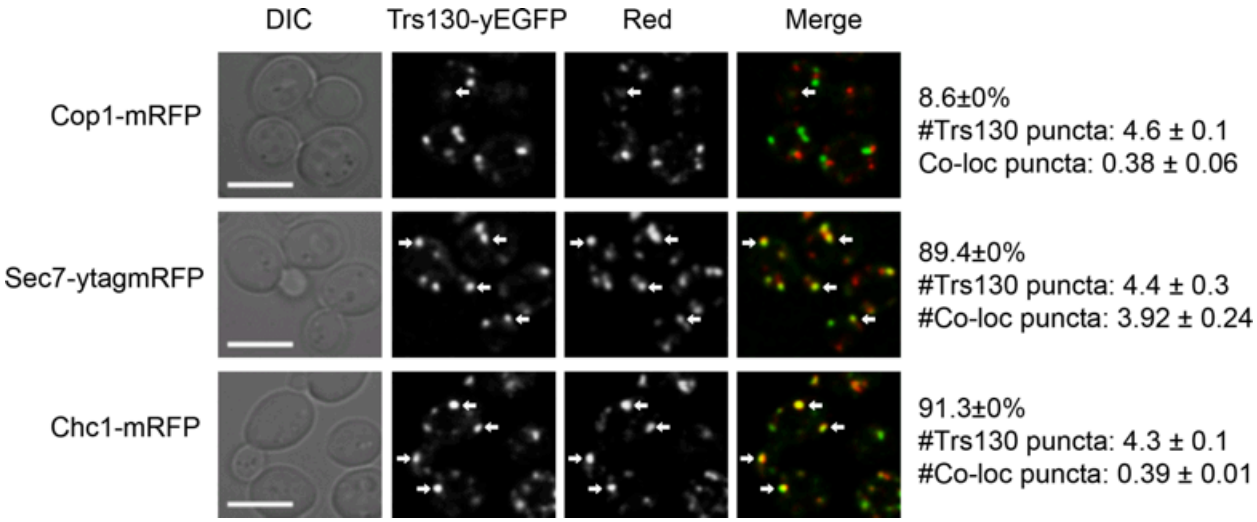


**Figure 20. TRAPPII-specific subunit Trs130 co-localizes with Sec7 and Chc1.**
Cells expressing red fluorescently tagged Golgi markers and green fluorescently tagged Trs130 were visualized using live confocal microscopy. Co-localization was determined by how much of the Trs130 signal co-localized with red signal. The quantification is shown as mean ± STDEV. Scale bar, 5 μm, arrows show co-localization, n=24 cells for each marker. Results are representative of at least two independent experiments.

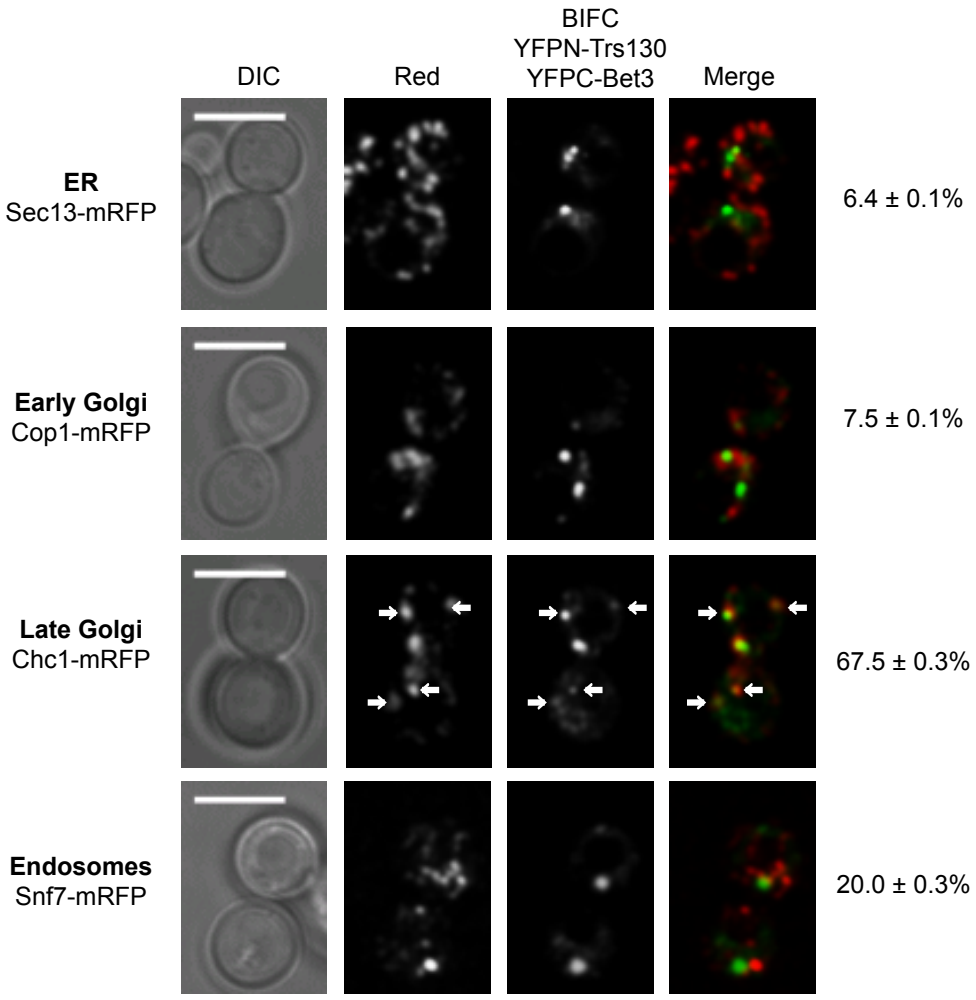


**Figure 21. Interaction of Trs130 and Bet3 co-localizes with the late Golgi marker.** BiFC was performed with YFP-N tagged Trs130 and YFP-C tagged Bet3 to form puncta that co-localize with Chc1-mRFP, a late Golgi marker. The BiFC Trs130-Bet3 puncta did not co-localize highly with the ER marker, the early Golgi marker, or the endosomal marker (Sec13, Cop1, and Snf7 respectively). The quantification is shown as mean ± STDEV. Scale bar, 5 μm, arrows show co-localization, n=20 cells for each marker. Results are representative of at least two independent experiments.

**C. Discussion**

The results in this chapter validate the placement of TRAPPII on the late Golgi. The *in vivo* live-cell microscopy of Trs120-20 pair as well as the Trs130-Bet3 pair highly co-localize with late Golgi markers and less so with Cop1, the early Golgi marker. Trs120-Trs20 co-localize to Chc1 ~87% (Figure 19) however Trs130-Bet3 only co-localizes ~70% (Figure 21). This difference can be due to the use of varied yeast strain backgrounds. The red-tagged strains used for co-localization of Trs130-Bet3 was obtained from the (Huh et al. 2003) whereas Trs20WT and *trs20ts* were obtained from M. Sacher (Concordia University). Alternatively, different pairs of TRAPP subunits may be formed in sub-complexes, which is the reason multiple pairs are checked. Due to the role of Trs20 in assembly of TRAPPII, perhaps it is found at the late Golgi with Trs120 in higher occurrence than the rest of TRAPPII.

If TRAPPII acts as a GEF for Ypt31 in later secretory or recycling steps, where the Ypt31/32 effectors Sec2, Rcy1, and Myo2 are already identified (Ortiz et al. 2002, Chen et al. 2005, Lipatova et al. 2008), TRAPPII should also be found in some abundance with endosomes. Surprisingly, there is only ~20% co-localization of BiFC Trs130-Bet3 with the endosomal marker Snf7-mRFP (Figure 21). This could be explained by the fact that Snf7 is not found in all endosomes. The creators of the Snf7-mRFP strain suggests that the tagged protein may not be fully function due it's localization pattern (Huh et al. 2003). If this finding is accurate, it may be that the majority of TRAPPII is found on the Golgi, and cycles to endosomes. This would cause most of the fluorescence signal to accumulate from BiFC to the late Golgi, and less to

the smaller scattered endosomal structures. Other endosomal markers are needed to validate the co-localization of TRAPPII with endosomes.

Further studies are necessary to visualize the presence of TRAPPI complex in vivo and confirm its localization to the early Golgi. Hopefully, the advance of novel microscopic techniques will greatly simplify the *in vivo* visualization of TRAPP subunits and complexes. It is yet unclear whether TRAPP undergoes a conversion, from TRAPPI to TRAPPII during the process of Golgi maturation. Instead, there may also be two separate pools of TRAPPs, which regulate the amount of activated Ypts. Furthermore, there are still many questions about the other roles of TRAPP, besides the GEF activity it has on the Ypts, as tethers or their involvement in disease states (Kim, Lipatova, and Segev 2016).

# CHAPTER 4. DISCUSSION

In this chapter: A.) the conclusions made in Chapters 2 and 3 are unified, B.) implications of these conclusions on the field of intracellular trafficking and Golgi homeostasis are discussed and C.) several new questions that arise from this research are examined.

## A. Summary of conclusions

The aim of this research study was to analyze the distribution and function of Rab GTPase and their GEFs in the yeast Golgi. Specifically, I determined the localization of Ypt1 and Ypt31 and TRAPPII to Golgi sub-compartments and analyzed the effect of Ypts on Golgi cisternal progression.

From Chapter 2, the following major conclusions can be made: Golgi markers can be established to the early and late Golgi, Ypt1 and Ypt31 GTPases are polarized to the opposite sides of the Golgi, early and late respectively, the Ypts co-localize on a transitional cisternae, and the Ypts regulate two distinct Golgi cisternal progressions steps. We conclude that as the analysis reported in the microscopy from Chapter 3, TRAPPII mainly localizes to the late Golgi shown by BiFC Trs120-Trs20, BiFC Trs130-Bet3, and Trs130 co-localization with Golgi markers. Moreover, TRAPPII exhibits polarized localization in the Golgi similar to that shown for Ypt31 in Chapter 2. The combined emerging picture from the results in these two chapters is illustrated in Figure 22.

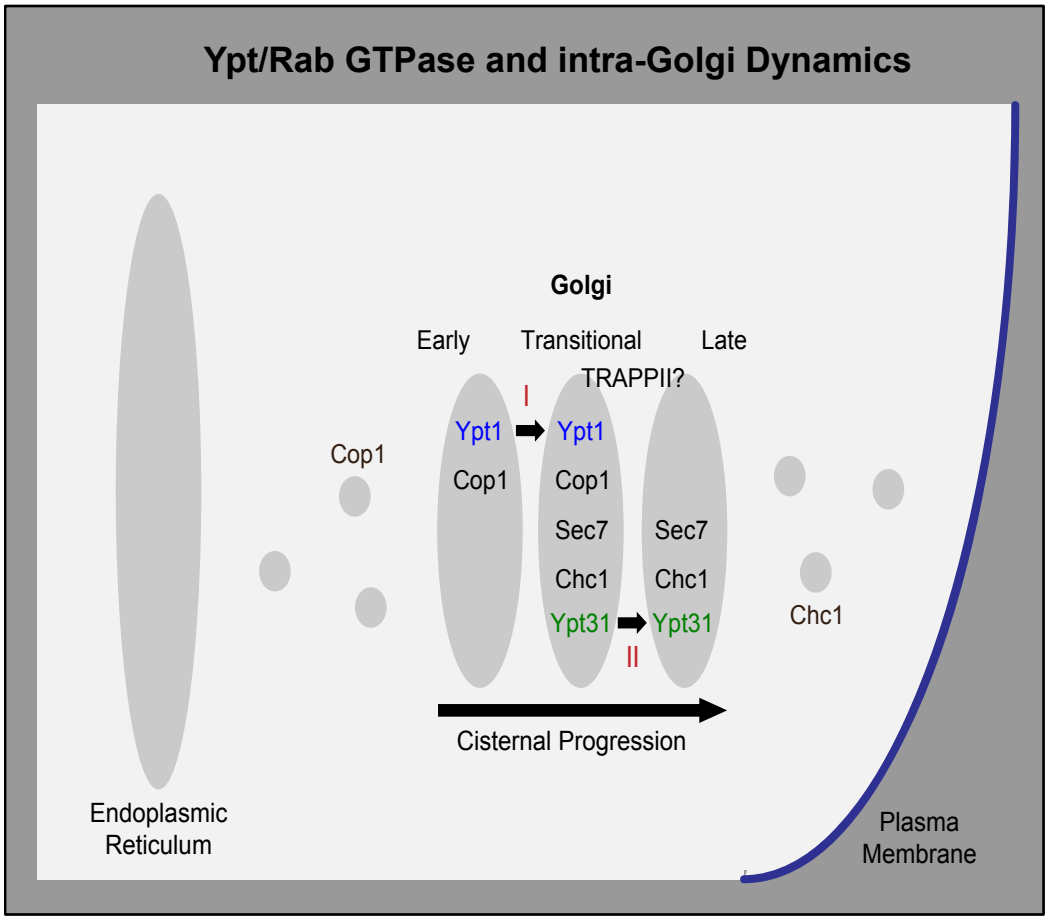


**Figure 22. Graphical summary of results.** The Golgi is the main sorting compartment of the secretory pathway between the endoplasmic reticulum (ER) and the plasma membrane (PM). Ypt1 and Ypt31 GTPases, in blue and green respectively, are polarized to opposite sides of the Golgi. Ypt1 is found mainly at the early Golgi and regulates the cisternal progression step of early to transitional Golgi (indicated by the arrow and red I). Ypt31 is found at the late Golgi and regulates the cisternal progression step of transitional to late Golgi (indicated by the arrow and red II). TRAPPII has the same localization pattern as Ypt31 and is found to localize with Sec7 and Chc1. The remaining question is whether the high levels of TRAPPII co-localization with Sec7 and Chc1 is solely to the late Golgi compartment, or is also found at the transitional compartment.

## B. Implications of results

### i. Resolving the Golgi localization of Ypt1

In Chapter 2, I establish that Golgi proteins can be visualized by live-cell confocal microscopy and organized to the early, transitional, and late compartments in yeast. This allows for more clarity in future localization of proteins to Golgi cisternae. Currently, Sec7 and Chc1 are both considered late Golgi markers and they co-localize extensively. However, I found that Sec7 also highly localizes to a Golgi transitional compartment when compared to Chc1. Therefore, using these two markers interchangeably as late Golgi markers could lead to inaccurate conclusions.

The accepted fact that Sec7 is a late Golgi marker was one of the issues leading to the conflict of the intra-Golgi localization of Ypt1. Ypt1 was proposed to have a functional role at the late Golgi based on co-localization with Sec7 (Sclafani et al. 2010, Suda et al. 2013). In these studies, fluorescently tagged Ypts were expressed from the chromosome at the locus of an auxotrophic marker as a secondary copy. These tagged variants were expressed over 4-5 fold higher than the endogenous protein when checked by western blotting (Rivera-Molina and Novick 2009). The results of Chapter 2 show that the use of Sec7 as a late Golgi marker combined with elevated expression levels of the tagged Ypts led to Golgi cisternal progression defects and the placement of Ypt1 at the late Golgi.

Also in Chapter 2, I propose that the Ypt1-Sec7 co-localization is due to the Rab conversion that occurs as the Golgi cisterna matures to gain late Golgi markers and Ypt31 while losing Ypt1 and early Golgi markers. The process of Rab conversion was shown to occur on endosomes with Rab5 labeled early endosomes to Rab7 labeled late

endosomes (Rink et al. 2005). I propose that in the Golgi, this process occurs at a transitional compartment. Based on the finding that Ypt1 polarizes to the early Golgi, I expect that Ypt1 would not have a role at the late Golgi. However, Ypt1 was reported to have a role in endosome to trans-Golgi transport. This idea stemmed from the accumulation of a SNARE protein, GFP-SNC1, in a Ypt1 mutant (Sclafani et al. 2010). A study performed by the Segev lab determined that this accumulation is due to a defect in ER-phagy (Lipatova et al. 2013). Thus, there is no evidence either for the localization or function of Ypt1 at the late Golgi.

ii. Genetic support for Golgi cisternal progression

Originally, the Golgi was sub-compartmentalized into cis, medial, and trans compartments identified by glycoenzyme content and subcellular fractionation studies (Farquhar and Palade 1981, Goldberg and Kornfeld 1983, Nilsson, Au, and Bergeron 2009). Two recent studies show that Golgi cisternal progression occurs in yeast, and this dynamic process can be visualized using early and late Golgi markers (Losev et al. 2006, Matsuura-Tokita et al. 2006). Using the time-lapse imaging techniques described in these studies and others, I found that overexpressing or hyper-activating Ypt1 or Ypt31 leads to temporal changes in cisternal progression. Ypt1 regulates an early to transitional compartmental progression step, and the effect of Ypt31 is centered on the late Golgi. During the process of cisternal maturation, the transitional compartment, what I describe as the transient Golgi compartment in Chapter 2, loses Ypt1 and early Golgi proteins and gains Ypt31 and late Golgi proteins in a sequential manner. The terms cis, medial, and trans are not used here to describe the compartments because this terminology specifies the enzymatic reaction that occur. Instead, I use the terms

early, transitional, and late compartments to take into account the temporal aspect of Golgi maturation.

There are only two other studies that provide genetic evidence of Golgi maturation. Bhave et al. in 2014 showed that depletion of Arf1 GTPase leads to fewer and bigger Sec7-labeled compartments (Bhave et al. 2014). They conclude that the Sec7-labeled compartments are late Golgi, however, it is probably the transitional compartment that they observed. Additionally, they discovered that in *arf1Δ* cells, the early cisternae persist longer and show evidence of the Vrg4 to Sec7 cisternal transition occurring slower, while late Golgi dynamics remained the same. Based on the above results, Arf1 must have a role in early to transitional Golgi, similar to that of Ypt1. The authors conclude that Arf1 regulates cisternal progression, however, this study fails to determine whether Arf1 is a regulator or merely a component of Golgi dynamics. To determine whether Arf1 is truly a regulator of Golgi dynamics, further analysis of Arf1 needs to be performed in a nucleotide-dependent manner (i.e. activated state).

A second study examined the mechanics of Golgi dynamics when Cop1 is sequestered to the mitochondria or ribosomes (Papanikou et al. 2015). Cop1 is a coat protein implicated in intra-Golgi transport for Golgi structure maintenance. Papanikou et al. found that when Cop1 is unavailable, reduced secretion still continues. They determined the secretion was due to the formation of hybrid Golgi structures, which contain early (GFP-Vrg4) and late Golgi (Sec7-DsRed) proteins. Although the hybrid structure described by Papanikou et al. is similar to the transitional compartment, there are some differences. As described earlier, the transitional compartment is found transiently in a wild-type situation and is more prevalent upon Ypt1 overexpression,

however, separate early and late Golgi compartments can still be distinguished. In the Cop1 disrupted cell, the hybrid compartment is the only Golgi structure available. Additionally, they show that Sec7 and Kex2 are recycled from the hybrid Golgi, however Vrg4 remains. They conclude that Cop1 is the component responsible for trafficking early Golgi proteins such as Vrg4 to newly forming Golgi, making it necessary for Golgi cisternal maturation, and that some other factor, theorized to be Chc1, is responsible for trafficking late Golgi proteins.

Adding to the current knowledge, my work describes Vrg4 or Cop1 to Sec7 as the early to transitional Golgi maturation step, and I found the existence of a novel subsequent maturation step, the transitional to late Golgi visualize by Sec7 to Chc1. I provide evidence that the GTPases Ypt1 and Ypt31 regulate these two steps respectively based on their ability to increase the speed of cisternal progression in their hyper-activated states.

iii. Views for TRAPP as a GEF

As discussed in Chapter 3, there is disagreement on whether the target of GEF activity of TRAPPII is Ypt1 or Ypt31/32. This was partially due to the mis-localization of Ypt1 to the late Golgi (Sclafani et al. 2010), which was already discussed above. Additional support for the view that TRAPPII is not a Ypt31/32 GEF is based on negative results and structural studies. Some studies showed that GEF activity for Ypt31/32 was not found from purified TRAPPII and that tagged Ypt31/32 could not pull down any TRAPPII specific subunits (Wang and Ferro-Novick 2002, Yip, Berscheminski, and Walz 2010). Other studies showed that TRAPP purification can lead to oligomerization and also can change which side of the complex is open to allow

a Ypt to bind for GEF activity (Choi et al. 2011, Brunet et al. 2012, Brunet et al. 2013). Therefore, conclusions about the TRAPP complexes cannot be made solely on negative results and in-vitro experiments, which may affect the nature of the complex.

From my in-vivo live-microscopy analysis, it can be concluded that TRAPPII is mainly localized on late Golgi, with similar polarized localization patterns as Ypt31. Since the GEF must be present upstream of the GTPase it activates, and the TRAPPII subunits co-localize with the late Golgi markers Sec7 and Chc1, I propose that TRAPPII is not the GEF for Ypt1, which co-localizes with early Golgi markers. These results as well as others previously discussed in Chapter 3 support the model that TRAPPII acts as a GEF for Ypt31 and not Ypt1.

**C. Open questions**

i. How are the two steps of Golgi cisternal progression coordinated?

As discussed above, Ypt1 and Ypt31 regulate two distinct steps of Golgi cisternal progression, early to transitional and transitional to late. The molecular mechanism of this process is unknown. Overexpression or hyper-activation of one of the Ypts only affects its own progression step, while there is no change in the progression step of the other Ypt. At a glance, this implies that there is no crosstalk or coordination between these two Ypts and their transport steps. However, this could be due to the addition of the overexpressed and/or hyper-activated Ypts from an external source. Under native conditions, there may be coordination by the regulators of Ypts to maintain similar levels of Ypt1 and Ypt31.

There is evidence that a GAP cascades occurs in the Golgi with Ypt32 and Ypt1 (Rivera-Molina and Novick 2009, Suda et al. 2013). This proposed GAP cascade would ensure that Ypt1 is not activated above the levels of Ypt31. Concurrently, to ensure that Ypt31 is activated to the same level as Ypt1, a GEF cascade would be an elegant solution. In this scenario, Ypt1 would interact with TRAPPII as an effector to recruit it for Ypt31/32 activation. However, a GEF cascade has not yet been shown between Ypt1 and Ypt31. Even without a GEF cascade, The TRAPP complex is an ideal candidate for regulating the levels of stimulated Ypts. One possibility is that the availability of TRAPPI or TRAPPII causes both Ypts to be activated at similar levels. The other possibility is that TRAPPI converts to TRAPPII as the Golgi matures to first activate Ypt1 and then activate Ypt31/32. The first question to address is whether TRAPP coordinates cisternal progression, and if not, to determine what other factors are involved in coordinating the levels of Ypts. The next question does not depend on the first, but addresses whether TRAPPI converts to TRAPPII as the Golgi matures.

ii. Which effectors of Ypt1 and Ypt31 are involved in cisternal progression?

Many effectors have been identified for these Ypts and their mammalian homologs. However, only some effectors are associated with the Golgi. In yeast, GTP-loaded purified Ypt1 was shown to bind with the COG tethering complex through its subunits Sec34/35 (Suvorova, Duden, and Lupashin 2002). Rab1 effectors, GM130 with GRASP65 and Golgin84 and Uso1, p115 in yeast, are Golgi related and have been implicated with Golgi ribbon homeostasis in mammalian cells (discussed in detail later) and could be the effector(s) involved in maintaining cisternal progression (Moyer, Allan, and Balch 2001, Diao et al. 2003, Sapperstein et al. 1996, Sapperstein et al. 1995, Cao,

Ballew, and Barlowe 1998, An et al. 2009, Satoh et al. 2003). For Ypt31 or Rab11, the effector Gyp1, is the proposed GAP for Ypt1 to function in a GAP cascade and could play a role in coordinating levels of activated Ypt1 and Ypt31 (Rivera-Molina and Novick 2009). The most promising candidate, Sec7, is proposed to be an effector of both Ypt1 and Ypt31. An earlier study performed by the Segev lab linked the Ypts to Sec7 with a genetic interaction, overexpression of Ypt1, Ypt31, or Ypt32 suppressed temperature sensitive growth phenotypes of Sec7 mutants (Jones et al. 1999). A recent study determined that Ypt1 and Ypt31 recruits Sec7 to liposomes in a GTP dependent manner and labels Sec7 as an effector of both Ypts (McDonold and Fromme 2014). Moreover, Sec7 is a promising candidate, as it acts as a GEF for Arf1, earlier discussed to be another component that is involved in cisternal progression.

iii. How does the partial sequestration of Ypt1 to autophagic pathways affect Golgi transport and cisternal progression?

In this study, I demonstrate that changes in levels of Ypt1 affect the dynamics of Golgi cisternal progression. However, in additional to its role in secretion and Golgi homeostasis, several studies from the Segev lab show that Ypt1 is required for general autophagy, as well as selective ER-phagy (Lipatova et al. 2012, Lipatova et al. 2013, Lipatova and Segev 2015). During nutrient starvation, the process of non-selective macro-autophagy is activated to engulf cellular components for degradation and recycling (Feng et al. 2014). The initial step of autophagy is the formation of the pre-autophagosomal structure, PAS, which requires Ypt1. Trs85, a component of TRAPPIII, recruits and activates Ypt1 to interact with its effector, Atg11, to organize other autophagic, Atg, proteins, which comprise the PAS (Lipatova et al. 2012). Under

conditions of stress or starvation where these pathways are activated, Ypt1 must be sequestered to the autophagic pathway. If there were a readily available pool of Ypts for all these pathways, the overexpression of Ypts would not have caused the changes of Golgi protein localization shown in Chapter 2. Currently, it is not known whether autophagy or Atgs affect secretion (Deretic, Jiang, and Dupont 2012). Moreover, it is not known whether the induction of non-selective autophagy will alter Golgi dynamics. If Golgi dynamics are reduced or halted when autophagy is activated, this would effectively switch major protein trafficking components away from secretion to autophagy. The cell would be investing in recycling cellular components for survival rather than transport of components for growth. This model would place Rab GTPases as a global regulator of multiple cellular pathways, not just of individual pathways steps.

iv. Is Ypt6 involved in the regulation of cisternal progression?

Besides Ypt1 and Ypt31/32, there are two other Ypts involved with exocytosis, Sec4 and Ypt6. Sec4 is not associated with the Golgi but regulates the transport of secretory vesicles at a stage after the Golgi and before the plasma membrane (Salminen and Novick 1989). Thus, Sec4 is probably not involved in Golgi compartmental regulation. Ypt6 is a non-essential GTPase that has a human homolog, Rab6, which localizes to the Golgi and has a role in its structural organization (Starr et al. 2010, Storrie et al. 2012). The role of Ypt6 is still controversial due to evidence for regulation of intra-Golgi transport as well as retrograde traffic from late endosomes to the Golgi (Li and Warner 1996, Siniossoglou, Peak-Chew, and Pelham 2000, Luo and Gallwitz 2003). Two recent studies show evidence of crosstalk occurring between Ypt6 and Ypt31/32. The first study shows that Ypt6 localizes to the Golgi and dissociates to

the cytosol when Ypt31/32 arrives. This study suggests that the putative GAP for Ypt6, Gyp6, is recruited by Ypt32 to facilitate the removal of Ypt6 in a GAP cascade (Suda et al. 2013). The second study shows that Trs130 interacts with Gyp6. A possible model is suggested where TRAPPII coordinates the recruitment of Ypt31/32 with the removal of Ypt6 (Brunet et al. 2016). These links found between Ypt6 and Ypt31/32 allow for coordination of these Ypts. Since Ypt31/32 is involved in regulation of cisternal progression, an open question to explore is whether Ypt6 or Rab6 also a role.

v. Do mammalian Rab1 and Rab11 regulate Golgi stacks?

To determine whether the results found in this study are relevant for human cells, it is important to determine if the mammalian homologs of Ypt1 and Ypt31, Rab1 and Rab11 respectively, regulate the progression of Golgi in mammalian cells. Mammalian Golgi is formed in paralleled stacks and linked together (Marra et al. 2007). The initial question to be addressed is whether the process of Golgi cisternal progression occurs within these Golgi stacks, or if they are stationary as described by the anterograde vesicular transport in a stable Golgi model (Orci et al. 1997, Orci et al. 2000). If some form of Golgi maturation does occur within the stacks, it would be beneficial to know whether Rabs play a role in the regulation of that process. Two recent studies have shown evidence for and against Cisternal maturation in mammalian Golgi stacks and thus the field is not yet unified on a single Golgi model (Lavieu, Zheng, and Rothman 2013, Rizzo et al. 2013).

Regardless of whether the Golgi undergoes maturation in mammalian cells, Rab1 and Rab11 may have roles in stabilizing or regulating Golgi stack homeostasis. A recent study showed that a Rab1 mutant that cannot perform nucleotide exchange in rat

embryonic fibroblasts causes Golgi stack dispersion and disassembly (Wilson et al. 1994). It would be interesting to study what hyper-activated Rab1 or Rab11 would do to the structure of the mammalian Golgi stacks. GM130, mentioned above as an effector of Rab1, is implicated as having an important role for membrane incorporation into Golgi stacks and in the absence of GM130, the Golgi ribbon is broken down (Marra et al. 2007). Although there are indications that Rab1 is involved in mammalian Golgi structure, the exact function and mechanism of these Rab GTPases in regulating Golgi membrane dynamics is still an open question.

# CHAPTER 5. MATERIALS AND METHODS

All materials and methods are taken the three published papers (Kim et al. 2016, Taussig et al. 2013, Lipatova et al. 2012) unless otherwise noted.

## A. Antibodies and reagents

The sources of antibodies used in this study are detailed below in the sections for their specific use. All reagents were purchased from Fisher Scientific (Bridgewater, NJ) except for: media components other than amino acids from US Biological (Swampscott, MA); ProtoGel for immuno-blots from National Diagnostics (Atlanta, GA); detection reagents for immuno-blots from GE Healthcare Life Sciences (Buckinghamshire, UK); film from Denville Scientific (Holliston, MA); glass beads from BioSpec Products (Bartlesville, OK); PCR reagents, restriction enzymes and buffers from New England BioLabs (Ipswich, MA); hygromycin B (Hyg) and geneticin (G418) from Invitrogen (Carlsbad, CA); and nourseothricin (Nat) from Jena Bioscience (Jena, Germany).

## B. Protein level analysis

Levels of Ypt1 and Ypt31 in cell lysates were determined from exponentially growing cells normalized to the same OD600 as previously described (Lipatova et al. 2012). Lysates were subjected to immuno-blot analysis using affinity-purified rabbit anti-Ypt1 or anti-Ypt31 antibodies (Jedd, Mulholland, and Segev 1997). Loading control was determined using rabbit anti-G6PDH antibodies (Sigma). Quantification of bands was performed with ImageJ software (National Institute of Health).

For Chapter 3, anti-GFP (mouse, Roche) and anti-Trs20 (rabbit, generaously provided by M. Sacher) were used. To compare the expression of yeast proteins for this study, 5 OD600 units of cells were harvested for each sample. Each was resuspended in 10% TCA, and lysed with glass beads in the presence of urea, as described previously (Graham and Emr 1991), except that TCA was used at a final concentration of 10%, and samples were vortexed with glass beads for 3 min.

**C. Fluorescence microscopy**

Fluorescence microscopy of cells grown to mid-log phase (in flasks) was done using a Zeiss Confocal LSM700 microscope controlled by Zen software. Images were captured using a 100x/1.45 NA objective. Laser lines used: 488nm for GFP/YFP/FITC, 555nm for mCherry/mRFP/Texas Red, and 639nm for Alexa Fluor® 647. To limit photo bleaching, all images were taken as fast as possible and within 10 minutes of slide preparation and using minimal laser strength.

i. Live-cell imaging

For live-cell imaging Z-stacks were taken at 0.35 μm increments. Only the microscopy for Figure 6 was performed on a deconvolution Zeiss Axiovision microscope (Carl Zeiss, Thornwood, NY) with FITC, fluorescein isothiocyanate (yEVenus) and Texas Red (mCherry) filters. Co-localization was quantified by counting puncta that do or do not overlap through several z-stacks and the stack with the highest amount of co-localization was selected. Random images of Golgi marker co-localization from Figure 5 were processed with the JACoP plugin to determine the Pearson's coefficient

of co-localization (by pixels). Pearson's coefficient confirmed the relative map of the Golgi proteins determined by counting puncta.

ii. Immunofluorescence

Immunofluorescence was done with Ibidi µ-slide 8-well coated (Poly-L-Lysine) microscopy chambers using affinity-purified anti-Ypt1 and anti-Ypt31 antibodies as previously described (Jedd, Mulholland, and Segev 1997). The following dye-conjugated secondary antibodies were purchased from Jackson Immunoresearch: Texas Red® dye-conjugated AffiniPure Goat Anti-Rabbit IgG; Alexa Fluor® 647-conjugated AffiniPure Goat Anti-Rabbit IgG; Fluorescein (FITC)-conjugated AffiniPure Goat Anti-Rabbit IgG. Co-localization was quantified by counting puncta that do or do not overlap on a single focal plane. Only the microscopy for Figure 24, Appendix was performed on a deconvolution Zeiss Axiovision microscope (Carl Zeiss, Thornwood, NY) with a FITC, fluorescein isothiocyanate filter.

iii. Time-lapse microscopy

Time-lapse microscopy was performed using the Zen software. One focal plane was followed for approximately 2 minutes. The resulting movies were analyzed using Fiji software (Schindelin et al. 2012). Images were measured for photobleach-correction and then adjusted with Gaussian filters. Single puncta were selected to track over time and measured for average fluorescence intensity. The resulting curves were adjusted to the same minimum/maximum range (0-1) using the equation previously detailed (Daboussi, Costaguta, and Payne 2012). Puncta were chosen as being a single color followed closely by the second color in the order of anterograde traffic as previously described (Losev et al. 2006). Statistical significance of the time-lapse curve

calculations were tested using the unpaired, Student's *t*-Test with GraphPad Software (http://www.graphpad.com/quickcalcs/ttest1/?Format=50).

iv. BiFC microscopy

For the bimolecular fluorescence complementation (BiFC) assays, cells (NSY128) were transformed with two plasmids expressing Trs120-YFP-C and YFPN-Trs20 or YFP-N-Trs20-D46Y; or CFP-N-Bet3 with CFP-C-Trs20 or CFPC-Trs20-D46Y for Figure 19. For Figure 21, Trs130-YFP-N and Bet3-YFP-C expression plasmids were used. Independent transformants were grown to mid-log phase, and YFP or CFP fluorescence were visualized using a Zeiss Confocal LSM 700 microscope.

## D. Construction of yeast strains and growth

The yeast strains used in this thesis are listed in Table IV. Strains were constructed by transformation and homologous recombination. Golgi proteins were tagged on the chromosome at their C-termini with mRFP, GFP, mCherry, or yEGFP using a standard technique (Wach et al., 1997) using appropriate plasmids listed in the plasmid table. All GFP-tagged strains were checked to ensure that the tagged product is stable by using immuno-blot analysis and mouse monoclonal anti-GFP antibodies (Roche Diagnostics). Media preparation and yeast culture growth were done as previously described in Segev and Botstein (Segev and Botstein 1987).

**Table IV. Yeast Strains used for this study**

| NSY number | Alias | Genotype | Reference |
|---|---|---|---|
| NSY862 | Cop1-mRFP | *mat alpha his3 delta1 leu2 delta 0 lys2 delta 0 ura3 delta 0 COP1::mRFP-kanMX6* | (Huh et al. 2003) |
| NSY1733 | Cop1-mRFP Vrg4-yEGFP | *NSY862 VRG4::yEGFP-nat* | (Kim et al. 2016) |
| NSY1734 | Cop1-mRFP Sec7-yEGFP | *NSY862 SEC7::yEGFP-nat* | (Kim et al. 2016) |
| NSY1735 | Cop1-mRFP Chc1-GFP | *NSY862 CHC1::GFP-hyg* | (Kim et al. 2016) |
| NSY863 | Chc1-mRFP | *mat alpha his3 delta1 leu2 delta 0 lys2 delta 0 ura3 delta 0 CHC1::mRFP-kanMX6* | (Huh et al. 2003) |
| NSY1736 | Chc1-mRFP Vrg4-yEGFP | *NSY863 VRG4::yEGFP-nat* | (Kim et al. 2016) |
| NSY1737 | Chc1-mRFP Cop1-GFP | *NSY863 COP1::GFP-hyg* | (Kim et al. 2016) |
| NSY1738 | Chc1-mRFP Sec7-yEGFP | *NSY863 SEC7::yEGFP-nat* | (Kim et al. 2016) |
| NSY825 | WT- BY4741 | *mat a leu2 delta 0 ura3 delta 0 his3 delta 1 met15 delta 0* | (Brachmann et al. 1998) |
| NSY1739 | Sec7-mCherry | BY4741 SEC7::mCherry-NatR | (Kim et al. 2016) |
| NSY1740 | Vrg4-yEGFP | BY4741 VRG4::yEGFP-NatR | (Kim et al. 2016) |
| NSY1221 | yEGFP-Ypt31/ypt31Δ | *mat alpha ade2 ura3-52 leu2-3,112 his3 delta 200 lys2 ypt32::kan yEGFP-Ypt31(LYS2) in Ypt31 locus* | (Kim et al. 2016) |
| NSY1741 | yEGFP-Ypt31/ypt31Δ Sec7-mRFP | *mat alpha ade2 ura3-52 leu2-3,112 his3 delta 200 lys2 ypt32::kan yEGFP-Ypt31(LYS2) in Ypt31 locus SEC7::mRFP-HygR* | (Kim et al. 2016) |
| NSY1742 | Chc1-GFP | BY4741 CHC1::GFP-HygR | (Kim et al. 2016) |
| NSY1743 | Chc1-GFP Sec7-mRFP | BY4741 CHC1::GFP-HygR SEC7::mRFP-G418R | (Kim et al. 2016) |
| NSY1744 | Sec7-mRFP | BY4741 SEC7::mRFP-G418R | (Kim et al. 2016) |
| NSY1745 | Cop1-GFP Sec7-mRFP | BY4741 SEC7::mRFP-G418R COP1::GFP-HygR | (Kim et al. 2016) |
| NSY128 | WT- DBY4985 | *mat alpha ade2 his3 delta 200 leu2-3,112 lys2-801 ura3-52* | David Botstein |
| NSY1746 | Chc1-GFP | NSY128 CHC1::GFP-HygR | (Kim et al. 2016) |

| | | | |
|---|---|---|---|
| NSY1747 | Chc1-GFP Sec7-mRFP | NSY128 CHC1::GFP-HygR SEC7::mRFP-G418R | (Kim et al. 2016) |
| NSY1748 | Cop1-GFP | NSY128 COP1::GFP-HygR | (Kim et al. 2016) |
| NSY1749 | Cop1-GFP Sec7-mRFP | NSY128 COP1::GFP-HygR SEC7::mRFP-G418R | (Kim et al. 2016) |
| NSY1541 | *ypt1Δ* + pRS316-Ypt1 | NSY128 pRS316-YPT1 yptt1 delta::HygR | (Lipatova et al. 2013) |
| NSY302 | *ypt31Δ/ypt32Δ* + pRS316-Ypt31 | *mat alpha ade2 his3 delta 200 leu2-3 lys2 ura3-52 deltaYPT31::HIS2 pRS316-Ypt31 deltaYPT32::KanR pRS316-Ypt31* | (Jedd, Mulholland, and Segev 1997) |
| NSY220 | WT- YPT1 | *mat alpha ura3-52 lys2 his4* | (Liang et al. 2007) |
| NSY222 | *ypt1ts* | *mat alpha ura3-52 his4 ypt1A136D* | (Liang et al. 2007) |
| NSY125 | WT- YPT31/32 | *mat a ura3-52 lys2 his4* | (Jones et al. 1999) |
| NSY348 | *ypt31Δ/ypt32ts* | *mat a ura3-52 lys2 his4-539 deltaYPT31::HIS3 ypt32-A141D* | (Jones et al. 1999) |
| NSY1750 | YPT1 Sec7-mRFP | NSY1081 SEC7::mRFP-G418R | (Kim et al. 2016) |
| NSY1754 | YPT1 Sec7-mRFP Cop1-GFP | NSY1081 SEC7::mRFP-G418R COP1::GFP-HygR | (Kim et al. 2016) |
| NSY1756 | YPT1 Sec7-mRFP Chc1-GFP | NSY1081 SEC7::mRFP-G418R CHC1::GFP-HygR | (Kim et al. 2016) |
| NSY1751 | *ypt1ts* Sec7-mRFP | NSY1082 SEC7::mRFP-G418R | (Kim et al. 2016) |
| NSY1758 | *ypt1ts* Sec7-mRFP Cop1-GFP | NSY1082 SEC7::mRFP-G418R COP1::GFP-HygR | (Kim et al. 2016) |
| NSY1760 | *ypt1ts* Sec7-mRFP Chc1-GFP | NSY1082 SEC7::mRFP-G418R CHC1::GFP-HygR | (Kim et al. 2016) |
| NSY1752 | YPT31/32 Sec7-mRFP | NSY125 SEC7::mRFP-G418R | (Kim et al. 2016) |
| NSY1762 | YPT31/32 Sec7-mRFP Cop1-GFP | NSY125 SEC7::mRFP-G418R COP1::GFP-HygR | (Kim et al. 2016) |
| NSY1764 | YPT31/32 Sec7-mRFP Chc1-GFP | NSY125 SEC7::mRFP-G418R CHC1::GFP-HygR | (Kim et al. 2016) |
| NSY1753 | *ypt31Δ/ypt32ts* Sec7-mRFP | NSY348 SEC7::mRFP-G418R | (Kim et al. 2016) |
| NSY1766 | *ypt31Δ/ypt32ts* Sec7-mRFP Cop1-GFP | NSY349 SEC7::mRFP-G418R COP1::GFP-HygR | (Kim et al. 2016) |
| NSY1768 | *ypt31Δ/ypt32ts* Sec7-mRFP Chc1-GFP | NSY350 SEC7::mRFP-G418R CHC1::GFP-HygR | (Kim et al. 2016) |

| | | | |
|---|---|---|---|
| NSY1770 | Trs130-yEGFP | BY4741 TRS130::yEGFP-Nat$^R$ | This study |
| NSY1771 | Trs130-yEGFP Cop1-mRFP | BY4741 TRS130::yEGFP-Nat$^R$ COP1::mRFP | This study |
| NSY1772 | Trs130-yEGFP Sec7-ytagmRFP | BY4741 TRS130::yEGFP-Nat$^R$ SEC7::ytagmRFP | This study |
| NSY1773 | Trs130-yEGFP Chc1-mRFP | BY4741 TRS130::yEGFP-Nat$^R$ | This study |
| NSY864 | Sec13-mRFP | *mat alpha his3 delta1 leu2 delta 0 lys2 delta 0 ura3 delta 0 SEC13::mRFP-kanMX6* | (Huh et al. 2003) |
| NSY865 | Snf7-mRFP | *mat alpha his3 delta1 leu2 delta 0 lys2 delta 0 ura3 delta 0 SNF7::mRFP-kanMX6* | (Huh et al. 2003) |
| NSY752 | Y2H-haploid-alpha | *MATα trp1-901 leu2-3,112 ura3-52 his3-200 gal4Δ gal80Δ gal2-ade2 lys2::gal1-his3 met2::gal7-lacZ* | (James, Halladay, and Craig 1996) |
| NSY468 | Y2H-haploid-A | *MATa trp1-901 leu2-3,112 ura3-52 his3-200 gal4Δ gal80Δ GAL2-ADE2 LYS2:GAL1-HIS3 met2::GAL7-lacZ* | (James, Halladay, and Craig 1996) |
| NSY125 | WT- YPT1 | DBY1034 *MATa his4-539 lys2-801 ura3-52* | David Botstein |
| NSY55 | *ypt1-1* | DBY1803 *MATa his4-539 lys2-801 ura3-52 ypt1-T40K* | David Botstein |

**E. Construction of plasmids**

The plasmids used in this thesis are listed in Table V. Plasmid for expression of mCherry-Ypt1 was constructed by sub-cloning mCherry to replace yEVenus in pNS1430. pNS220 (pRS316-Ypt31) was described in (Jedd, Mulholland, and Segev 1997). pNS939 (pRS317-Ypt31) was made by sub-cloning the Ypt31 containing ClaI-XbaI fragment from pRS316-Ypt31 into pRS317. pNS939 (pRS317-yEGFP-Ypt31) was made as follows: first, PciI site was removed from the vector backbone and introduced upstream of Ypt31 by site-directed mutagenesis, then yEGFP was cloned in frame with Ypt31 using PciI. pNS993 was previously described (Liang et al. 2007). pNS1556 (Ypt1Q67L in a 2μ *LEU2*) was made by site-directed mutagenesis of pNS993. pNS1557 (pFA6a-GFP-HygR) was made by replacing G418R cassette with HygR cassette using BglII and SacI sites. pNS1533 (pKT-yEGFP-NatR) was made by replacing G418R cassette with NatR cassette using BglII and SacI sites. The *CEN* plasmids, pNS1558 and pNS1559 were constructed by sub-cloning Ypt1Q67L and Ypt31Q72L from the 2μ plasmids pNS1556 and pNS782, respectively, using the Sal1 and Xba1 sites of pNS245 (*CEN Leu2*).

**Table V. Plasmids used for this study**

| PNS number | Alias | Genotype | Reference |
|---|---|---|---|
| pNS245 | empty *CEN* | pRS315 *CEN, LEU2,* Amp$^r$ | (Sikorski and Hieter 1989) |
| pNS1430 | yEVenus-Ypt1 | pRS315-yEVenus-*YPT1* | (Taussig et al. 2013) |
| pNS1431 | mCherry-Ypt1 | pRS315-mCherry-*YPT1* | (Kim et al. 2016) |
| pNS1364 | *CEN* Ypt1 | pRS315-*YPT1* | (Lipatova et al. 2012) |
| pNS661 | GFP-Ypt31 | pRS315-GFP-*YPT31* | Ruth Collins |
| pNS221 | *CEN* Ypt31 | pRS315-*YPT31* | (Jedd, Mulholland, and Segev 1997) |
| pNS246 | empty *CEN* | pRS316 *CEN, URA3,* Amp$^r$ | (Sikorski and Hieter 1989) |
| pNS636 | *CEN* Ypt1 | pRS316-*YPT1* | Ruth Collins |
| pNS220 | *CEN* Ypt31 | pRS316-*YPT31* | (Jedd, Mulholland, and Segev 1997) |
| pNS719 | empty *CEN* | pRS317 *CEN, LYS2, Amp$^r$* | (Eriksson et al. 2004) |
| pNS939 | *CEN* Ypt31 | pRS317-*YPT31* | (Kim et al. 2016) |
| pNS994 | yEGFP-Ypt31 | pRS317-yEGFP-*YPT31* | (Kim et al. 2016) |
| pNS180 | empty 2µ | pRS425 2µ, *LEU2,* Amp$^r$ | (Sikorski and Hieter 1989) |
| pNS993 | 2µ Ypt1 | YEp423-*YPT1 LEU2* | (Liang et al. 2007) |
| pNS1556 | 2µ Ypt1-GTP | YEp423-*YPT1Q67L* | (Kim et al. 2016) |
| pNS781 | 2µ Ypt31 | pRS425-*Ypt31* | Scott Emr |
| pNS782 | 2µ Ypt31-GTP | pRS425-*YPT31Q72L* | Scott Emr |
| pNS274 | empty 2µ | YEp24 2µ, *URA3,* Amp$^r$ | New England Biolabs, MA |

| | | | |
|---|---|---|---|
| pNS489 | 2μ Ypt1 | YEp24-*YPT1* | (Morozova et al. 2006) |
| pNS229 | 2μ Ypt31 | YEp24-*YPT31* | (Jones et al. 1999) |
| pNS1527 | tagging plasmid | pFA6a-mRFP-G418$^r$ | (Huh et al. 2003) |
| pNS1557 | tagging plasmid | pFA6a-GFP-Hyg$^r$ | (Kim et al. 2016) |
| pNS1506 | tagging plasmid | pKT127-yEGFP replaced with mCherry-G418r replaced with Natr | (Lipatova and Segev 2015) |
| pNS1533 | tagging plasmid | pKT127-yEGFP-G418r replaced with Nat$^r$ | (Kim et al. 2016) |
| pNS1558 | *CEN* Ypt1-GTP | pRS315-YPT1Q67L | (Kim et al. 2016) |
| pNS1559 | *CEN* Ypt31-GTP | pRS315-YPT31Q72L | (Kim et al. 2016) |
| pNS1432 | CFP-N-Bet3 | pRS416-CFP-N-BET3 | (Taussig et al. 2013) |
| pNS1428 | CFP-C-Trs20 | pRS413-CFP-C-TRS20 | (Taussig et al. 2013) |
| pNS1429 | CFP-C-Trs20D46Y | pRS413-CFP-C-*trs20D46Y* | (Taussig et al. 2013) |
| pNS1435 | YFP-C-Trs120 | pRS413-YFP-C-TRS120 | (Taussig et al. 2013) |
| pNS1433 | YFP-N-Trs20 | pRS416-YFP-N-TRS20 | (Taussig et al. 2013) |
| pNS1434 | YFP-N-Trs20D46Y | pRS416-YFP-N-*trs20D46Y* | (Taussig et al. 2013) |
| pNS1560 | Tagging plasmid | pFA6a-ytagmRFP-G418$^r$ | This study |
| pNS1561 | YFP-N-Trs130 | pRS-YFP-N-TRS130 | This study |
| pNS1562 | YFP-C-Bet3 | pRS-YFP-C-BET3 | This study |
| pNS1101 | AD | pACT2-Gal4-activation domain- LEU2, Amp$^R$ | Clontech |
| pNS206 | BD | pGBDU-C2-Gal4-binding domain-URA3, Amp$^R$ | (James, Halladay, and Craig 1996) |
| pNS1390 | AD-Atg11 | pACT2-ATG11 | (Lipatova et al. 2012) |
| pNS1342 | AD-Atg11 CC2-3 | pACT2-ATG11-CC2-3 | (Lipatova et al. 2012) |

| | | | |
|---|---|---|---|
| pNS969 | BD-Ypt1Q | pGBDU -C2-YPT1-Q67L | (Lipatova et al. 2012) |
| pNS1392 | BD-Ypt6Q | pGBDU -C2-YPT6-Q69L | (Lipatova et al. 2012) |
| pNS1391 | BD-Ypt31Q | pGBDU-C2-YPT31Q72L | (Lipatova et al. 2012) |
| pNS1390 | BD-Sec4Q | pGBDU-C2-SEC4-Q79L | (Lipatova et al. 2012) |

## APPENDIX

In this dissertation, I have shown a role for Ypt1 in the secretory transport pathway, specifically with Golgi cisternal progression dynamics. However, Ypt1 has another cellular function, the regulation of autophagic pathways. Three studies have shown that Trs85 is a part of the TRAPPIII complex and is also involved in autophagy (Meiling-Wesse et al. 2005, Nazarko et al. 2005, Lynch-Day et al. 2010). In this appendix, I present two figures that I contributed for a study published by the Segev lab. This study demonstrates that the Trs85-Ypt1-Atg11 module organizes the pre-autophagosomal structure, or PAS (Lipatova et al. 2012).

Lynch-Day et al. show that Trs85 is the GEF for Ypt1 in autophagy. Furthermore, the activated GTP-locked mutant of Ypt1, Ypt1Q67L, is able to suppress the Trs85 deletion phenotype (Lynch-Day et al. 2010). However, this study did not determine the role for activated Ypt1 in autophagy. First, I show that Ypt1Q67L interacts with Atg11 by yeast-2-hybrid, Y2H, analysis (Figure 23). The interaction of Ypt1 is with the coiled-coil 2 and 3, CC2-3, domains of Atg11. This interaction is Ypt specific, as none of the other secretory pathway Ypts interacts with Atg11. The protein levels of these Ypts were determined by western blotting to ensure that the negative results are not due to low expression from the Y2H plasmids (Figure 23).

To confirm the Ypt1Q-Atg11 interaction, pull-downs from yeast and bacteria were performed (Lipatova et al. 2012). Once Atg11 was established as an effector of Ypt1, this interaction was visualized *in vivo* using BiFC analysis. A negative control, Ypt1-1 mutant protein was used for all these assays. This mutant has an amino acid substitution (T40K) in the effector-binding domain that abolishes the Ypt1-Atg11

interaction. This mutant was unable to interact with Atg11 in Y2H, pull-down and BiFC analysis. However, for BiFC analysis, we wanted to ensure that the Ypt1-1 mutant protein was still capable of producing a punctate signal. Tagged-Ypt1-1 proved non-functional as a sole-copy in the cell, therefore, IF was performed with anti-Ypt1 antibodies in a wild type and *ypt1-1* mutant strains (Figure 24). These IF results provided evidence that Ypt1 and Ypt1-1 proteins share the same punctate pattern. Other results from this study show that the Trs85-Ypt1-Atg11 module is required for organizing autophagy proteins, Atgs, at the pre-autophagosomal, PAS, which is required for the onset of autophagy. Furthermore, because Trs85 and Atg11 are not involved in the secretory pathway or for ER-to-Golgi transport, this study provided further evidence that Ypts/Rabs can regulate two independent transport pathways with different GEF/effector accessory factors.

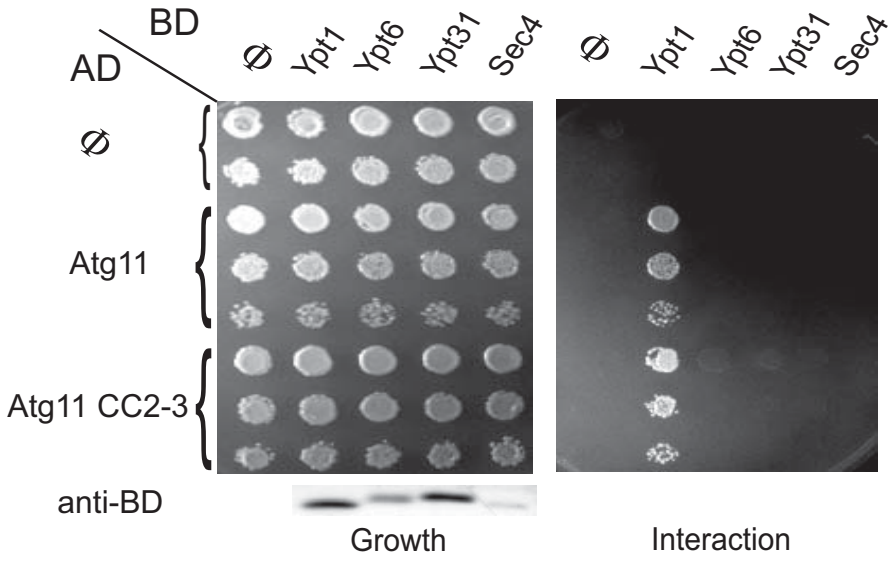


**Figure 23. Ypt1 interacts with Atg11 CC2-3 domain.** Ypt1, but not the other Ypts in the secretory pathway, interacts with Atg11 in the yeast-two-hybrid (Y2H) assay. Immuno-blot analysis performed with the anti-binding domain, anti-BD, antibody shows expression of the different Ypt proteins. Growth is shown on synthetic dextrose-Ura-Leu plates, whereas interaction is shown on synthetic dextrose-Ura-Leu-His plates. One to two 10-fold dilutions are shown from top to bottom. Results are representative of at least two independent experiments. Empty AD and BD plasmids served as negative controls for interaction.

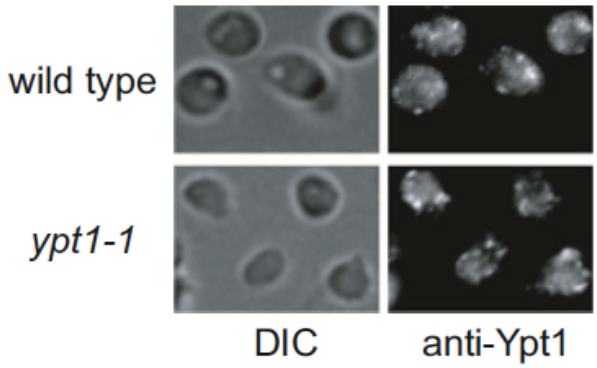


**Figure 24. Intracellular localization of the Ypt1-1 mutant protein is similar to that of wild type Ypt1.** Ypt1 localization was determined by IF using anti-Ypt1 antibodies in wild type and *ypt1-1* mutant strains. Images were acquired using a Zeiss deconvolution Axioscope microscope with the FITC filter. DIC, differential interference contrast.

## CITED LITERATURE


Albert, S., E. Will, and D. Gallwitz. 1999. "Identification of the catalytic domains and their functionally critical arginine residues of two yeast GTPase-activating proteins specific for Ypt/Rab transport GTPases." *EMBO J* 18 (19):5216-25. doi: 10.1093/emboj/18.19.5216.

An, Y., C. Y. Chen, B. Moyer, P. Rotkiewicz, M. A. Elsliger, A. Godzik, I. A. Wilson, and W. E. Balch. 2009. "Structural and functional analysis of the globular head domain of p115 provides insight into membrane tethering." *J Mol Biol* 391 (1):26-41. doi: 10.1016/j.jmb.2009.04.062.

Barrowman, J., D. Bhandari, K. Reinisch, and S. Ferro-Novick. 2010. "TRAPP complexes in membrane traffic: convergence through a common Rab." *Nat Rev Mol Cell Biol* 11 (11):759-63. doi: 10.1038/nrm2999.

Beitz, J. M. 2014. "Parkinson's disease: a review." *Front Biosci (Schol Ed)* 6:65-74.

Bhave, M., E. Papanikou, P. Iyer, K. Pandya, B. K. Jain, A. Ganguly, C. Sharma, K. Pawar, J. Austin, 2nd, K. J. Day, O. W. Rossanese, B. S. Glick, and D. Bhattacharyya. 2014. "Golgi enlargement in Arf-depleted yeast cells is due to altered dynamics of cisternal maturation." *J Cell Sci* 127 (Pt 1):250-7. doi: 10.1242/jcs.140996.

Brachmann, C. B., A. Davies, G. J. Cost, E. Caputo, J. Li, P. Hieter, and J. D. Boeke. 1998. "Designer deletion strains derived from Saccharomyces cerevisiae S288C: a useful set of strains and plasmids for PCR-mediated gene disruption and other applications." *Yeast* 14 (2):115-32. doi: 10.1002/(SICI)1097-0061(19980130)14:2<115::AID-YEA204>3.0.CO;2-2.

Brunet, S., B. Noueihed, N. Shahrzad, D. Saint-Dic, B. Hasaj, T. L. Guan, A. Moores, C. Barlowe, and M. Sacher. 2012. "The SMS domain of Trs23p is responsible for the in vitro appearance of the TRAPP I complex in Saccharomyces cerevisiae." *Cell Logist* 2 (1):28-42. doi: 10.4161/cl.19414.

Brunet, S., and M. Sacher. 2014. "In sickness and in health: the role of TRAPP and associated proteins in disease." *Traffic* 15 (8):803-18. doi: 10.1111/tra.12183.

Brunet, S., N. Shahrzad, D. Saint-Dic, H. Dutczak, and M. Sacher. 2013. "A trs20 mutation that mimics an SEDT-causing mutation blocks selective and non-

selective autophagy: a model for TRAPP III organization." *Traffic* 14 (10):1091-104. doi: 10.1111/tra.12095.

Brunet, Stephanie, Djenann Saint-Dic, Miroslav P. Milev, Tommy Nilsson, and MICHAEL SACHER. 2016. "The TRAPP subunit Trs130p interacts with the GAP Gyp6p to mediate Ypt6p dynamics at the late Golgi." *Frontiers in Cell and Developmental Biology* 4. doi: 10.3389/fcell.2016.00048.

Buggia-Prevot, V., C. G. Fernandez, S. Riordan, K. S. Vetrivel, J. Roseman, J. Waters, V. P. Bindokas, R. Vassar, and G. Thinakaran. 2014. "Axonal BACE1 dynamics and targeting in hippocampal neurons: a role for Rab11 GTPase." *Mol Neurodegener* 9:1. doi: 10.1186/1750-1326-9-1.

Cai, H., Y. Zhang, M. Pypaert, L. Walker, and S. Ferro-Novick. 2005. "Mutants in trs120 disrupt traffic from the early endosome to the late Golgi." *J Cell Biol* 171 (5):823-33. doi: 10.1083/jcb.200505145.

Cai, Y., H. F. Chin, D. Lazarova, S. Menon, C. Fu, H. Cai, A. Sclafani, D. W. Rodgers, E. M. De La Cruz, S. Ferro-Novick, and K. M. Reinisch. 2008. "The structural basis for activation of the Rab Ypt1p by the TRAPP membrane-tethering complexes." *Cell* 133 (7):1202-13. doi: 10.1016/j.cell.2008.04.049.

Calvo, A., N. Xiao, J. Kang, C. J. Best, I. Leiva, M. R. Emmert-Buck, C. Jorcyk, and J. E. Green. 2002. "Alterations in gene expression profiles during prostate cancer progression: functional correlations to tumorigenicity and down-regulation of selenoprotein-P in mouse and human tumors." *Cancer Res* 62 (18):5325-35.

Cao, X., N. Ballew, and C. Barlowe. 1998. "Initial docking of ER-derived vesicles requires Uso1p and Ypt1p but is independent of SNARE proteins." *EMBO J* 17 (8):2156-65. doi: 10.1093/emboj/17.8.2156.

Caro, L. G., and G. E. Palade. 1964. "Protein Synthesis, Storage, and Discharge in the Pancreatic Exocrine Cell. An Autoradiographic Study." *J Cell Biol* 20:473-95.

Chang, J. Y., M. H. Lee, S. R. Lin, L. Y. Yang, H. S. Sun, C. I. Sze, Q. Hong, Y. S. Lin, Y. T. Chou, L. J. Hsu, M. S. Jan, C. X. Gong, and N. S. Chang. 2015. "Trafficking protein particle complex 6A delta (TRAPPC6ADelta) is an extracellular plaque-forming protein in the brain." *Oncotarget* 6 (6):3578-89. doi: 10.18632/oncotarget.2876.

Chen, S. H., S. Chen, A. A. Tokarev, F. Liu, G. Jedd, and N. Segev. 2005. "Ypt31/32 GTPases and their novel F-box effector protein Rcy1 regulate protein recycling." *Mol Biol Cell* 16 (1):178-92. doi: 10.1091/mbc.E04-03-0258.

Chen, S. H., A. H. Shah, and N. Segev. 2011. "Ypt31/32 GTPases and their F-Box effector Rcy1 regulate ubiquitination of recycling proteins." *Cell Logist* 1 (1):21-31. doi: 10.4161/cl.1.1.14695.

Cheng, K. W., J. P. Lahad, W. L. Kuo, A. Lapuk, K. Yamada, N. Auersperg, J. Liu, K. Smith-McCune, K. H. Lu, D. Fishman, J. W. Gray, and G. B. Mills. 2004. "The RAB25 small GTPase determines aggressiveness of ovarian and breast cancers." *Nat Med* 10 (11):1251-6. doi: 10.1038/nm1125.

Choi, C., M. Davey, C. Schluter, P. Pandher, Y. Fang, L. J. Foster, and E. Conibear. 2011. "Organization and assembly of the TRAPPII complex." *Traffic* 12 (6):715-25. doi: 10.1111/j.1600-0854.2011.01181.x.

Chung, Y. C., W. C. Wei, S. H. Huang, C. M. Shih, C. P. Hsu, K. J. Chang, and W. T. Chao. 2014. "Rab11 regulates E-cadherin expression and induces cell transformation in colorectal carcinoma." *BMC Cancer* 14:587. doi: 10.1186/1471-2407-14-587.

Cooper, A. A., A. D. Gitler, A. Cashikar, C. M. Haynes, K. J. Hill, B. Bhullar, K. Liu, K. Xu, K. E. Strathearn, F. Liu, S. Cao, K. A. Caldwell, G. A. Caldwell, G. Marsischky, R. D. Kolodner, J. Labaer, J. C. Rochet, N. M. Bonini, and S. Lindquist. 2006. "Alpha-synuclein blocks ER-Golgi traffic and Rab1 rescues neuron loss in Parkinson's models." *Science* 313 (5785):324-8. doi: 10.1126/science.1129462.

Dabbeekeh, J. T., S. L. Faitar, C. P. Dufresne, and J. K. Cowell. 2007. "The EVI5 TBC domain provides the GTPase-activating protein motif for RAB11." *Oncogene* 26 (19):2804-8. doi: 10.1038/sj.onc.1210081.

Daboussi, L., G. Costaguta, and G. S. Payne. 2012. "Phosphoinositide-mediated clathrin adaptor progression at the trans-Golgi network." *Nat Cell Biol* 14 (3):239-48. doi: 10.1038/ncb2427.

Deretic, V., S. Jiang, and N. Dupont. 2012. "Autophagy intersections with conventional and unconventional secretion in tissue development, remodeling and inflammation." *Trends Cell Biol* 22 (8):397-406. doi: 10.1016/j.tcb.2012.04.008.

Diao, A., D. Rahman, D. J. Pappin, J. Lucocq, and M. Lowe. 2003. "The coiled-coil membrane protein golgin-84 is a novel rab effector required for Golgi ribbon formation." *J Cell Biol* 160 (2):201-12. doi: 10.1083/jcb.200207045.

Du, L. L., R. N. Collins, and P. J. Novick. 1998. "Identification of a Sec4p GTPase-activating protein (GAP) as a novel member of a Rab GAP family." *J Biol Chem* 273 (6):3253-6.

Eriksson, P., L. R. Thomas, A. Thorburn, and D. J. Stillman. 2004. "pRS yeast vectors with a LYS2 marker." *Biotechniques* 36 (2):212-3.

Farquhar, M. G., and G. E. Palade. 1981. "The Golgi apparatus (complex)-(1954-1981)-from artifact to center stage." *J Cell Biol* 91 (3 Pt 2):77s-103s.

Feng, Y., D. He, Z. Yao, and D. J. Klionsky. 2014. "The machinery of macroautophagy." *Cell Res* 24 (1):24-41. doi: 10.1038/cr.2013.168.

Gentzsch, M., X. B. Chang, L. Cui, Y. Wu, V. V. Ozols, A. Choudhury, R. E. Pagano, and J. R. Riordan. 2004. "Endocytic trafficking routes of wild type and DeltaF508 cystic fibrosis transmembrane conductance regulator." *Mol Biol Cell* 15 (6):2684-96. doi: 10.1091/mbc.E04-03-0176.

Giorgini, F., and J. R. Steinert. 2013. "Rab11 as a modulator of synaptic transmission." *Commun Integr Biol* 6 (6):e26807. doi: 10.4161/cib.26807.

Glick, B. S., and A. Luini. 2011. "Models for Golgi traffic: a critical assessment." *Cold Spring Harb Perspect Biol* 3 (11):a005215. doi: 10.1101/cshperspect.a005215.

Glick, B. S., and A. Nakano. 2009. "Membrane traffic within the Golgi apparatus." *Annu Rev Cell Dev Biol* 25:113-32. doi: 10.1146/annurev.cellbio.24.110707.175421.

Goldberg, D. E., and S. Kornfeld. 1983. "Evidence for extensive subcellular organization of asparagine-linked oligosaccharide processing and lysosomal enzyme phosphorylation." *J Biol Chem* 258 (5):3159-65.

Goldenberg, M. M. 2012. "Multiple sclerosis review." *P T* 37 (3):175-84.

Goody, R. S., and W. Hofmann-Goody. 2002. "Exchange factors, effectors, GAPs and motor proteins: common thermodynamic and kinetic principles for different functions." *Eur Biophys J* 31 (4):268-74. doi: 10.1007/s00249-002-0225-3.

Goud, B., A. Salminen, N. C. Walworth, and P. J. Novick. 1988. "A GTP-binding protein required for secretion rapidly associates with secretory vesicles and the plasma membrane in yeast." *Cell* 53 (5):753-68.

Graham, T. R., and S. D. Emr. 1991. "Compartmental organization of Golgi-specific protein modification and vacuolar protein sorting events defined in a yeast sec18 (NSF) mutant." *J Cell Biol* 114 (2):207-18.

Hamilton, G., S. E. Harris, G. Davies, D. C. Liewald, A. Tenesa, J. M. Starr, D. Porteous, and I. J. Deary. 2011. "Alzheimer's disease genes are associated with measures of cognitive ageing in the lothian birth cohorts of 1921 and 1936." *Int J Alzheimers Dis* 2011:505984. doi: 10.4061/2011/505984.

Hanahan, D., and R. A. Weinberg. 2000. "The hallmarks of cancer." *Cell* 100 (1):57-70.

Hardy, J. 2006. "A hundred years of Alzheimer's disease research." *Neuron* 52 (1):3-13. doi: 10.1016/j.neuron.2006.09.016.

Haubruck, H., R. Prange, C. Vorgias, and D. Gallwitz. 1989. "The ras-related mouse ypt1 protein can functionally replace the YPT1 gene product in yeast." *EMBO J* 8 (5):1427-32.

Hoppenbrouwers, I. A., Y. S. Aulchenko, G. C. Ebers, S. V. Ramagopalan, B. A. Oostra, C. M. van Duijn, and R. Q. Hintzen. 2008. "EVI5 is a risk gene for multiple sclerosis." *Genes Immun* 9 (4):334-7. doi: 10.1038/gene.2008.22.

Hu, C. D., A. V. Grinberg, and T. K. Kerppola. 2005. "Visualization of protein interactions in living cells using bimolecular fluorescence complementation (BiFC) analysis." *Curr Protoc Protein Sci* Chapter 19:Unit 19 10. doi: 10.1002/0471140864.ps1910s41.

Huang, J., C. L. Birmingham, S. Shahnazari, J. Shiu, Y. T. Zheng, A. C. Smith, K. G. Campellone, W. D. Heo, S. Gruenheid, T. Meyer, M. D. Welch, N. T. Ktistakis, P. K. Kim, D. J. Klionsky, and J. H. Brumell. 2011. "Antibacterial autophagy occurs at PI(3)P-enriched domains of the endoplasmic reticulum and requires Rab1 GTPase." *Autophagy* 7 (1):17-26.

Huang, S., and M. P. Czech. 2007. "The GLUT4 glucose transporter." *Cell Metab* 5 (4):237-52. doi: 10.1016/j.cmet.2007.03.006.

Huh, W. K., J. V. Falvo, L. C. Gerke, A. S. Carroll, R. W. Howson, J. S. Weissman, and E. K. O'Shea. 2003. "Global analysis of protein localization in budding yeast." *Nature* 425 (6959):686-91. doi: 10.1038/nature02026.

James, P., J. Halladay, and E. A. Craig. 1996. "Genomic libraries and a host strain designed for highly efficient two-hybrid selection in yeast." *Genetics* 144 (4):1425-36.

Jang, S. B., Y. G. Kim, Y. S. Cho, P. G. Suh, K. H. Kim, and B. H. Oh. 2002. "Crystal structure of SEDL and its implications for a genetic disease spondyloepiphyseal dysplasia tarda." *J Biol Chem* 277 (51):49863-9. doi: 10.1074/jbc.M207436200.

Jedd, G., J. Mulholland, and N. Segev. 1997. "Two new Ypt GTPases are required for exit from the yeast trans-Golgi compartment." *J Cell Biol* 137 (3):563-80.

Jedd, G., C. Richardson, R. Litt, and N. Segev. 1995. "The Ypt1 GTPase is essential for the first two steps of the yeast secretory pathway." *J Cell Biol* 131 (3):583-90.

Jones, S., G. Jedd, R. A. Kahn, A. Franzusoff, F. Bartolini, and N. Segev. 1999. "Genetic interactions in yeast between Ypt GTPases and Arf guanine nucleotide exchangers." *Genetics* 152 (4):1543-56.

Jones, S., R. J. Litt, C. J. Richardson, and N. Segev. 1995. "Requirement of nucleotide exchange factor for Ypt1 GTPase mediated protein transport." *J Cell Biol* 130 (5):1051-61.

Jones, S., C. Newman, F. Liu, and N. Segev. 2000. "The TRAPP complex is a nucleotide exchanger for Ypt1 and Ypt31/32." *Mol Biol Cell* 11 (12):4403-11.

Kerppola, T. K. 2008. "Bimolecular fluorescence complementation (BiFC) analysis as a probe of protein interactions in living cells." *Annu Rev Biophys* 37:465-87. doi: 10.1146/annurev.biophys.37.032807.125842.

Kessler, A., E. Tomas, D. Immler, H. E. Meyer, A. Zorzano, and J. Eckel. 2000. "Rab11 is associated with GLUT4-containing vesicles and redistributes in response to insulin." *Diabetologia* 43 (12):1518-27. doi: 10.1007/s001250051563.

Khattak, N. A., and A. Mir. 2014. "Computational analysis of TRAPPC9: candidate gene for autosomal recessive non-syndromic mental retardation." *CNS Neurol Disord Drug Targets* 13 (4):699-711.

Kim, J. J., Z. Lipatova, U. Majumdar, and N. Segev. 2016. "Regulation of Golgi Cisternal Progression by Ypt/Rab GTPases." *Dev Cell* 36 (4):440-52. doi: 10.1016/j.devcel.2016.01.016.

Kim, J. J., Z. Lipatova, and N. Segev. 2016. "TRAPP Complexes in Secretion and Autophagy." *Front Cell Dev Biol* 4:20. doi: 10.3389/fcell.2016.00020.

Kim, Y. G., S. Raunser, C. Munger, J. Wagner, Y. L. Song, M. Cygler, T. Walz, B. H. Oh, and M. Sacher. 2006. "The architecture of the multisubunit TRAPP I complex suggests a model for vesicle tethering." *Cell* 127 (4):817-30. doi: 10.1016/j.cell.2006.09.029.

Knodler, A., S. Feng, J. Zhang, X. Zhang, A. Das, J. Peranen, and W. Guo. 2010. "Coordination of Rab8 and Rab11 in primary ciliogenesis." *Proc Natl Acad Sci U S A* 107 (14):6346-51. doi: 10.1073/pnas.1002401107.

Landles, C., and G. P. Bates. 2004. "Huntingtin and the molecular pathogenesis of Huntington's disease. Fourth in molecular medicine review series." *EMBO Rep* 5 (10):958-63. doi: 10.1038/sj.embor.7400250.

Lavieu, G., H. Zheng, and J. E. Rothman. 2013. "Stapled Golgi cisternae remain in place as cargo passes through the stack." *Elife* 2:e00558. doi: 10.7554/eLife.00558.

Lee, M. T., A. Mishra, and D. G. Lambright. 2009. "Structural mechanisms for regulation of membrane traffic by rab GTPases." *Traffic* 10 (10):1377-89. doi: 10.1111/j.1600-0854.2009.00942.x.

Leung, K. F., R. Baron, and M. C. Seabra. 2006. "Thematic review series: lipid posttranslational modifications. geranylgeranylation of Rab GTPases." *J Lipid Res* 47 (3):467-75. doi: 10.1194/jlr.R500017-JLR200.

Li, B., and J. R. Warner. 1996. "Mutation of the Rab6 homologue of Saccharomyces cerevisiae, YPT6, inhibits both early Golgi function and ribosome biosynthesis." *J Biol Chem* 271 (28):16813-9.

Li, X., E. Sapp, A. Valencia, K. B. Kegel, Z. H. Qin, J. Alexander, N. Masso, P. Reeves, J. J. Ritch, S. Zeitlin, N. Aronin, and M. Difiglia. 2008. "A function of huntingtin in guanine nucleotide exchange on Rab11." *Neuroreport* 19 (16):1643-7. doi: 10.1097/WNR.0b013e328315cd4c.

Liang, Y., N. Morozova, A. A. Tokarev, J. W. Mulholland, and N. Segev. 2007. "The role of Trs65 in the Ypt/Rab guanine nucleotide exchange factor function of the TRAPP II complex." *Mol Biol Cell* 18 (7):2533-41. doi: 10.1091/mbc.E07-03-0221.

Lipatova, Z., N. Belogortseva, X. Q. Zhang, J. Kim, D. Taussig, and N. Segev. 2012. "Regulation of selective autophagy onset by a Ypt/Rab GTPase module." *Proc Natl Acad Sci U S A* 109 (18):6981-6. doi: 10.1073/pnas.1121299109.

Lipatova, Z., A. U. Hain, V. Y. Nazarko, and N. Segev. 2015. "Ypt/Rab GTPases: principles learned from yeast." *Crit Rev Biochem Mol Biol* 50 (3):203-11. doi: 10.3109/10409238.2015.1014023.

Lipatova, Z., J. J. Kim, and N. Segev. 2015. "Ypt1 and TRAPP interactions: optimization of multicolor bimolecular fluorescence complementation in yeast." *Methods Mol Biol* 1298:107-16. doi: 10.1007/978-1-4939-2569-8_9.

Lipatova, Z., and N. Segev. 2014. "Ypt/Rab GTPases regulate two intersections of the secretory and the endosomal/lysosomal pathways." *Cell Logist* 4 (3):e954870. doi: 10.4161/21592780.2014.954870.

Lipatova, Z., and N. Segev. 2015. "A Role for Macro-ER-Phagy in ER Quality Control." *PLoS Genet* 11 (7):e1005390. doi: 10.1371/journal.pgen.1005390.

Lipatova, Z., A. H. Shah, J. J. Kim, J. W. Mulholland, and N. Segev. 2013. "Regulation of ER-phagy by a Ypt/Rab GTPase module." *Mol Biol Cell* 24 (19):3133-44. doi: 10.1091/mbc.E13-05-0269.

Lipatova, Z., A. A. Tokarev, Y. Jin, J. Mulholland, L. S. Weisman, and N. Segev. 2008. "Direct interaction between a myosin V motor and the Rab GTPases Ypt31/32 is required for polarized secretion." *Mol Biol Cell* 19 (10):4177-87. doi: 10.1091/mbc.E08-02-0220.

Losev, E., C. A. Reinke, J. Jellen, D. E. Strongin, B. J. Bevis, and B. S. Glick. 2006. "Golgi maturation visualized in living yeast." *Nature* 441 (7096):1002-6. doi: 10.1038/nature04717.

Luo, Z., and D. Gallwitz. 2003. "Biochemical and genetic evidence for the involvement of yeast Ypt6-GTPase in protein retrieval to different Golgi compartments." *J Biol Chem* 278 (2):791-9. doi: 10.1074/jbc.M209120200.

Lynch-Day, M. A., D. Bhandari, S. Menon, J. Huang, H. Cai, C. R. Bartholomew, J. H. Brumell, S. Ferro-Novick, and D. J. Klionsky. 2010. "Trs85 directs a Ypt1 GEF, TRAPPIII, to the phagophore to promote autophagy." *Proc Natl Acad Sci U S A* 107 (17):7811-6. doi: 10.1073/pnas.1000063107.

Marie, M., H. A. Dale, R. Sannerud, and J. Saraste. 2009. "The function of the intermediate compartment in pre-Golgi trafficking involves its stable connection with the centrosome." *Mol Biol Cell* 20 (20):4458-70. doi: 10.1091/mbc.E08-12-1229.

Marra, P., L. Salvatore, A. Mironov, Jr., A. Di Campli, G. Di Tullio, A. Trucco, G. Beznoussenko, A. Mironov, and M. A. De Matteis. 2007. "The biogenesis of the Golgi ribbon: the roles of membrane input from the ER and of GM130." *Mol Biol Cell* 18 (5):1595-608. doi: 10.1091/mbc.E06-10-0886.

Matsuura-Tokita, K., M. Takeuchi, A. Ichihara, K. Mikuriya, and A. Nakano. 2006. "Live imaging of yeast Golgi cisternal maturation." *Nature* 441 (7096):1007-10. doi: 10.1038/nature04737.

McCarthy, S. E., J. Gillis, M. Kramer, J. Lihm, S. Yoon, Y. Berstein, M. Mistry, P. Pavlidis, R. Solomon, E. Ghiban, E. Antoniou, E. Kelleher, C. O'Brien, G. Donohoe, M. Gill, D. W. Morris, W. R. McCombie, and A. Corvin. 2014. "De novo mutations in schizophrenia implicate chromatin remodeling and support a genetic overlap with autism and intellectual disability." *Mol Psychiatry* 19 (6):652-8. doi: 10.1038/mp.2014.29.

McDonold, C. M., and J. C. Fromme. 2014. "Four GTPases differentially regulate the Sec7 Arf-GEF to direct traffic at the trans-golgi network." *Dev Cell* 30 (6):759-67. doi: 10.1016/j.devcel.2014.07.016.

Meiling-Wesse, K., U. D. Epple, R. Krick, H. Barth, A. Appelles, C. Voss, E. L. Eskelinen, and M. Thumm. 2005. "Trs85 (Gsg1), a component of the TRAPP complexes, is required for the organization of the preautophagosomal structure

during selective autophagy via the Cvt pathway." *J Biol Chem* 280 (39):33669-78. doi: 10.1074/jbc.M501701200.

Morozova, N., Y. Liang, A. A. Tokarev, S. H. Chen, R. Cox, J. Andrejic, Z. Lipatova, V. A. Sciorra, S. D. Emr, and N. Segev. 2006. "TRAPPII subunits are required for the specificity switch of a Ypt-Rab GEF." *Nat Cell Biol* 8 (11):1263-9. doi: 10.1038/ncb1489.

Moyer, B. D., B. B. Allan, and W. E. Balch. 2001. "Rab1 interaction with a GM130 effector complex regulates COPII vesicle cis--Golgi tethering." *Traffic* 2 (4):268-76.

Nazarko, T. Y., J. Huang, J. M. Nicaud, D. J. Klionsky, and A. A. Sibirny. 2005. "Trs85 is required for macroautophagy, pexophagy and cytoplasm to vacuole targeting in Yarrowia lipolytica and Saccharomyces cerevisiae." *Autophagy* 1 (1):37-45.

Nilsson, T., C. E. Au, and J. J. Bergeron. 2009. "Sorting out glycosylation enzymes in the Golgi apparatus." *FEBS Lett* 583 (23):3764-9. doi: 10.1016/j.febslet.2009.10.064.

Orci, L., M. Ravazzola, A. Volchuk, T. Engel, M. Gmachl, M. Amherdt, A. Perrelet, T. H. Sollner, and J. E. Rothman. 2000. "Anterograde flow of cargo across the golgi stack potentially mediated via bidirectional "percolating" COPI vesicles." *Proc Natl Acad Sci U S A* 97 (19):10400-5. doi: 10.1073/pnas.190292497.

Orci, L., M. Stamnes, M. Ravazzola, M. Amherdt, A. Perrelet, T. H. Sollner, and J. E. Rothman. 1997. "Bidirectional transport by distinct populations of COPI-coated vesicles." *Cell* 90 (2):335-49.

Ortiz, D., M. Medkova, C. Walch-Solimena, and P. Novick. 2002. "Ypt32 recruits the Sec4p guanine nucleotide exchange factor, Sec2p, to secretory vesicles; evidence for a Rab cascade in yeast." *J Cell Biol* 157 (6):1005-15. doi: 10.1083/jcb.200201003.

Palade, G. 1975. "Intracellular aspects of the process of protein synthesis." *Science* 189 (4206):867. doi: 10.1126/science.189.4206.867-b.

Papanikou, E., K. J. Day, J. Austin, and B. S. Glick. 2015. "COPI selectively drives maturation of the early Golgi." *Elife* 4. doi: 10.7554/eLife.13232.

Papanikou, E., and B. S. Glick. 2009. "The yeast Golgi apparatus: insights and mysteries." *FEBS Lett* 583 (23):3746-51. doi: 10.1016/j.febslet.2009.10.072.

Papanikou, E., and B. S. Glick. 2014. "Golgi compartmentation and identity." *Curr Opin Cell Biol* 29:74-81. doi: 10.1016/j.ceb.2014.04.010.

Pfeffer, S. 2005. "A model for Rab GTPase localization." *Biochem Soc Trans* 33 (Pt 4):627-30. doi: 10.1042/BST0330627.

Pfeffer, S. R. 2013. "Rab GTPase regulation of membrane identity." *Curr Opin Cell Biol* 25 (4):414-9. doi: 10.1016/j.ceb.2013.04.002.

Pinar, M., H. N. Arst, Jr., A. Pantazopoulou, V. G. Tagua, V. de los Rios, J. Rodriguez-Salarichs, J. F. Diaz, and M. A. Penalva. 2015. "TRAPPII regulates exocytic Golgi exit by mediating nucleotide exchange on the Ypt31 ortholog RabERAB11." *Proc Natl Acad Sci U S A* 112 (14):4346-51. doi: 10.1073/pnas.1419168112.

Pind, S. N., C. Nuoffer, J. M. McCaffery, H. Plutner, H. W. Davidson, M. G. Farquhar, and W. E. Balch. 1994. "Rab1 and Ca2+ are required for the fusion of carrier vesicles mediating endoplasmic reticulum to Golgi transport." *J Cell Biol* 125 (2):239-52.

Plutner, H., A. D. Cox, S. Pind, R. Khosravi-Far, J. R. Bourne, R. Schwaninger, C. J. Der, and W. E. Balch. 1991. "Rab1b regulates vesicular transport between the endoplasmic reticulum and successive Golgi compartments." *J Cell Biol* 115 (1):31-43.

Preuss, D., J. Mulholland, A. Franzusoff, N. Segev, and D. Botstein. 1992. "Characterization of the Saccharomyces Golgi complex through the cell cycle by immunoelectron microscopy." *Mol Biol Cell* 3 (7):789-803.

Rambourg, A., and Y. Clermont. 1990. "Three-dimensional electron microscopy: structure of the Golgi apparatus." *Eur J Cell Biol* 51 (2):189-200.

Richards, P., C. Didszun, S. Campesan, A. Simpson, B. Horley, K. W. Young, P. Glynn, K. Cain, C. P. Kyriacou, F. Giorgini, and P. Nicotera. 2011. "Dendritic spine loss and neurodegeneration is rescued by Rab11 in models of Huntington's disease." *Cell Death Differ* 18 (2):191-200. doi: 10.1038/cdd.2010.127.

Rines, D. R., D. Thomann, J. F. Dorn, P. Goodwin, and P. K. Sorger. 2011. "Live cell imaging of yeast." *Cold Spring Harb Protoc* 2011 (9). doi: 10.1101/pdb.top065482.

Rink, J., E. Ghigo, Y. Kalaidzidis, and M. Zerial. 2005. "Rab conversion as a mechanism of progression from early to late endosomes." *Cell* 122 (5):735-49. doi: 10.1016/j.cell.2005.06.043.

Rivera-Molina, F. E., and P. J. Novick. 2009. "A Rab GAP cascade defines the boundary between two Rab GTPases on the secretory pathway." *Proc Natl Acad Sci U S A* 106 (34):14408-13. doi: 10.1073/pnas.0906536106.

Rizzo, R., S. Parashuraman, P. Mirabelli, C. Puri, J. Lucocq, and A. Luini. 2013. "The dynamics of engineered resident proteins in the mammalian Golgi complex relies on cisternal maturation." *J Cell Biol* 201 (7):1027-36. doi: 10.1083/jcb.201211147.

Rosenstein, B. J., and G. R. Cutting. 1998. "The diagnosis of cystic fibrosis: a consensus statement. Cystic Fibrosis Foundation Consensus Panel." *J Pediatr* 132 (4):589-95.

Sacher, M., J. Barrowman, D. Schieltz, J. R. Yates, 3rd, and S. Ferro-Novick. 2000. "Identification and characterization of five new subunits of TRAPP." *Eur J Cell Biol* 79 (2):71-80. doi: 10.1078/S0171-9335(04)70009-6.

Sacher, M., J. Barrowman, W. Wang, J. Horecka, Y. Zhang, M. Pypaert, and S. Ferro-Novick. 2001. "TRAPP I implicated in the specificity of tethering in ER-to-Golgi transport." *Mol Cell* 7 (2):433-42.

Sacher, M., Y. Jiang, J. Barrowman, A. Scarpa, J. Burston, L. Zhang, D. Schieltz, J. R. Yates, 3rd, H. Abeliovich, and S. Ferro-Novick. 1998. "TRAPP, a highly conserved novel complex on the cis-Golgi that mediates vesicle docking and fusion." *EMBO J* 17 (9):2494-503. doi: 10.1093/emboj/17.9.2494.

Salminen, A., and P. J. Novick. 1987. "A ras-like protein is required for a post-Golgi event in yeast secretion." *Cell* 49 (4):527-38.

Salminen, A., and P. J. Novick. 1989. "The Sec15 protein responds to the function of the GTP binding protein, Sec4, to control vesicular traffic in yeast." *J Cell Biol* 109 (3):1023-36.

Sapperstein, S. K., V. V. Lupashin, H. D. Schmitt, and M. G. Waters. 1996. "Assembly of the ER to Golgi SNARE complex requires Uso1p." *J Cell Biol* 132 (5):755-67.

Sapperstein, S. K., D. M. Walter, A. R. Grosvenor, J. E. Heuser, and M. G. Waters. 1995. "p115 is a general vesicular transport factor related to the yeast endoplasmic reticulum to Golgi transport factor Uso1p." *Proc Natl Acad Sci U S A* 92 (2):522-6.

Satoh, A., Y. Wang, J. Malsam, M. B. Beard, and G. Warren. 2003. "Golgin-84 is a rab1 binding partner involved in Golgi structure." *Traffic* 4 (3):153-61.

Schindelin, J., I. Arganda-Carreras, E. Frise, V. Kaynig, M. Longair, T. Pietzsch, S. Preibisch, C. Rueden, S. Saalfeld, B. Schmid, J. Y. Tinevez, D. J. White, V. Hartenstein, K. Eliceiri, P. Tomancak, and A. Cardona. 2012. "Fiji: an open-source platform for biological-image analysis." *Nature methods* 9 (7):676-82. doi: 10.1038/nmeth.2019.

Schwenk, R. W., J. J. Luiken, and J. Eckel. 2007. "FIP2 and Rip11 specify Rab11a-mediated cellular distribution of GLUT4 and FAT/CD36 in H9c2-hIR cells." *Biochem Biophys Res Commun* 363 (1):119-25. doi: 10.1016/j.bbrc.2007.08.111.

Sclafani, A., S. Chen, F. Rivera-Molina, K. Reinisch, P. Novick, and S. Ferro-Novick. 2010. "Establishing a role for the GTPase Ypt1p at the late Golgi." *Traffic* 11 (4):520-32. doi: 10.1111/j.1600-0854.2010.01031.x.

Segev, N. 1991. "Mediation of the attachment or fusion step in vesicular transport by the GTP-binding Ypt1 protein." *Science* 252 (5012):1553-6.

Segev, N. 2001a. "Ypt and Rab GTPases: insight into functions through novel interactions." *Curr Opin Cell Biol* 13 (4):500-11.

Segev, N. 2001b. "Ypt/rab gtpases: regulators of protein trafficking." *Sci STKE* 2001 (100):re11. doi: 10.1126/stke.2001.100.re11.

Segev, N. 2011. "Coordination of intracellular transport steps by GTPases." *Semin Cell Dev Biol* 22 (1):33-8. doi: 10.1016/j.semcdb.2010.11.005.

Segev, N., and D. Botstein. 1987. "The ras-like yeast YPT1 gene is itself essential for growth, sporulation, and starvation response." *Mol Cell Biol* 7 (7):2367-77.

Segev, N., J. Mulholland, and D. Botstein. 1988. "The yeast GTP-binding YPT1 protein and a mammalian counterpart are associated with the secretion machinery." *Cell* 52 (6):915-24.

Sheff, M. A., and K. S. Thorn. 2004. "Optimized cassettes for fluorescent protein tagging in Saccharomyces cerevisiae." *Yeast* 21 (8):661-70. doi: 10.1002/yea.1130.

Shimada, K., K. Uzawa, M. Kato, Y. Endo, M. Shiiba, H. Bukawa, H. Yokoe, N. Seki, and H. Tanzawa. 2005. "Aberrant expression of RAB1A in human tongue cancer." *Br J Cancer* 92 (10):1915-21. doi: 10.1038/sj.bjc.6602594.

Shimomura, O., F. H. Johnson, and Y. Saiga. 1962. "Extraction, purification and properties of aequorin, a bioluminescent protein from the luminous hydromedusan, Aequorea." *J Cell Comp Physiol* 59:223-39.

Shorter, J., and G. Warren. 2002. "Golgi architecture and inheritance." *Annu Rev Cell Dev Biol* 18:379-420. doi: 10.1146/annurev.cellbio.18.030602.133733.

Sikorski, R. S., and P. Hieter. 1989. "A system of shuttle vectors and yeast host strains designed for efficient manipulation of DNA in Saccharomyces cerevisiae." *Genetics* 122 (1):19-27.

Silvis, M. R., C. A. Bertrand, N. Ameen, F. Golin-Bisello, M. B. Butterworth, R. A. Frizzell, and N. A. Bradbury. 2009. "Rab11b regulates the apical recycling of the cystic fibrosis transmembrane conductance regulator in polarized intestinal epithelial cells." *Mol Biol Cell* 20 (8):2337-50. doi: 10.1091/mbc.E08-01-0084.

Siniossoglou, S., S. Y. Peak-Chew, and H. R. Pelham. 2000. "Ric1p and Rgp1p form a complex that catalyses nucleotide exchange on Ypt6p." *EMBO J* 19 (18):4885-94. doi: 10.1093/emboj/19.18.4885.

Starr, T., Y. Sun, N. Wilkins, and B. Storrie. 2010. "Rab33b and Rab6 are functionally overlapping regulators of Golgi homeostasis and trafficking." *Traffic* 11 (5):626-36. doi: 10.1111/j.1600-0854.2010.01051.x.

Storrie, B., M. Micaroni, G. P. Morgan, N. Jones, J. A. Kamykowski, N. Wilkins, T. H. Pan, and B. J. Marsh. 2012. "Electron tomography reveals Rab6 is essential to the trafficking of trans-Golgi clathrin and COPI-coated vesicles and the maintenance of Golgi cisternal number." *Traffic* 13 (5):727-44. doi: 10.1111/j.1600-0854.2012.01343.x.

Strom, M., P. Vollmer, T. J. Tan, and D. Gallwitz. 1993. "A yeast GTPase-activating protein that interacts specifically with a member of the Ypt/Rab family." *Nature* 361 (6414):736-9. doi: 10.1038/361736a0.

Suda, Y., K. Kurokawa, R. Hirata, and A. Nakano. 2013. "Rab GAP cascade regulates dynamics of Ypt6 in the Golgi traffic." *Proc Natl Acad Sci U S A* 110 (47):18976-81. doi: 10.1073/pnas.1308627110.

Suda, Y., and A. Nakano. 2012. "The yeast Golgi apparatus." *Traffic* 13 (4):505-10. doi: 10.1111/j.1600-0854.2011.01316.x.

Sultana, A., Y. Jin, C. Dregger, E. Franklin, L. S. Weisman, and A. R. Khan. 2011. "The activation cycle of Rab GTPase Ypt32 reveals structural determinants of effector recruitment and GDI binding." *FEBS Lett* 585 (22):3520-7. doi: 10.1016/j.febslet.2011.10.013.

Suvorova, E. S., R. Duden, and V. V. Lupashin. 2002. "The Sec34/Sec35p complex, a Ypt1p effector required for retrograde intra-Golgi trafficking, interacts with Golgi SNAREs and COPI vesicle coat proteins." *J Cell Biol* 157 (4):631-43. doi: 10.1083/jcb.200111081.

Takahashi, S., K. Kubo, S. Waguri, A. Yabashi, H. W. Shin, Y. Katoh, and K. Nakayama. 2012. "Rab11 regulates exocytosis of recycling vesicles at the plasma membrane." *J Cell Sci* 125 (Pt 17):4049-57. doi: 10.1242/jcs.102913.

Tan, T. J., P. Vollmer, and D. Gallwitz. 1991. "Identification and partial purification of GTPase-activating proteins from yeast and mammalian cells that preferentially act on Ypt1/Rab1 proteins." *FEBS Lett* 291 (2):322-6.

Taussig, D., Z. Lipatova, J. J. Kim, X. Zhang, and N. Segev. 2013. "Trs20 is required for TRAPP II assembly." *Traffic* 14 (6):678-90. doi: 10.1111/tra.12065.

Taussig, D., Z. Lipatova, and N. Segev. 2014. "Trs20 is required for TRAPP III complex assembly at the PAS and its function in autophagy." *Traffic* 15 (3):327-37. doi: 10.1111/tra.12145.

Thomas, J. D., Y. J. Zhang, Y. H. Wei, J. H. Cho, L. E. Morris, H. Y. Wang, and X. F. Zheng. 2014. "Rab1A is an mTORC1 activator and a colorectal oncogene." *Cancer Cell* 26 (5):754-69. doi: 10.1016/j.ccell.2014.09.008.

Tisdale, E. J., J. R. Bourne, R. Khosravi-Far, C. J. Der, and W. E. Balch. 1992. "GTP-binding mutants of rab1 and rab2 are potent inhibitors of vesicular transport from the endoplasmic reticulum to the Golgi complex." *J Cell Biol* 119 (4):749-61.

Tokarev, A. A., D. Taussig, G. Sundaram, Z. Lipatova, Y. Liang, J. W. Mulholland, and N. Segev. 2009. "TRAPP II complex assembly requires Trs33 or Trs65." *Traffic* 10 (12):1831-44. doi: 10.1111/j.1600-0854.2009.00988.x.

Udayar, V., V. Buggia-Prevot, R. L. Guerreiro, G. Siegel, N. Rambabu, A. L. Soohoo, M. Ponnusamy, B. Siegenthaler, J. Bali, Aesg, M. Simons, J. Ries, M. A. Puthenveedu, J. Hardy, G. Thinakaran, and L. Rajendran. 2013. "A paired RNAi and RabGAP overexpression screen identifies Rab11 as a regulator of beta-amyloid production." *Cell Rep* 5 (6):1536-51. doi: 10.1016/j.celrep.2013.12.005.

Ullrich, O., S. Reinsch, S. Urbe, M. Zerial, and R. G. Parton. 1996. "Rab11 regulates recycling through the pericentriolar recycling endosome." *J Cell Biol* 135 (4):913-24.

Venditti, R., T. Scanu, M. Santoro, G. Di Tullio, A. Spaar, R. Gaibisso, G. V. Beznoussenko, A. A. Mironov, A. Mironov, Jr., L. Zelante, M. R. Piemontese, A. Notarangelo, V. Malhotra, B. M. Vertel, C. Wilson, and M. A. De Matteis. 2012. "Sedlin controls the ER export of procollagen by regulating the Sar1 cycle." *Science* 337 (6102):1668-72. doi: 10.1126/science.1224947.

Wang, W., and S. Ferro-Novick. 2002. "A Ypt32p exchange factor is a putative effector of Ypt1p." *Mol Biol Cell* 13 (9):3336-43. doi: 10.1091/mbc.01-12-0577.

Wang, W., M. Sacher, and S. Ferro-Novick. 2000. "TRAPP stimulates guanine nucleotide exchange on Ypt1p." *J Cell Biol* 151 (2):289-96.

Welz, T., J. Wellbourne-Wood, and E. Kerkhoff. 2014. "Orchestration of cell surface proteins by Rab11." *Trends Cell Biol* 24 (7):407-15. doi: 10.1016/j.tcb.2014.02.004.

Wen, J., C. W. Hanna, S. Martell, P. C. Leung, S. M. Lewis, W. P. Robinson, M. D. Stephenson, and E. Rajcan-Separovic. 2015. "Functional consequences of copy number variants in miscarriage." *Mol Cytogenet* 8:6. doi: 10.1186/s13039-015-0109-8.

Westlake, C. J., J. R. Junutula, G. C. Simon, M. Pilli, R. Prekeris, R. H. Scheller, P. K. Jackson, and A. G. Eldridge. 2007. "Identification of Rab11 as a small GTPase binding protein for the Evi5 oncogene." *Proc Natl Acad Sci U S A* 104 (4):1236-41. doi: 10.1073/pnas.0610500104.

Wilson, B. S., C. Nuoffer, J. L. Meinkoth, M. McCaffery, J. R. Feramisco, W. E. Balch, and M. G. Farquhar. 1994. "A Rab1 mutant affecting guanine nucleotide exchange promotes disassembly of the Golgi apparatus." *J Cell Biol* 125 (3):557-71.

Xu, B. H., X. X. Li, Y. Yang, M. Y. Zhang, H. L. Rao, H. Y. Wang, and X. F. Zheng. 2015. "Aberrant amino acid signaling promotes growth and metastasis of hepatocellular carcinomas through Rab1A-dependent activation of mTORC1 by Rab1A." *Oncotarget* 6 (25):20813-28. doi: 10.18632/oncotarget.5175.

Yip, C. K., J. Berscheminski, and T. Walz. 2010. "Molecular architecture of the TRAPPII complex and implications for vesicle tethering." *Nat Struct Mol Biol* 17 (11):1298-304. doi: 10.1038/nsmb.1914.

Zeigerer, A., M. A. Lampson, O. Karylowski, D. D. Sabatini, M. Adesnik, M. Ren, and T. E. McGraw. 2002. "GLUT4 retention in adipocytes requires two intracellular insulin-regulated transport steps." *Mol Biol Cell* 13 (7):2421-35. doi: 10.1091/mbc.E02-02-0071.

Zerial, M., and H. McBride. 2001. "Rab proteins as membrane organizers." *Nat Rev Mol Cell Biol* 2 (2):107-17. doi: 10.1038/35052055.

Zhang, J., X. Liu, A. Datta, K. Govindarajan, W. L. Tam, J. Han, J. George, C. Wong, K. Ramnarayanan, T. Y. Phua, W. Y. Leong, Y. S. Chan, N. Palanisamy, E. T. Liu, K. M. Karuturi, B. Lim, and L. D. Miller. 2009. "RCP is a human breast cancer-promoting gene with Ras-activating function." *J Clin Invest* 119 (8):2171-83. doi: 10.1172/JCI37622.

Zhang, Y., S. Liu, H. Wang, W. Yang, F. Li, F. Yang, D. Yu, F. V. Ramsey, G. P. Tuszyski, and W. Hu. 2015. "Elevated NIBP/TRAPPC9 mediates tumorigenesis of cancer cells through NFkappaB signaling." *Oncotarget* 6 (8):6160-78. doi: 10.18632/oncotarget.3349.

Zhao, S. L., J. Hong, Z. Q. Xie, J. T. Tang, W. Y. Su, W. Du, Y. X. Chen, R. Lu, D. F. Sun, and J. Y. Fang. 2011. "TRAPPC4-ERK2 interaction activates ERK1/2, modulates its nuclear localization and regulates proliferation and apoptosis of

colorectal cancer cells." *PLoS One* 6 (8):e23262. doi: 10.1371/journal.pone.0023262.

Zoppino, F. C., R. D. Militello, I. Slavin, C. Alvarez, and M. I. Colombo. 2010. "Autophagosome formation depends on the small GTPase Rab1 and functional ER exit sites." *Traffic* 11 (9):1246-61. doi: 10.1111/j.1600-0854.2010.01086.x.

# VITA

NAME: Jane Jinmyung Kim

EDUCATION: Ph.D., Biological Sciences, University of Illinois at Chicago, Chicago, Illinois, 2016

B.A., Chemistry concentration in Biochemistry and Molecular Biology, Kalamazoo College, Kalamazoo, Michigan 2008

TEACHING: Teaching assistant for;
BioS100: Biology of Cells and Organisms, UIC (2 semesters),
BioS220: Mendelian and Molecular Genetics, UIC (10 semesters)
BioS222: Cell Biology, UIC (1 semester)
BioS351: Microbiology Lab, UIC (1 semester)

Undergraduate mentoring in lab- trained and worked with 5 undergrads during my tenure as a graduate student.

PUBLICATIONS:

first author Kim, J.J., Lipatova, Z., Majumdar, U., and Segev, N. (2016) Regulation of Golgi Cisternal Progression by Ypt/Rab GTPases. Dev. Cell. 36:440-452

co-first-author Kim, J.J., Lipatova, Z., and Segev, N. (2016) TRAPP complexes in secretion and autophagy. Review, Front. Cell Dev. Biol. 4:20-31

Kim, J.J.[1], Lipatova, Z.[1], and Segev, N. (2015) Ypt1 and TRAPP interactions: Optimization of multi-color bimolecular fluorescence complementation in yeast. Methods Mol. Biol. 1298:107-16

co-author Lipatova, Z., Shah, A.H., Kim, J.J., Mulholland, J.W., and Segev, N. (2013) Regulation of ER-phagy by a Ypt/Rab GTPase module. MBoC 24:3133-3144.

Taussig, D., Lipatova, Z., Kim, J.J., Zhang, X.Q., and Segev, N. (2013) Trs20 is required for TRAPPII assembly. Traffic 14:678-690.

Lipatova, Z., Belogortseva, N., Zhang, X.Q., Kim, J., Taussig, D., and Segev, N. (2012) Regulation of selective autophagy onset by a Ypt/Rab GTPase module. PNAS 109:6981-6986.

PRESENTATIONS: Poster; The Annual Meeting The American Society of Cell Biology, San Diego, CA 2015

**1st prize Poster**; Molecular Biology and Genetics Departmental Retreat, Lake Geneva, WI 2014

Poster; The Annual Meeting The American Society of Cell Biology, New Orleans LA 2013

**3rd prize Poster**; Molecular Biology and Genetics Departmental Retreat, Lake Geneva, WI 2013

Poster; Chicago Symposium for Cell Signaling, Chicago IL 2013

Poster; The Annual Meeting The American Society of Cell Biology, San Francisco, CA 2012

Poster; Molecular Biology and Genetics Departmental Retreat, Lake Geneva WI 2012

Poster; Chicago Symposium for Cell Signaling, Chicago IL 2012

Poster; Chicago Signal Transduction Symposium Chicago, IL 2011

MEMBERSHIPS: American Society of Cell Biology Graduate- Student Member

HONORS: Graduate Student Research Achievement Award, Department of Biological Sciences, UIC, 2016

Graduate Student Research Achievement Award, Department of Biological Sciences, UIC, 2015

## ELSEVIER LICENSE
## TERMS AND CONDITIONS

Jul 06, 2016

This Agreement between Jane J Kim ("You") and Elsevier ("Elsevier") consists of your license details and the terms and conditions provided by Elsevier and Copyright Clearance Center.

| | |
|---|---|
| License Number | 3823781053720 |
| License date | Mar 07, 2016 |
| Licensed Content Publisher | Elsevier |
| Licensed Content Publication | Developmental Cell |
| Licensed Content Title | Regulation of Golgi Cisternal Progression by Ypt/Rab GTPases |
| Licensed Content Author | Jane J. Kim,Zhanna Lipatova,Uddalak Majumdar,Nava Segev |
| Licensed Content Date | 22 February 2016 |
| Licensed Content Volume Number | 36 |
| Licensed Content Issue Number | 4 |
| Start Page | 440 |
| End Page | 452 |
| Type of Use | reuse in a thesis/dissertation |
| Portion | full article |
| Format | both print and electronic |
| Are you the author of this Elsevier article? | Yes |
| Will you be translating? | No |
| Order reference number | |
| Title of your thesis/dissertation | Ypts and TRAPPs in Golgi Dynamics |
| Expected completion date | Jun 2016 |
| Estimated size (number of pages) | 100 |
| Elsevier VAT number | GB 494 6272 12 |
| Requestor Location | Jane J Kim<br>360 E. South Water St.<br>Apt 3106<br><br>CHICAGO, IL 60601<br>United States<br>Attn: Jane J Kim |
| Billing Type | Invoice |
| Billing Address | Jane J Kim<br>360 E. South Water St.<br>Apt 3106<br><br>CHICAGO, IL 60601 |

| | |
|---|---|
| | United States<br>Attn: Jane J Kim |
| Total | 0.00 USD |
| Total | 0.00 USD |

Terms and Conditions

## INTRODUCTION

1. The publisher for this copyrighted material is Elsevier. By clicking "accept" in connection with completing this licensing transaction, you agree that the following terms and conditions apply to this transaction (along with the Billing and Payment terms and conditions established by Copyright Clearance Center, Inc. ("CCC"), at the time that you opened your Rightslink account and that are available at any time at http://myaccount.copyright.com).

## GENERAL TERMS

2. Elsevier hereby grants you permission to reproduce the aforementioned material subject to the terms and conditions indicated.
3. Acknowledgement: If any part of the material to be used (for example, figures) has appeared in our publication with credit or acknowledgement to another source, permission must also be sought from that source. If such permission is not obtained then that material may not be included in your publication/copies. Suitable acknowledgement to the source must be made, either as a footnote or in a reference list at the end of your publication, as follows:
"Reprinted from Publication title, Vol /edition number, Author(s), Title of article / title of chapter, Pages No., Copyright (Year), with permission from Elsevier [OR APPLICABLE SOCIETY COPYRIGHT OWNER]." Also Lancet special credit - "Reprinted from The Lancet, Vol. number, Author(s), Title of article, Pages No., Copyright (Year), with permission from Elsevier."
4. Reproduction of this material is confined to the purpose and/or media for which permission is hereby given.
5. Altering/Modifying Material: Not Permitted. However figures and illustrations may be altered/adapted minimally to serve your work. Any other abbreviations, additions, deletions and/or any other alterations shall be made only with prior written authorization of Elsevier Ltd. (Please contact Elsevier at permissions@elsevier.com)
6. If the permission fee for the requested use of our material is waived in this instance, please be advised that your future requests for Elsevier materials may attract a fee.
7. Reservation of Rights: Publisher reserves all rights not specifically granted in the combination of (i) the license details provided by you and accepted in the course of this licensing transaction, (ii) these terms and conditions and (iii) CCC's Billing and Payment terms and conditions.
8. License Contingent Upon Payment: While you may exercise the rights licensed immediately upon issuance of the license at the end of the licensing process for the transaction, provided that you have disclosed complete and accurate details of your proposed use, no license is finally effective unless and until full payment is received from you (either by publisher or by CCC) as provided in CCC's Billing and Payment terms and conditions. If full payment is not received on a timely basis, then any license preliminarily granted shall be deemed automatically revoked and shall be void as if never granted. Further, in the event that you breach any of these terms and conditions or any of CCC's Billing and Payment terms and conditions, the license is automatically revoked and shall be void as if never granted. Use of materials as described in a revoked license, as well as any use of the materials beyond the scope of an unrevoked license, may constitute copyright infringement and publisher reserves the right to take any and all action to protect its copyright in the materials.
9. Warranties: Publisher makes no representations or warranties with respect to the licensed material.
10. Indemnity: You hereby indemnify and agree to hold harmless publisher and CCC, and

their respective officers, directors, employees and agents, from and against any and all claims arising out of your use of the licensed material other than as specifically authorized pursuant to this license.
11. No Transfer of License: This license is personal to you and may not be sublicensed, assigned, or transferred by you to any other person without publisher's written permission.
12. No Amendment Except in Writing: This license may not be amended except in a writing signed by both parties (or, in the case of publisher, by CCC on publisher's behalf).
13. Objection to Contrary Terms: Publisher hereby objects to any terms contained in any purchase order, acknowledgment, check endorsement or other writing prepared by you, which terms are inconsistent with these terms and conditions or CCC's Billing and Payment terms and conditions. These terms and conditions, together with CCC's Billing and Payment terms and conditions (which are incorporated herein), comprise the entire agreement between you and publisher (and CCC) concerning this licensing transaction. In the event of any conflict between your obligations established by these terms and conditions and those established by CCC's Billing and Payment terms and conditions, these terms and conditions shall control.
14. Revocation: Elsevier or Copyright Clearance Center may deny the permissions described in this License at their sole discretion, for any reason or no reason, with a full refund payable to you. Notice of such denial will be made using the contact information provided by you. Failure to receive such notice will not alter or invalidate the denial. In no event will Elsevier or Copyright Clearance Center be responsible or liable for any costs, expenses or damage incurred by you as a result of a denial of your permission request, other than a refund of the amount(s) paid by you to Elsevier and/or Copyright Clearance Center for denied permissions.

**LIMITED LICENSE**

The following terms and conditions apply only to specific license types:
15. **Translation**: This permission is granted for non-exclusive world **English** rights only unless your license was granted for translation rights. If you licensed translation rights you may only translate this content into the languages you requested. A professional translator must perform all translations and reproduce the content word for word preserving the integrity of the article.
16. **Posting licensed content on any Website**: The following terms and conditions apply as follows: Licensing material from an Elsevier journal: All content posted to the web site must maintain the copyright information line on the bottom of each image; A hyper-text must be included to the Homepage of the journal from which you are licensing at http://www.sciencedirect.com/science/journal/xxxxx or the Elsevier homepage for books at http://www.elsevier.com; Central Storage: This license does not include permission for a scanned version of the material to be stored in a central repository such as that provided by Heron/XanEdu.
Licensing material from an Elsevier book: A hyper-text link must be included to the Elsevier homepage at http://www.elsevier.com . All content posted to the web site must maintain the copyright information line on the bottom of each image.

**Posting licensed content on Electronic reserve**: In addition to the above the following clauses are applicable: The web site must be password-protected and made available only to bona fide students registered on a relevant course. This permission is granted for 1 year only. You may obtain a new license for future website posting.
17. **For journal authors:** the following clauses are applicable in addition to the above:
**Preprints:**
A preprint is an author's own write-up of research results and analysis, it has not been peer-reviewed, nor has it had any other value added to it by a publisher (such as formatting, copyright, technical enhancement etc.).
Authors can share their preprints anywhere at any time. Preprints should not be added to or enhanced in any way in order to appear more like, or to substitute for, the final versions of

articles however authors can update their preprints on arXiv or RePEc with their Accepted Author Manuscript (see below).
If accepted for publication, we encourage authors to link from the preprint to their formal publication via its DOI. Millions of researchers have access to the formal publications on ScienceDirect, and so links will help users to find, access, cite and use the best available version. Please note that Cell Press, The Lancet and some society-owned have different preprint policies. Information on these policies is available on the journal homepage.
**Accepted Author Manuscripts:** An accepted author manuscript is the manuscript of an article that has been accepted for publication and which typically includes author-incorporated changes suggested during submission, peer review and editor-author communications.
Authors can share their accepted author manuscript:

- immediately
    - via their non-commercial person homepage or blog
    - by updating a preprint in arXiv or RePEc with the accepted manuscript
    - via their research institute or institutional repository for internal institutional uses or as part of an invitation-only research collaboration work-group
    - directly by providing copies to their students or to research collaborators for their personal use
    - for private scholarly sharing as part of an invitation-only work group on commercial sites with which Elsevier has an agreement
- after the embargo period
    - via non-commercial hosting platforms such as their institutional repository
    - via commercial sites with which Elsevier has an agreement

In all cases accepted manuscripts should:

- link to the formal publication via its DOI
- bear a CC-BY-NC-ND license - this is easy to do
- if aggregated with other manuscripts, for example in a repository or other site, be shared in alignment with our hosting policy not be added to or enhanced in any way to appear more like, or to substitute for, the published journal article.

**Published journal article (JPA):** A published journal article (PJA) is the definitive final record of published research that appears or will appear in the journal and embodies all value-adding publishing activities including peer review co-ordination, copy-editing, formatting, (if relevant) pagination and online enrichment.
Policies for sharing publishing journal articles differ for subscription and gold open access articles:
**Subscription Articles:** If you are an author, please share a link to your article rather than the full-text. Millions of researchers have access to the formal publications on ScienceDirect, and so links will help your users to find, access, cite, and use the best available version.
Theses and dissertations which contain embedded PJAs as part of the formal submission can be posted publicly by the awarding institution with DOI links back to the formal publications on ScienceDirect.
If you are affiliated with a library that subscribes to ScienceDirect you have additional private sharing rights for others' research accessed under that agreement. This includes use for classroom teaching and internal training at the institution (including use in course packs and courseware programs), and inclusion of the article for grant funding purposes.
**Gold Open Access Articles:** May be shared according to the author-selected end-user license and should contain a CrossMark logo, the end user license, and a DOI link to the formal publication on ScienceDirect.
Please refer to Elsevier's posting policy for further information.

18. **For book authors** the following clauses are applicable in addition to the above: Authors are permitted to place a brief summary of their work online only. You are not allowed to download and post the published electronic version of your chapter, nor may you scan the printed edition to create an electronic version. **Posting to a repository:** Authors are permitted to post a summary of their chapter only in their institution's repository.
19. **Thesis/Dissertation**: If your license is for use in a thesis/dissertation your thesis may be submitted to your institution in either print or electronic form. Should your thesis be published commercially, please reapply for permission. These requirements include permission for the Library and Archives of Canada to supply single copies, on demand, of the complete thesis and include permission for Proquest/UMI to supply single copies, on demand, of the complete thesis. Should your thesis be published commercially, please reapply for permission. Theses and dissertations which contain embedded PJAs as part of the formal submission can be posted publicly by the awarding institution with DOI links back to the formal publications on ScienceDirect.

**Elsevier Open Access Terms and Conditions**

You can publish open access with Elsevier in hundreds of open access journals or in nearly 2000 established subscription journals that support open access publishing. Permitted third party re-use of these open access articles is defined by the author's choice of Creative Commons user license. See our open access license policy for more information.
**Terms & Conditions applicable to all Open Access articles published with Elsevier:**
Any reuse of the article must not represent the author as endorsing the adaptation of the article nor should the article be modified in such a way as to damage the author's honour or reputation. If any changes have been made, such changes must be clearly indicated.
The author(s) must be appropriately credited and we ask that you include the end user license and a DOI link to the formal publication on ScienceDirect.
If any part of the material to be used (for example, figures) has appeared in our publication with credit or acknowledgement to another source it is the responsibility of the user to ensure their reuse complies with the terms and conditions determined by the rights holder.
**Additional Terms & Conditions applicable to each Creative Commons user license:**
**CC BY:** The CC-BY license allows users to copy, to create extracts, abstracts and new works from the Article, to alter and revise the Article and to make commercial use of the Article (including reuse and/or resale of the Article by commercial entities), provided the user gives appropriate credit (with a link to the formal publication through the relevant DOI), provides a link to the license, indicates if changes were made and the licensor is not represented as endorsing the use made of the work. The full details of the license are available at http://creativecommons.org/licenses/by/4.0.
**CC BY NC SA:** The CC BY-NC-SA license allows users to copy, to create extracts, abstracts and new works from the Article, to alter and revise the Article, provided this is not done for commercial purposes, and that the user gives appropriate credit (with a link to the formal publication through the relevant DOI), provides a link to the license, indicates if changes were made and the licensor is not represented as endorsing the use made of the work. Further, any new works must be made available on the same conditions. The full details of the license are available at http://creativecommons.org/licenses/by-nc-sa/4.0.
**CC BY NC ND:** The CC BY-NC-ND license allows users to copy and distribute the Article, provided this is not done for commercial purposes and further does not permit distribution of the Article if it is changed or edited in any way, and provided the user gives appropriate credit (with a link to the formal publication through the relevant DOI), provides a link to the license, and that the licensor is not represented as endorsing the use made of the work. The full details of the license are available at http://creativecommons.org/licenses/by-nc-nd/4.0.
Any commercial reuse of Open Access articles published with a CC BY NC SA or CC BY NC ND license requires permission from Elsevier and will be subject to a fee.
Commercial reuse includes:

- Associating advertising with the full text of the Article
- Charging fees for document delivery or access
- Article aggregation
- Systematic distribution via e-mail lists or share buttons

Posting or linking by commercial companies for use by customers of those companies.

20. **Other Conditions**:

v1.8

**Questions? customercare@copyright.com or +1-855-239-3415 (toll free in the US) or +1-978-646-2777.**

## JOHN WILEY AND SONS LICENSE TERMS AND CONDITIONS

Jul 06, 2016

This Agreement between Jane J Kim ("You") and John Wiley and Sons ("John Wiley and Sons") consists of your license details and the terms and conditions provided by John Wiley and Sons and Copyright Clearance Center.

| | |
|---|---|
| License Number | 3823781200158 |
| License date | Mar 07, 2016 |
| Licensed Content Publisher | John Wiley and Sons |
| Licensed Content Publication | Traffic |
| Licensed Content Title | Trs20 is Required for TRAPP II Assembly |
| Licensed Content Author | David Taussig,Zhanna Lipatova,Jane J. Kim,XuiQi Zhang,Nava Segev |
| Licensed Content Date | Mar 25, 2013 |
| Licensed Content Pages | 13 |
| Type of use | Dissertation/Thesis |
| Requestor type | Author of this Wiley article |
| Format | Print and electronic |
| Portion | Full article |
| Will you be translating? | No |
| Title of your thesis / dissertation | Ypts and TRAPPs in Golgi Dynamics |
| Expected completion date | Jun 2016 |
| Expected size (number of pages) | 100 |
| Requestor Location | Jane J Kim<br>360 E. South Water St.<br>Apt 3106<br><br>CHICAGO, IL 60601<br>United States<br>Attn: Jane J Kim |
| Publisher Tax ID | EU826007151 |
| Billing Type | Invoice |
| Billing Address | Jane J Kim<br>360 E. South Water St.<br>Apt 3106<br><br>CHICAGO, IL 60601<br>United States<br>Attn: Jane J Kim |
| Total | 0.00 USD |
| Terms and Conditions | |

## TERMS AND CONDITIONS

This copyrighted material is owned by or exclusively licensed to John Wiley & Sons, Inc. or

one of its group companies (each a"Wiley Company") or handled on behalf of a society with which a Wiley Company has exclusive publishing rights in relation to a particular work (collectively "WILEY"). By clicking "accept" in connection with completing this licensing transaction, you agree that the following terms and conditions apply to this transaction (along with the billing and payment terms and conditions established by the Copyright Clearance Center Inc., ("CCC's Billing and Payment terms and conditions"), at the time that you opened your RightsLink account (these are available at any time at http://myaccount.copyright.com).

**Terms and Conditions**

- The materials you have requested permission to reproduce or reuse (the "Wiley Materials") are protected by copyright.

- You are hereby granted a personal, non-exclusive, non-sub licensable (on a stand-alone basis), non-transferable, worldwide, limited license to reproduce the Wiley Materials for the purpose specified in the licensing process. This license, **and any CONTENT (PDF or image file) purchased as part of your order,** is for a one-time use only and limited to any maximum distribution number specified in the license. The first instance of republication or reuse granted by this license must be completed within two years of the date of the grant of this license (although copies prepared before the end date may be distributed thereafter). The Wiley Materials shall not be used in any other manner or for any other purpose, beyond what is granted in the license. Permission is granted subject to an appropriate acknowledgement given to the author, title of the material/book/journal and the publisher. You shall also duplicate the copyright notice that appears in the Wiley publication in your use of the Wiley Material. Permission is also granted on the understanding that nowhere in the text is a previously published source acknowledged for all or part of this Wiley Material. Any third party content is expressly excluded from this permission.

- With respect to the Wiley Materials, all rights are reserved. Except as expressly granted by the terms of the license, no part of the Wiley Materials may be copied, modified, adapted (except for minor reformatting required by the new Publication), translated, reproduced, transferred or distributed, in any form or by any means, and no derivative works may be made based on the Wiley Materials without the prior permission of the respective copyright owner.**For STM Signatory Publishers clearing permission under the terms of the STM Permissions Guidelines only, the terms of the license are extended to include subsequent editions and for editions in other languages, provided such editions are for the work as a whole in situ and does not involve the separate exploitation of the permitted figures or extracts,** You may not alter, remove or suppress in any manner any copyright, trademark or other notices displayed by the Wiley Materials. You may not license, rent, sell, loan, lease, pledge, offer as security, transfer or assign the Wiley Materials on a stand-alone basis, or any of the rights granted to you hereunder to any other person.

- The Wiley Materials and all of the intellectual property rights therein shall at all times remain the exclusive property of John Wiley & Sons Inc, the Wiley Companies, or their respective licensors, and your interest therein is only that of having possession of and the right to reproduce the Wiley Materials pursuant to Section 2 herein during the continuance of this Agreement. You agree that you own no right, title or interest in or to the Wiley Materials or any of the intellectual property rights therein. You shall have no rights hereunder other than the license as provided for above in Section 2. No right, license or interest to any trademark, trade name, service mark or other branding ("Marks") of WILEY or its licensors is granted hereunder, and you agree that you

shall not assert any such right, license or interest with respect thereto

- NEITHER WILEY NOR ITS LICENSORS MAKES ANY WARRANTY OR REPRESENTATION OF ANY KIND TO YOU OR ANY THIRD PARTY, EXPRESS, IMPLIED OR STATUTORY, WITH RESPECT TO THE MATERIALS OR THE ACCURACY OF ANY INFORMATION CONTAINED IN THE MATERIALS, INCLUDING, WITHOUT LIMITATION, ANY IMPLIED WARRANTY OF MERCHANTABILITY, ACCURACY, SATISFACTORY QUALITY, FITNESS FOR A PARTICULAR PURPOSE, USABILITY, INTEGRATION OR NON-INFRINGEMENT AND ALL SUCH WARRANTIES ARE HEREBY EXCLUDED BY WILEY AND ITS LICENSORS AND WAIVED BY YOU.

- WILEY shall have the right to terminate this Agreement immediately upon breach of this Agreement by you.

- You shall indemnify, defend and hold harmless WILEY, its Licensors and their respective directors, officers, agents and employees, from and against any actual or threatened claims, demands, causes of action or proceedings arising from any breach of this Agreement by you.

- IN NO EVENT SHALL WILEY OR ITS LICENSORS BE LIABLE TO YOU OR ANY OTHER PARTY OR ANY OTHER PERSON OR ENTITY FOR ANY SPECIAL, CONSEQUENTIAL, INCIDENTAL, INDIRECT, EXEMPLARY OR PUNITIVE DAMAGES, HOWEVER CAUSED, ARISING OUT OF OR IN CONNECTION WITH THE DOWNLOADING, PROVISIONING, VIEWING OR USE OF THE MATERIALS REGARDLESS OF THE FORM OF ACTION, WHETHER FOR BREACH OF CONTRACT, BREACH OF WARRANTY, TORT, NEGLIGENCE, INFRINGEMENT OR OTHERWISE (INCLUDING, WITHOUT LIMITATION, DAMAGES BASED ON LOSS OF PROFITS, DATA, FILES, USE, BUSINESS OPPORTUNITY OR CLAIMS OF THIRD PARTIES), AND WHETHER OR NOT THE PARTY HAS BEEN ADVISED OF THE POSSIBILITY OF SUCH DAMAGES. THIS LIMITATION SHALL APPLY NOTWITHSTANDING ANY FAILURE OF ESSENTIAL PURPOSE OF ANY LIMITED REMEDY PROVIDED HEREIN.

- Should any provision of this Agreement be held by a court of competent jurisdiction to be illegal, invalid, or unenforceable, that provision shall be deemed amended to achieve as nearly as possible the same economic effect as the original provision, and the legality, validity and enforceability of the remaining provisions of this Agreement shall not be affected or impaired thereby.

- The failure of either party to enforce any term or condition of this Agreement shall not constitute a waiver of either party's right to enforce each and every term and condition of this Agreement. No breach under this agreement shall be deemed waived or excused by either party unless such waiver or consent is in writing signed by the party granting such waiver or consent. The waiver by or consent of a party to a breach of any provision of this Agreement shall not operate or be construed as a waiver of or consent to any other or subsequent breach by such other party.

- This Agreement may not be assigned (including by operation of law or otherwise) by you without WILEY's prior written consent.

- Any fee required for this permission shall be non-refundable after thirty (30) days

from receipt by the CCC.

- These terms and conditions together with CCC's Billing and Payment terms and conditions (which are incorporated herein) form the entire agreement between you and WILEY concerning this licensing transaction and (in the absence of fraud) supersedes all prior agreements and representations of the parties, oral or written. This Agreement may not be amended except in writing signed by both parties. This Agreement shall be binding upon and inure to the benefit of the parties' successors, legal representatives, and authorized assigns.

- In the event of any conflict between your obligations established by these terms and conditions and those established by CCC's Billing and Payment terms and conditions, these terms and conditions shall prevail.

- WILEY expressly reserves all rights not specifically granted in the combination of (i) the license details provided by you and accepted in the course of this licensing transaction, (ii) these terms and conditions and (iii) CCC's Billing and Payment terms and conditions.

- This Agreement will be void if the Type of Use, Format, Circulation, or Requestor Type was misrepresented during the licensing process.

- This Agreement shall be governed by and construed in accordance with the laws of the State of New York, USA, without regards to such state's conflict of law rules. Any legal action, suit or proceeding arising out of or relating to these Terms and Conditions or the breach thereof shall be instituted in a court of competent jurisdiction in New York County in the State of New York in the United States of America and each party hereby consents and submits to the personal jurisdiction of such court, waives any objection to venue in such court and consents to service of process by registered or certified mail, return receipt requested, at the last known address of such party.

**WILEY OPEN ACCESS TERMS AND CONDITIONS**

Wiley Publishes Open Access Articles in fully Open Access Journals and in Subscription journals offering Online Open. Although most of the fully Open Access journals publish open access articles under the terms of the Creative Commons Attribution (CC BY) License only, the subscription journals and a few of the Open Access Journals offer a choice of Creative Commons Licenses. The license type is clearly identified on the article.

**The Creative Commons Attribution License**

The Creative Commons Attribution License (CC-BY) allows users to copy, distribute and transmit an article, adapt the article and make commercial use of the article. The CC-BY license permits commercial and non-

**Creative Commons Attribution Non-Commercial License**

The Creative Commons Attribution Non-Commercial (CC-BY-NC)License permits use, distribution and reproduction in any medium, provided the original work is properly cited and is not used for commercial purposes.(see below)

**Creative Commons Attribution-Non-Commercial-NoDerivs License**

The Creative Commons Attribution Non-Commercial-NoDerivs License (CC-BY-NC-ND) permits use, distribution and reproduction in any medium, provided the original work is properly cited, is not used for commercial purposes and no modifications or adaptations are made. (see below)

**Use by commercial "for-profit" organizations**

Use of Wiley Open Access articles for commercial, promotional, or marketing purposes

requires further explicit permission from Wiley and will be subject to a fee.
Further details can be found on Wiley Online Library
http://olabout.wiley.com/WileyCDA/Section/id-410895.html

**Other Terms and Conditions:**

**v1.10 Last updated September 2015**

**Questions? customercare@copyright.com or +1-855-239-3415 (toll free in the US) or +1-978-646-2777.**